THE REFLECTANCE OF SOME III - V ALLOY SEMICONDUCTORS

by

ALAN G. THOMPSON

Submitted in partial fulfillment
of the requirements for the degree of
Doctor of Philosophy

Department of Physics,
Faculty of Pure and Applied Science,
The University of Ottawa,
Ottawa, Canada.

1966

ABSTRACT

Apparatus to measure the reflectance of small semiconducting specimens at room and liquid nitrogen temperatures was designed and constructed. Measurements were made on the GaAs - GaP alloy system between 2 and 6eV, and some new interband transitions observed and identified. Apparatus to measure electroreflectance at room temperature was constructed, and measurements made on the GaAs - GaP alloys. The results enabled further conclusions on the optical properties and band structure of GaAs, GaP and their alloys, to be made. Alloys of the InAs - GaAs system of a high quality were grown using a new technique, and electroreflectance measurements on these materials furthered the reflectance work of Woolley and Blazey (W 30). Some semi-empirical work was done on the effective masses and fundamental energy gaps of the III - V alloy systems, which enabled some general conclusions to be drawn.

STATEMENT of ORIGINALITY

So far as the author is aware, the following parts of the present work are original:-

1. The Reflectance measurements on $GaAs_{1-x}P_x$ at room temperature between 2 and 6eV.
2. The Electroreflectance measurements on an alloy system i.e. $GaAs_{1-x}P_x$ between 1 and 6eV.
3. The Electroreflectance measurements on $In_{1-x}Ga_xAs$ between 2 and 6eV.
4. The Calculation of Electron Effective Masses in alloys between the III - V compounds by an approach other than a simple linear interpolation.
5. The development of a General Empirical Formula giving the magnitude of the departure from linearity of E_o for the III - V alloys, based on curve-fitting previously obtained results to a second-order equation.

Other work on the room-temperature reflectance (2 to 6eV) of $GaAs_{1-x}P_x$ was done concurrently but independently of the above study (S 30, W 43).

Professor Cardona collaborated on some of the conclusions based on the $GaAs_{1-x}P_x$ electroreflectance work (T 12).

ACKNOWLEDGEMENTS

I would like to thank Professor J.M. Robson for affording me the facilities of the Physics Department. I would also like to thank:- Dr M. Rubenstein of Westinghouse Labs, for providing the GaAs - GaP specimens; Messrs A. Croxon and J. Broome, for constructing the reflectance cryostat; R. Hart for building the associated vacuum system; P.M. Lazzier, for building and calibrating the furnaces and making some of the X-ray measurements; A.F. Seeley for his general assistance and forbearance; the Physics Department workshop staff; O. Bercle for reproducing most of the diagrams shown herein, Miss L.T. Sawyer, for typing this thesis.

I have benefitted from discussions with Drs J. Lucsin, T.E. Fischer and E.M. Williams, and my colleagues in the Physics Department.

I am most grateful to Professor M. Cardona for extending to me the use of the laboratory at Brown University, Physics Department and for the helpful discussions which ensued.

The inspiration and assistance provided throughout the course of research by my supervisor, Professor J.C. Woolley, is deeply appreciated.

The financial support of the Province of Ontario, and the National Research Council is gratefully acknowledged.

LIST OF CONTENTS

LIST OF FIGURES

LIST OF TABLES

SECTION I

INTRODUCTION

1.1 HISTORICAL INTRODUCTION

The first observation of a property of a semiconductor was made by Faraday (F 17) in 1833, when he noticed that the temperature coefficient of resistance of silver sulphide was negative. The photoconductivity effect was observed by Smith (S 50) in selenium in 1873, and rectification was obtained in lead sulphide and iron pyrites by Braun (B 39) a year later. The discovery of the Hall effect in 1879 (H 40) started a gradual understanding of the conduction processes in solids that culminated in the work of Bloch, Brillouin and Wilson. Modern theories are still largely founded upon the work of these three.

Academic interest grew slowly, but the need for high-frequency rectifiers in World War II greatly accelerated the quest for pure materials. This work resulted in the discovery of transistor action in 1949 (B 40), which was followed by intensive research into obtaining very pure materials and finding their properties.

Welker started research in 1952 on the III - V compounds (W 54) after correctly reasoning that their

properties should closely follow those of the corresponding group IV material. Certain members of this family of compounds have since become almost as important technologically as germanium and silicon.

1.2 BAND THEORY OF SOLIDS.

The first electron theory of solids, the Drude-Lorentz theory, qualitatively explained some of the properties of metals, with notable exceptions such as specific heats. It could not explain the differences between the various classes of solids (see e.g. K 25, S 51). The application of wave mechanics, by Sommerfeld in 1928, to an electron moving in a field - free space bounded by the surfaces of the solid, predicted a quasi-continuous range of energy levels (S 52). Whilst this theory was capable of explaining many properties of metals, it still gave no clues as to why crystalline solids should fall into the different categories of conductors and insulators.

Bloch modified the problem by pointing out that the electron moves in a periodic potential field, rather than a field - free space (B 41). In this way he showed that the quasi-continuous energy spectrum is broken up into regions of allowed and forbidden energy levels, whatever the form of the periodic potential. The existence of such forbidden bands then allowed the differences between metals, insulators and semiconductors to become apparent. This work was augmented by that of Brillouin (B 42) and Wilson (W 55, W 56).

The development of the theory from the foundations laid by these three workers is thoroughly dealt with in the standard texts (e.g. J 4, K 25, S 51) and will not be expounded here.

1.3 BAND STRUCTURE REPRESENTATIONS

The valence electrons in a crystal lattice are effectively free to move around, and their motion can be described by plane waves, having wave vectors k_i (where i specifies the direction). The energy band structure of the crystal is then the way in which the electron energy E depends upon the k_i.

There are two main ways of representing this band structure on paper. The first is to plot surfaces of constant energy, the paper being a certain plane in $\underline{k}$ space intersecting these surfaces. Typical examples are shown in the standard texts, eg S 51, pp 33 and 35. The second way is to plot energy versus $\underline{k}$ choosing certain directions of $\underline{k}$. It is found experimentally that most of the interesting band extrema in adamantine crystals occur either at the centre of the Brillouin zone i.e. 000, or in the ⟨111⟩ and ⟨100⟩ directions. Thus E is plotted against $\underline{k}$ in these two directions from k = 000, out to the first Brillouin zone boundaries at $k = \frac{2\pi}{a}(\frac{1}{2}, \frac{1}{2}, \frac{1}{2})$ and $k = \frac{2\pi}{a}(1, 0, 0)$, see Fig. 1.

The second representation is usually utilised when general band theory is being considered, and will be used extensively in this thesis. The manner in which

band structures and E - $\underline{k}$ diagrams are obtained theoretically will now be reviewed.

1.4 BAND CALCULATIONS

If the crystal periodic potential is known the band structure may be found but the inaccuracy in estimating such a potential plus the practical necessity of approximations has prevented accurate band calculations

The first step is to find the crystal structure of the lattice of the materials under consideration Using group theory it is found that the symmetry gives rise to a qualitative picture of the band structure, notably the degeneracy of the various levels This method is usually incapable of determining the relative positions of the levels etc. When spin is taken into account, certain degeneracies will be lifted, and symmetry calculations will say where but not by how much.

Having obtained a general picture, the next step is to calculate the form of the bands This entails certain assumptions and approximations The first approximation is that of reducing the problem to a "one - electron" case making an allowance for the effect of all the other electrons. A suitable periodic potential is then calculated from a knowledge of the lattice constant, atomic energy levels etc A set of one - electron wave equations for the more important

directions in the lattice is then set up, and the self-consistent solution of these equations will give the required energy band structure. With the growth of high-speed computers, these calculations have become quite refined, and give a good general picture of the band structure of the group IV elements, but fail to give detail such as relative energy level separations, and are not nearly so good for more complex crystal structures than diamond (see e.g. C 43).

The need for good band structures of all materials, particularly the III - V compounds, has given rise to several different methods based on the one described in the preceding paragraph, but using a semi-empirical approach. This work was developed quantitatively by Kane (K 26, K 27) after suggestions by Dresselhaus (D 15) and Herman (H 42, H 43).

The Schroedinger equation for an electron in a periodic potential V(r) is

$$\left[\frac{p^2}{2m} + V + \frac{\hbar}{4m^2c^2}(\text{grad } V \times p).\sigma\right]\psi = E_k\psi_k \qquad \text{(i)}$$

where p is a momentum operator.

σ is a spin operator.

Using Bloch functions

$$\psi_k = u_k(\underline{r})e^{i\underline{k}\cdot\underline{r}}$$

The equation for the lattice periodic function $u_k(\underline{r})$ follows:

$$(H_o + H_1 + H_2 + H_3)u_k = E_k' u_k \qquad \text{(ii)}$$

where

$H_o = \frac{p^2}{2m} + V(r)$, hamiltonian of the unperturbed problem.

$H_1 = \frac{\hbar}{m}\underline{k}.\underline{p}$, spin-independant perturbation for small k

$H_2 = \frac{\hbar}{4m^2c^2}(\text{grad } V \times \underline{p}).\underline{\sigma}$

$H_3 = \frac{\hbar}{4m^2c^2}(\text{grad } V \times \underline{k}).\underline{\sigma}$

} spin-dependent perturbation

and $E_{k'} = E_k - \frac{\hbar^2k^2}{2m}$

By expanding the wave functions of the perturbed problem in terms of the wave functions of the unperturbed problem, and using first order perturbation theory, a set of linear equations is obtained for the expansion coefficients whose secular determinant must vanish. Solving this equation gives energies to the first order, and higher orders can be calculated. The full development of this theory is

outside the scope of this work, but useful references are Callaway (C 42, C 43), Cardona (C 13) and Kane (B 4, K 27, M 22). The basic result is that by using some experimental energy gaps, other gaps and quantities such as effective masses may be predicted.

This method has developed into three other lines of approach. Cardona and Pollak (C 33, C 35, P 53) extended the $\underline{k}.\underline{p}$ analysis to a full zone method, which gives a complete band structure rather than merely the levels at the zone centre and edges. Brust (B 12) and Cohen and Bergstresser (C 37) have developed the empirical pseudo-potential method, in which the coefficients of the potential are adjusted so the solution gives agreement with experiment for one or more well-known gaps. They claim a high resolution for the group IV elements.

The problem of fitting an experimental band structure over a wide (up to 20eV) energy range to an empirical model is a very difficult one, however, and some sacrifices in local accuracy usually have to be made in order to obtain a good overall fit. Herman (H 38) claims to have overcome some of these difficulties. He starts with a first-principles method, namely a non-relativistic self-consistent calculation carried out very carefully, and modifies it to take care of relativistic and spin-

orbit effects etc He then adjusts some of the coefficients using well-established experimental values to bring the entire scheme into good agreement with the experimental energy level scheme. The adjustment required is small compared to that needed by Cohen and Bergstresser, and yet the scheme is not so empirical as the full zone $\underline{k}.\underline{p}$ analysis. This calculation also yields other parameters such as deformation potentials, pressure dependances etc., which are capable of being tested experimentally, so future developments in the above field are eagerly awaited.

1.5 BAND STRUCTURE OF Ge, Si, and III - V COMPOUNDS.

In this section, the band structure of some typical Group IV and Group III - V semiconductors will be discussed. Since this is of a review nature, detailed accounts will not be given, but will be referred to.

1.5 (a) Germanium and Silicon

Both of these Group IVB elements crystallise with the diamond structure. As can be seen from Fig 1 the band structures of Ge and Si are qualitatively similar, the main differences concerning the relative levels of the minima of the lowest conduction band. In Ge these are located on the eight ⟨111⟩ axes at the zone edges, but in Si they are located on the six ⟨100⟩ axes at $\underline{k} = 0.85.\frac{2\pi}{a}(100)$, that is, just inside the (100) edge. Optical absorption measurements (F 18) and magnetoresistance data (G 20) supported this theoretical prediction made by Herman (H 41). The values of the various energy gaps are listed in Table 1.

The valence band is triply degenerate at the Brillouin zone centre, where it is also at maximum energy. Because of the spin-orbit interaction however, one of these is split off from the other two by a small energy Δ_o (see Table 1; N.B. - Fig. 1 shows the band structure calculated without spin-orbit interaction

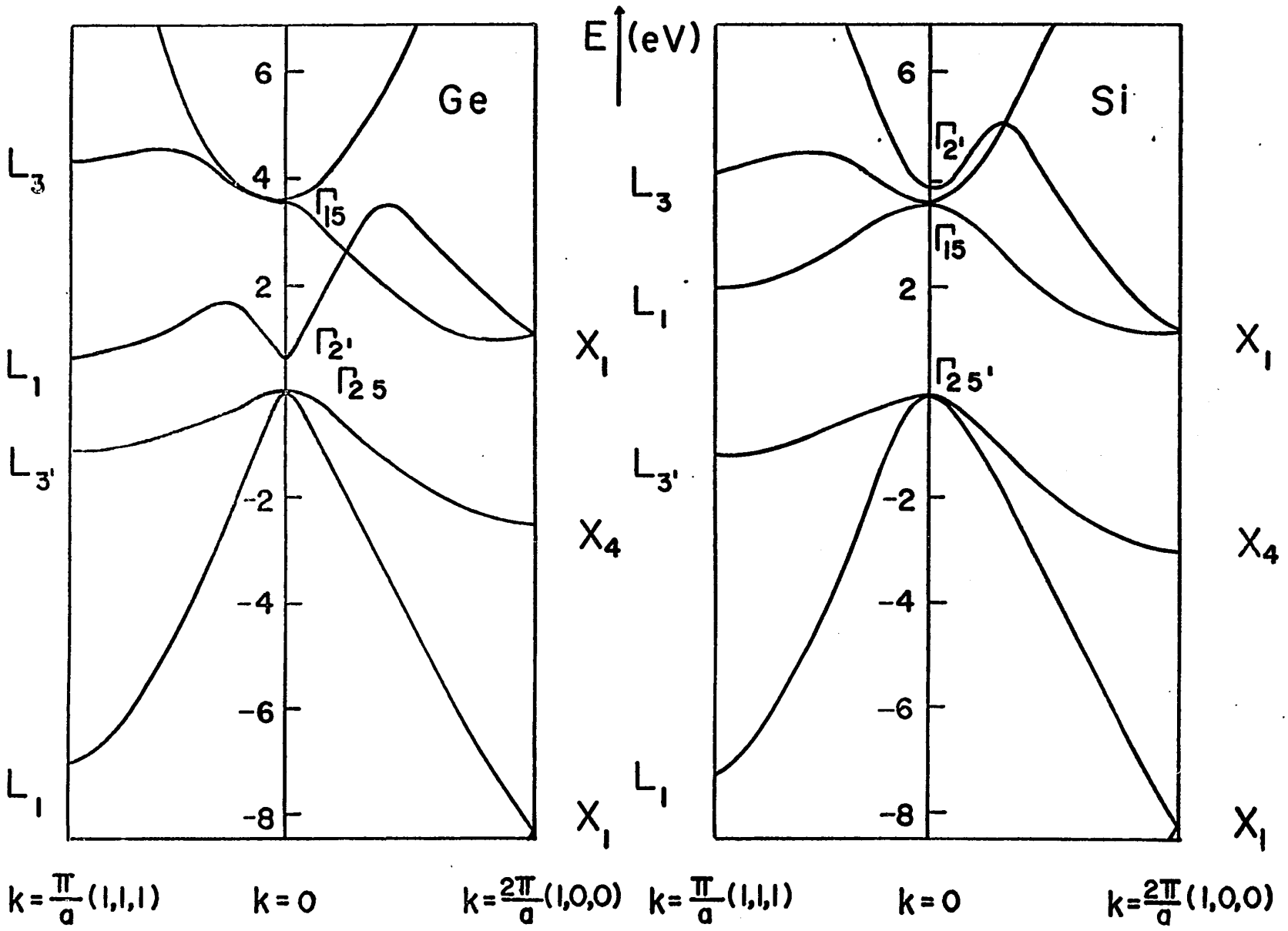

FIG I The Theoretical Band Structures of Ge and Si (without spin-orbit splitting - see B2)

effects being taken into account, and therefore does not show Δ_o). This split-off band is found to have spherical constant-energy surfaces, whilst the two degenerate branches have "warped" surfaces. It is usually possible, for the purpose of theoretical calculations, to replace these "warped" surfaces by pairs of spherical constant-energy surfaces having different effective masses $m_{v_1}^*$ and $m_{v_2}^*$ - hence the expressions "light" and "heavy" holes (D 15).

For energies not far removed from the conduction band edge, both Ge and Si have prolate spheroidal constant-energy surfaces, leading to two effective masses $m_{c_\perp}^*$ and $m_{c_{//}}^*$. The conduction band minimum at k = 000 has spherical constant energy surfaces in Ge, but Si probably does not have a minimum at this point (Γ_{15}) (C 33). Values of the various effective masses are given in S 51, pp. 347 and 350

1.5 (b) InSb and GaAs

These have been chosen for examples since they have both been widely investigated, and also illustrate the type of differences that can occur in the Groups IIIB-VB family of compounds. Most of this family crystallise with the zinc-blende structure, a sub-group of the

TABLE 1. Energy Gaps in Ge and Si

Energy Gap	Germanium		Silicon	
	4.2°K	290°K	4.2°K	290°K
E_g (opt). $= \Gamma_{25}' \rightarrow$ lowest minimum	0.741 (M 25)	0.665 (M 25)	1.156 (M 26)	1.114 (M 26)
E_o (direct) $= \Gamma_{25}' \rightarrow \Gamma_2'$	0.898 (Z 5)	0.806 (Z 5)	-	4.05 (C 49)
Δ_o		0.29 (C 13)		0.044 (C 13)

Table 1:

The values of the fundamental optical energy gap, (E_g), the lowest direct energy gap, (E_o), and the spin-orbit splitting at Γ, for Ge.and Si. All energies are in eV.

diamond structure with lower symmetry.

If spin is not considered, the only difference between diamond and zinc-blende band structures in a qualitative sense will be the splitting of the degenerate X_1 point (N.B. This notation is the group theoretical one, see Figs. 1 and 2). The detailed structure of the valence band of zinc-blende materials with and without spin effects being taken into account is shown in Fig. 2. The first diagram should be compared to Fig. 1 in order to see the differences in group-theoretical notation between diamond and zinc-blende lattices. As can be seen from Fig. 2, the structure incorporating spin-orbit effects is much more complex than the structure without, and, partly for this reason, it is customary to use the non-spin notation, and mention the splitting if it is important (e g. the X_{5_v} doublet, rather than the X_6 and X_7 levels). The main point is that the top of the valence band no longer lies at the exact centre of the zone, or Γ point, but is located a small distance along the $\langle 111 \rangle$ direction, or Λ_5 (assuming Γ_6 is the highest sub-band). The split-off valence band and the conduction band still have extrema at Γ

Both GaAs and InSb have direct fundamental energy gaps, since the lowest conduction band minimum occurs,

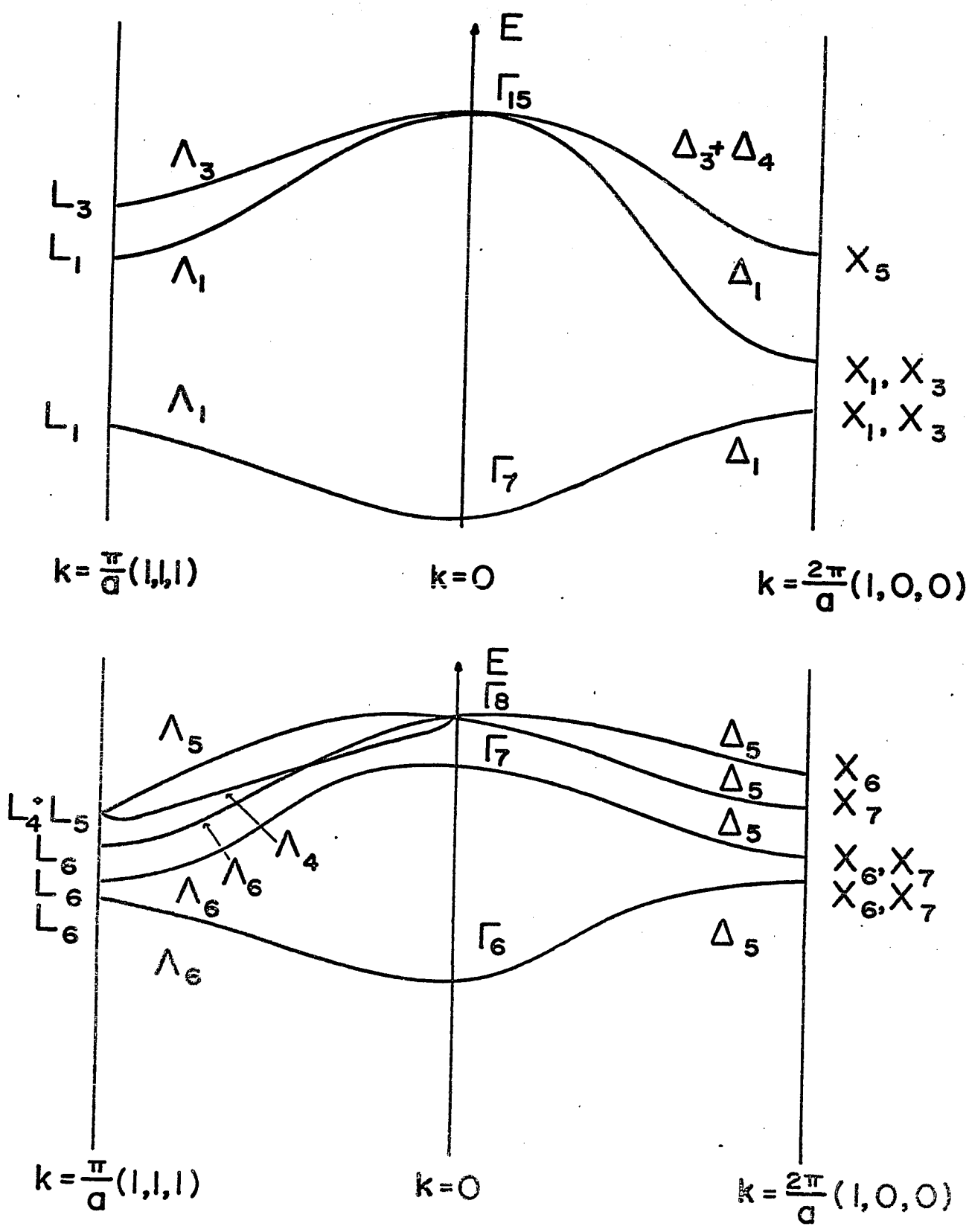

Fig 2 The Valence Band Schemes of Zinc-Blende Materials from Symmetry Considerations (a) without and (b) with spin effects (M22)

as in most III - V compounds, at Γ_{1c}. Otherwise they appear qualitatively similar to Ge and Si, with the symmetry exceptions noted earlier. However, InSb has a very small fundamental gap, and this leads to a departure from parabolicity in the conduction band, because of the influence of nearby bands (see Fig 3). The electron effective mass therefore varies according to the degree to which the band is filled, and the different definitions of effective mass (see Section VI) give different values (e.g.M 22, p. 34). Also, the value of the optical energy gap varies as a function of the impurity concentration of the specimen. This effect is named after Burstein (B 43) who explained its quantitative form in terms of the non-parabolicity of the conduction band and a low density of states, the latter causing the band to fill rapidly.

GaAs has a much larger energy gap than InSb, and has a practically parabolic conduction band. It was one of the first of the III - V compounds to receive theoretical attention, when Herman suggested it was qualitatively similar to Ge, and derived a theoretical energy band scheme (H 43). Optical reflectivity results (B 44) and magneto-resistance measurements (G 19) proved that, unlike Ge, the lowest conduction band minimum was

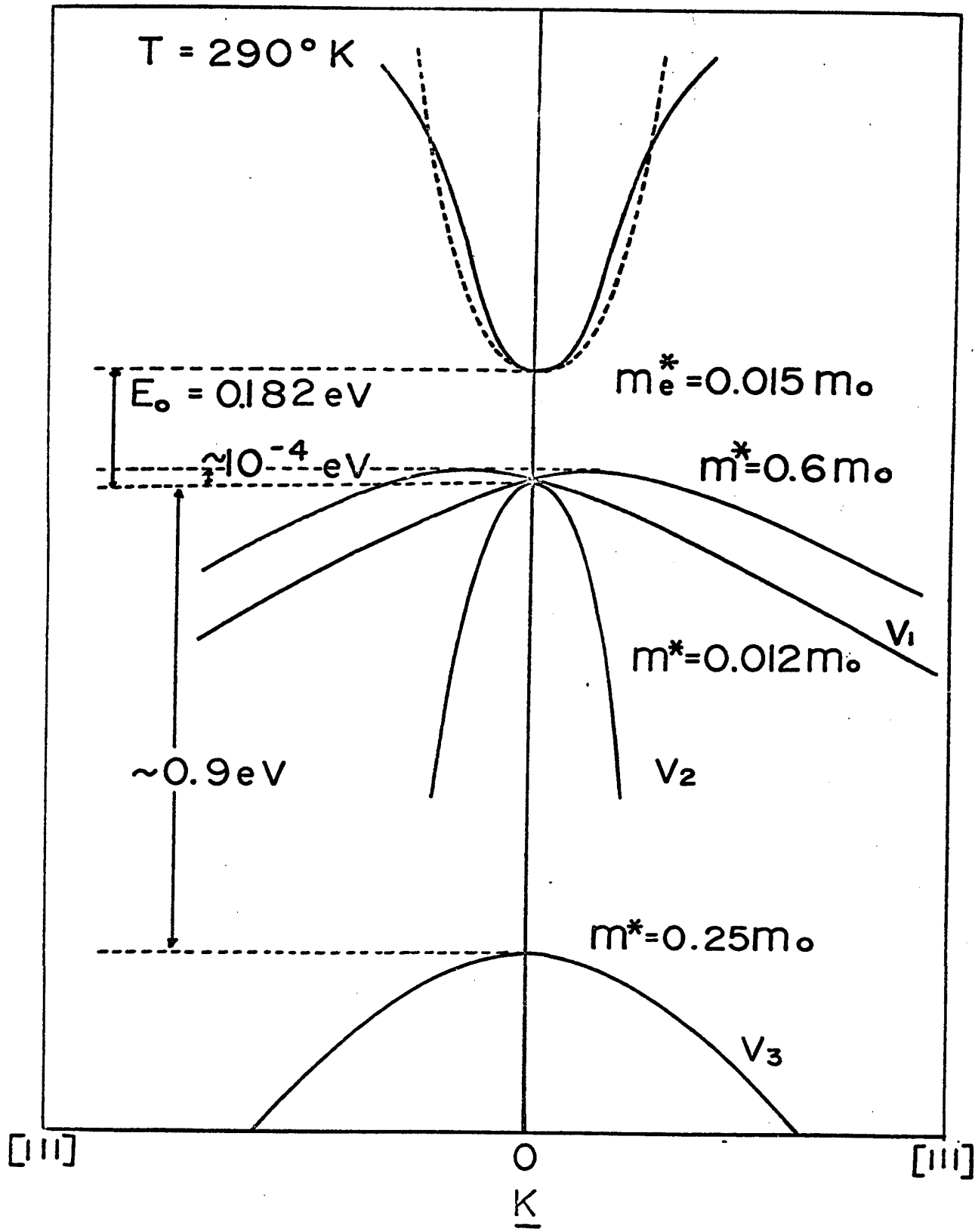

FIG 3 The Band Structure for InSb around Γ.

at $\underline{k} = 000$. The energy band scheme derived by the full zone $\underline{k}.\underline{p}$ method (P 53) is shown in Fig. 4.

The fundamental energy gaps, relative levels of the conduction band minima and other physical properties of the more common III - V compounds, where known, are shown in Table 2, together with references as to their source. Some review articles on band theory, the methods of calculating band structures, and other useful references are listed below:

Callaway (C 42)
Herman (H 9, H 27)
Long (L 1)
Nussbaum (N 1)
Pincherle (P 13)

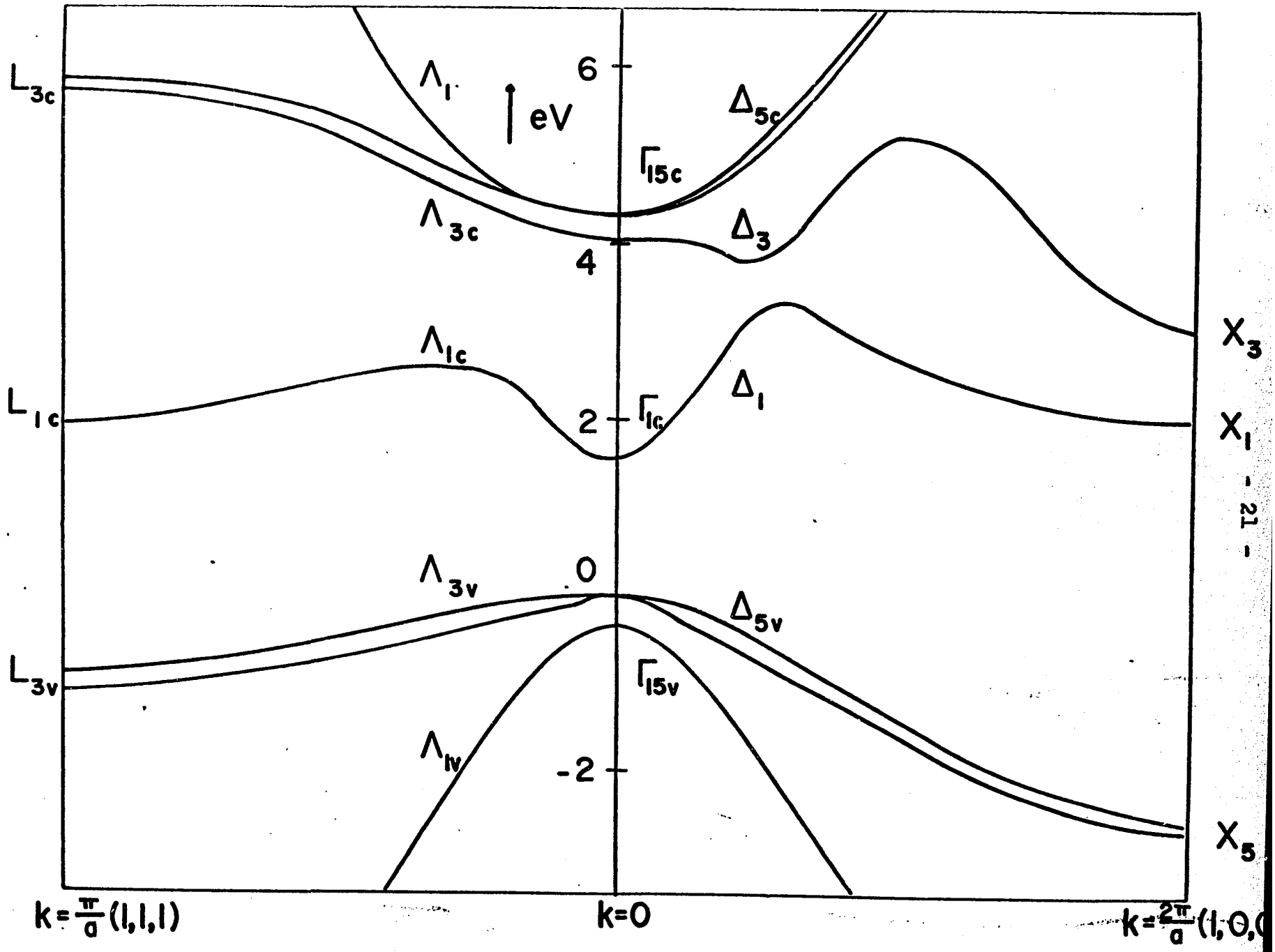

FIG 4 The Band Structure of GaAs (P 53)

TABLE 2. Energy Gaps and Physical Parameters in some of the III - V Compounds.

Compound	E_o (290°K) direct gap, eV.	Δ_{111}	Δ_{100}	Δ_o	Lattice Const. in Å (C23)	Melting Pt. in °C (M22)
GaP	2.742 (T12) 2.780 (S36)	~-.2* (H30)	-0.56* (H30) -0.55 (S36)	0.103 (T12) 0.127 (H2) 0.09 (S36)	5.451	1467
GaAs	1.441 (T12) 1.38 (S46) 1.436 (S55)	0.48* (H30)	0.33* (H30) 0.36 (E1)	0.339 (T12) 0.348 (S46)	5.654	1238
GaSb	0.725 (B10)	0.08* (H30)	0.40* (H30)	0.80 (C49)	6.096	706
InP	1.34 (C49)	0.7* (H30)	0.4* (H30)	0.11 (C49)	5.869	1058
InAs	0.360 (Z5) 0.35 (S1)	1.1* (H30)	1.2* (H30)	0.41 (B4)	6.059	942
InSb	0.182 (Z5)	0.6* (H30)	0.8* (H30)	~0.9 (C23) 0.82 (C49)	6.479	530

Table 2: Energies of the lowest direct gap, heights of the conduction band minima above that at Γ, and the spin-orbit splitting for some III - V compounds, in eV; N.B. low temperature data are indicated by an asterisk. Also included are the lattice constants and melting points.

SECTION II

ALLOY SEMICONDUCTORS

2 1 INTRODUCTION.

The term "alloy semiconductor" is generally taken to mean an alloy formed between two or more semiconducting elements or compounds, and which is itself a semiconductor. In this thesis the alloy systems considered are pseudo-binary Group III - V systems i.e., two III - V compounds are combined and have either the Group III or Group V element in common.

Another feature of these systems is that the alloy produced must form solid solutions so that only one phase is present. If this condition is not satisfied, the interpretation of the physical properties observed is usually extremely difficult and misleading. As will be seen later, satisfying this single-phase condition for all compositions leads to most of the problems of producing alloys between the III - V compounds. This statement is generally true for most alloy semiconducting systems.

Also, the great majority of alloy semiconductors are disordered, so that the mixed atoms lie randomly on the sites available. This lack of ordering has an important effect on the theory of these materials, as

will be seen in the next few pages. If ordering does take place, the result is usually called a compound e.g. $CdIn_2Se_4$, which forms in the $CdSe-In_2Se_3$ alloy system, at the 0.5 mole fraction composition (see ⅄ 53).

2.2 THE VIRTUAL CRYSTAL MODEL

The calculations of the band structure of alloys is extremely difficult, as indicated in Section 1.4. Very few such calculations have been made, and these will be dealt with later. However, there is a very useful general theory available, known as the virtual crystal model.

This concept was introduced by Nordheim (N 6), and extended by Muto (M 23) and Parmenter (P 47, P 48, P 49), the latter applying it specifically to semiconductors. The basic postulate of this theory is that the potential function through which an electron moves can be considered as two parts;

i.e. $$V_{alloy}(r) = V_p(r) + V_{np}(r) \qquad \text{(iii)}$$

where V_p = a periodic part, representing the "ideal" crystal, chosen to give the average alloy potential over all possible random arrangements of atoms on the lattice

and V_{np} = a non-periodic part, representing the effects of disorder, chosen to give the deviation of $V_{alloy}(r)$ from the average.

Both Nordheim and Muto applied first order perturbation theory to the problem by considering V_{np} as a perturbing

potential and V_p as the unperturbed case. Muto came to the conclusion that the disorder produced no changes in the energy levels to first order.

Parmenter extended this theory, and his results show that while higher order perturbation theory affects the centre of an unperturbed band very little, larger effects take place at the band edges. The net effect is that the edges of the allowed bands are "smeared" into the forbidden bands, but only to a finite extent; the concept of allowed and forbidden bands is therefore still applicable. Hence it is still reasonable to assign a wave vector and an energy band structure to an alloy, provided the effects of disorder are not large enough to invalidate the use of the perturbation treatment. This is usually the case of course, since a large disorder would result in a high free energy, which would effectively prevent the formation of an alloy (see Section 2.1).

The general result of the virtual crystal model is that certain physical quantities should vary linearly with alloying to a first approximation. Vegard's law, which states that alloys between two substances having the same crystal structure should show a linear dependence

on composition of the lattice parameter, is probably the best known result from the model. This law has been proved, with the exceptions usually having only small departures from linearity (e.g. W 58). Other properties which should also vary linearly with composition to a first approximation include energy gaps, effective masses, some lattice scattering parameters etc. Deviations from this law are naturally of some interest, and are discussed in Section VI.

First - principles band calculations have not been performed for alloy semiconductors, as the virtual crystal model is usually assumed to hold for some basic quantities, such as certain potentials. Bassani and Brust (B 2), computed the band structure of Ge - Si alloys using a pseudopotential method; the parameters were chosen from a linear interpolation between the parameters used previously for similar calculations on Ge and Si (see e.g. B 7, B 12). The energy levels all vary approximately linearly with alloy composition, any deviation taking the form of a convex (upwards) curve. This contrasts with the experimental evidence which suggests a slight concavity (downwards) for certain transitions (see Section 2.3(a)). Chang Yu-Won and Yu Qi-Hua made calculations on the GaAs - GaP system using a pseudopotential method

(Y 2), again using a linear interpolation between the potential coefficients calculated for GaAs and GaP. Further comment on this system will be made in Section 7.

2.3 REVIEW OF ALLOY SEMICONDUCTORS

In this section the history of alloy semiconductors as it affects this thesis will be reviewed, and a resumé of the results presented. For a detailed account of all semiconducting alloy systems see Woolley (W 53)

2.3 (a) The Ge-Si system

These were the first semiconducting alloys to be successfully synthesised, and have been more thoroughly studied than any other system. Stöhr and Klemm (S 53) obtained homogeneous specimens in the form of compressed powders after annealing for long times. Their investigations showed that single phase solid solution could be obtained over the complete alloy range Solid specimens were first obtained by Johnson and Christian (J 5) and they made infra-red absorption measurements on them. The latter were extended by Braunstein, Moore and Herman (B 17). Other measurements have been made on the Hall effect (B 45, D 8), magneto-resistance and conductivity (G 20), thermal conductivity (D 8, S 54), cyclotron resonance (D 16, O 3) and reflectivity (T 2, T 3) as a function of temperature and alloy composition Some of these properties have also been measured as a function of pressure, such as

Paul's work on the variation of fundamental optical gap (E_g) as a function of hydrostatic pressure (P 50). Recently, electroreflectance measurements have been reported (C 48).

As explained in Section 1.5, the conduction band structures of Ge and Si are quite different; some of the first evidence for this came from work on the variation of E_g with composition in the alloys, a distinct break in the curve being observed at $Ge_{0.85}Si_{0.15}$. This lead to the conclusion that between Ge and this composition, the lowest minima are in the ⟨111⟩ directions, at the zone edges, whilst above this composition up to Si the minima in the ⟨100⟩ directions are the lowest. This interpretation was confirmed by the magnetoresistance measurements mentioned above.

Theoretical work on this system has been extensive compared to other alloy systems. Herman's initial suggestions (H 41) were developed alongside the experimental work (see eg B 17, P 50), but the first calculations of complete band structures were made by Bassani and Brust (see Section 2.2) who obtained quite good quantitative agreement with experiment.

2.3 (b) The III - V Systems

Early attempts to alloy the III - V compounds

containing a common element were not encouraging, with the exception of InAs - InP and GaAs - GaP which were produced and investigated by Folberth (F 1) and Weiss (W 20). Shortly after this news, Woolley et al (W 1, W 3) and Goryunova et al (G 21, G 22) showed that solid solution occurred for all compositions in InSb - GaSb, but very long annealing times were required to produce equilibrium, even compressed powders taking several weeks when held within 50°C of the solidus curve Later work established that complete solid solution also occurred in InAs - GaAs (A 2, W 2), InAs - InSb (W 58), AlSb - InSb (W 58) and AlSb - GaSb (B 46). Reviews on the crystallography and preparation of alloys between the III - V compounds have been given by Woolley (W 53, W 57).

Many physical properties have been measured on these systems, and some references are summarised in Table 3 for infra-red absorption (or photoconductivity), reflectivity above the fundamental edge, and electrical transport properties, for some of the more important III - V alloy systems This table includes references published up to mid - 1966, and some of the work to be described in this thesis, together with other investigations done concurrently or after it, therefore appears

TABLE 3. References for the III - V alloy system

III - V Alloy System	E_g by Optical Absorption or Photoconductivity*	Reflectance Above E_g	Electrical Transport Properties	Electroluminescence
GaAs - GaP	A2, A7, F1, F2, K4, R8, S8*, T12, T13.	A9, B21, S30, T12, T16, W42, W43.	A11, F7, K4, T8, T13, W48.	A5, C22, F4, F10, G16, H4, H10, H11, H19, K4, K5, N7, P21, P29,
InAs - InP	D1, F1, O4.	-	E14, W20.	A3,
InSb - GaSb	B25, I5, W6, W16.	B49, W30	I6, W11.	R10.
InAs - GaAs	A2, H45, W15.	B49, C41, W30	A2, H45, W15.	M5, M12
InSb - InAs	W34, W59*	-	C44, W59	-
InSb - AlSb	-	-	A17.	-
GaSb - AlSb	B47, E1, M2*, M24	-	B48.	-
GaSb - GaAs	-	-	-	-
AlAs - GaAs	B36	-	-	

Table 3: References for certain physical properties of the III - V alloy systems which have been produced. It is believed complete up to mid 1966.

Most of the III - V alloy systems on which optical absorption measurements of E_g have been made show a linear or slightly monotonic variation with composition (see Section VI for further detail). However, GaAs - GaP does not (F 1, R 6), but shows an abrupt change of slope at approximately the equimolar composition. Also, the GaAs rich alloys show absorption characteristic of a direct transition, whilst the GaP rich alloys exhibit an indirect transition. Pressure measurements on GaP (P 3) showed it has the lowest conduction band minima in the ⟨100⟩ directions / change similar to that of the Ge-Si system therefore takes place, except that different directions in $\underline{k}$ space are involved since the GaAs conduction band minima occur at $\underline{k}$ = 000.

2.4 CURRENT INTERESTS AND CONTENTS

At the time this work was started, very little was known about GaP and its band structure. In particular, its reflectance spectrum was unlike most of the other III - V compounds, and subject to speculation (C 8). With this in mind, it was decided to measure the reflectance spectra of GaAs, GaP and GaAs - GaP alloys, since GaAs was comparatively well known. This reasoning was later fortified by the tremendously increased interest in the GaAs - GaP alloys by both the academic world and industry, mainly because they are capable of laser activity in the visible region, whereas GaAs radiates in the near infra-red (see Section VII and Table 3). GaAs has been used for a while for electrical devices, but interest is growing in the use of the alloys and GaP for rectifier and transistor action at high temperatures.

Apparatus to measure reflectance at room and liquid-nitrogen temperatures was therefore set up, after examining the various methods that had been used in the past. The results from the GaAs - GaP reflectance spectra were interesting, but still partly inconclusive (see Section III).

Another technique was resorted to which had been reported capable of higher resolution than reflectance, namely electroreflectance. The results from the electroreflectance spectra enabled further conclusions on the band structure of GaAs, GaP and their alloys to be drawn (see Section IV).

The different techniques of producing InAs - GaAs alloys were examined (/ 15) and specimens were produced. Electroreflectance measurements were made on these in an attempt to further the reflectance results of Woolley and Blazey (B 49, W 30) (Section V).

In Section VI some theoretical work on the variation of effective mass in alloys is presented, together with some semi-empirical observations on the variation of the fundamental energy gap in III - V alloy systems, with their bearing on the virtual crystal model, which arose from the effective mass investigation.

Conclusions on the above work are drawn, and suggestions for future lines of approach are made in Section VII.

The work outlined above forms part of a general programme of research into alloys involving the III - V compounds, directed by Professor John C. Woolley.

Started at Nottingham University (England) in 1955, this programme was continued in 1963 at Ottawa The research on which this thesis is based was started in August 1963, and finished in September 1966.

SECTION III

THE REFLECTANCE OF GaAs - GaP

3 1 INTRODUCTION

Many of the important properties of semiconductors are directly connected with their band structure. When endeavouring to find a band structure however, certain properties are more useful than others, and in particular a knowledge of certain energy gaps is necessary for both the pseudo-potential (B 7, C 37) and k p perturbation methods (C 13, C 33, P 53). These gaps are usually found by optical experiments, and are shown in Fig 5.

A study of the optical constants of a semiconductor over a wide energy range yields much useful information. At low energies, or long wavelengths, the absorption coefficient depends on the number of free carriers, lattice vibrations etc., so that a pure material generally is almost transparent in this region. At a certain wavelength the absorption coefficient rises sharply, this being known as the fundamental absorption edge. It corresponds to the energy required to excite an electron from the valence band to the lowest lying conduction band, the wavelength of the photon absorbed

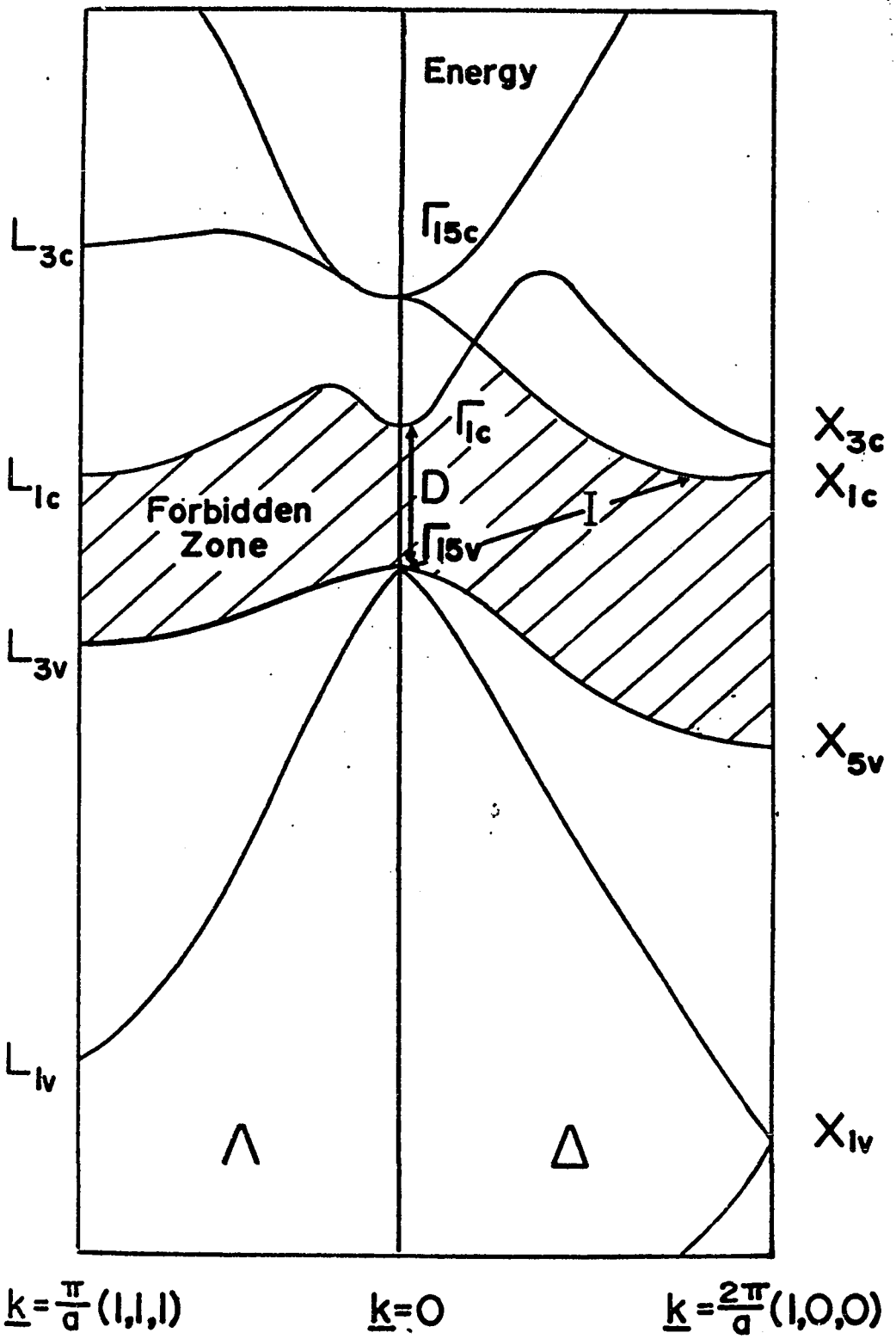

Transitions

$E_0=\Gamma_{15v}-\Gamma_1$

$E_0'=\Gamma_{15v}-\Gamma_{15c}$

$e_1=L_{3v}-L_{1c}$

$E_1=\Lambda_{3v}-\Lambda_{1c}$

$E_1'=L_{3v}-L_{3c}$

$E_2=X_5-X_1$

Relative Levels

Γ_1-L_1 (min)

$\Gamma_1-\Delta_1$ (min.)

$\Delta_0=\Gamma_{15v}$ splitting

$\Delta_1=\Lambda_{3v}$ splitting

$\Delta_2=X_3-X_1$

FIG 5 Generalised Band Structure for Zinc-Blende (without spin-orbit splitting) showing the location of some Optical Transitions

being given by

$$\Delta E = \frac{hc}{\lambda} \qquad \text{(iv)}$$

/t energies greater than that corresponding to this edge, the absorption coefficient is very high, and is associated with interband transitions Between about 8 and 16eV the reflectance decreases rapidly, indicating that the valence electrons are essentially unbound (P 2). Between 16 and 30eV additional absorption indicates transitions from filled d bands below the valence band to empty conduction band states (for general accounts see C 23, P 2, P 36).

Two types of transition can take place at the fundamental edge. The first involves only a photon, but the second involves phonons also i.e energy is either supplied by the crystal lattice or given up to it These are known as "direct" and "indirect" transitions respectively, since no movement in $\underline{k}$ space takes place for the former, but usually does for the latter (see Fig 5). The differences between the various types of transition and the analysis of their corresponding absorption edges is well documented in the literature (eg M 27, S 51) and will not be expanded here, since it does not directly concern this work

It can be seen therefore that the measurement of the optical absorption coefficient of a semiconductor will show the fundamental gap, and thus yield a value of the energy separation of the top valence band, Γ_{15v} (using III - V spinless representation) to the lowest conduction band minima, which is Γ_{1c} in the direct gap III - V compounds. Optical absorption measurements sometimes give another edge at higher energies due to transitions from the split-off valence band; the spin-orbit splitting Δ_o can thus be obtained. (The notation to be used in this thesis generally follows Cardona, C 8, C 23, the fundamental direct gap being E_o).

Measurement of further absorption edges at higher energies is rendered difficult by the extremely large absorption coefficients mentioned earlier. One has to use either very intense light sources and sensitive detection equipment, which results in experimental difficulties, or very thin specimens. The latter cannot be obtained by the usual grinding techniques, and usually take the form of thin films on transparent substrates. However, doubt has been cast on the properties of thin films being representative of the bulk material. Also many materials do not lend themselves to this technique of deposition, and the choice of substrate has to be made carefully. Work has been done

using thin films of varying thickness (C 3) but other methods of finding these higher energy gaps are available and one of these will now be outlined

3.2 THE THEORY OF REFLECTANCE

The complex refractive index of a material can be written $n^* = n - ik$. A plane electromagnetic wave of frequency ν and wavelength λ propagated through a material in the x direction has the form

$$x = A \exp\{2\pi i\nu(t - \frac{n^*x}{c})\}$$

$$= A \exp\{-\frac{2\pi\nu kx}{c}\} \exp\{2\pi i\nu(t - \frac{nx}{c})\} \qquad (v)$$

Now phase velocity $V = \frac{c}{n}$, and wavelength $\lambda = \frac{c}{\nu n}$, so (v) becomes

$$x = A \exp\{-\frac{\alpha x}{2}\} \exp\{2\pi i\nu(t - \frac{x}{V})\}$$

where $\alpha = \frac{4\pi k}{\lambda_o}$ is called the absorption coefficient and λ_o is the free space wavelength at the frequency ν. The complex dielectric constant $\varepsilon^* = \varepsilon_1 - i\varepsilon_2$ and $|\varepsilon| = |n^2|$, so the optical and dielectric constants are related by

$$\varepsilon_1 = n^2 - k^2$$

$$\varepsilon_2 = 2nk \qquad (vi)$$

It can thus be seen that the optical properties of a material closest related to the absorption coefficient are the imaginary parts of the refractive index and dielectric constant, k and ε_2 respectively.

For allowed transitions the imaginary part of the dielectric constant ϵ_2 is proportional to the joint density of states $\frac{dN}{dE}$, which has singularities or critical points whenever

$$\nabla_k (E_c - E_v) = 0$$

$$E_c - E_v = \hbar\omega \qquad \text{(vii)}$$

where E_c and E_v are the energies of the conduction and valence bands involved, and ω is the angular frequency of the radiation (= c/λ) (C 23). At high symmetry points in the energy band scheme, such as Γ, X and L in zinc blende structures,

$$\nabla_k E_c = \nabla_k E_v = 0$$

Thus structure in ϵ_2 should be present for the energy gaps at these points. However, the conditions in equation (vii) can be satisfied without either $\nabla_k E_{c,v}$ being zero, and would be expected at high symmetry directions such as [111] in zince blende. The critical points fall into four categories corresponding to minima, maxima, and two types of saddle points on the E - $\underline{k}$ curves; the saddle points give rise to the strongest structure in the joint density of states and hence in ϵ_2 also.

Therefore, by measuring ϵ_2 over the energy range of interest, the various transitions can be observed and

the values of the energy gaps used for band calculations etc. Now ϵ_2 can be measured indirectly from n and k, but this is usually difficult. The knowledge of one optical constant over a wide range of energy is sufficient, however to determine all others through the Kramers - Krönig relations. These state, for example,

$$\epsilon_1(\omega_o) = 1 + \frac{1}{\pi}\int_{-\infty}^{\infty} \epsilon_2(\omega)\,\frac{d\omega}{\omega - \omega_o} \qquad \text{(viii)}$$

The reflectance at near-normal incidence is experimentally the simplest constant to find over a wide energy range. The reflectance phase is then (J 3, P 4).

$$\theta_1(E_o) = \frac{1}{2\pi}\int_{o}^{\infty} \frac{d \ln |R(E)|}{dE} \ln \left|\frac{E + E_o}{E - E_o}\right| dE \qquad \text{(ix)}$$

A knowledge of R(E) over a wide range of energy is then sufficient to find θ_1 over a similar range. The optical constants n and k are then given as solutions to the equation.

$$(n - ik - 1)(n - ik + 1) = R^{\frac{1}{2}} e^{i\theta} \qquad \text{(x)}$$

The treatment of this equation by computer methods is dealt with in the literature, together with methods of extrapolating R(E) over an infinite range of energy,

(see e.g. C 16, P 2). Thus k, and hence ϵ_2 or α, can be calculated, and the resulting structure interpreted as being representative of the locations of the absorption edges.

Hence structure in the reflectance spectrum can be correlated with absorption edges and such structure will be expected to occur even for very large absorption coefficients. Also, if the absolute reflectance is known over a sufficiently wide energy range, the optical constants (n, k, ϵ_1, ϵ_2, α) may be found over the range of interest.

In practice, whilst the expected structure in the reflectance $R(E)$ is observed, other factors prevent a straightforward correlation with band structure. The surface of the material must be "atomically clean" i.e. there should be no damaged layers of the type produced by polishing. Etching helps to remove these layers, but results cannot usually be duplicated. Other surface treatments give differing results, and the best is probably cleavage (see C 23). For this reason, results must be interpreted with caution, a topical case being the "hyperfine structure" observed by Lukes and Schmidt in Si (L 4, L 7), which has been both interpreted theoretically (P 51) and repudiated (G 5).

The only criteria used to define the 'best' surface are highest reflectivity at the peaks and sharpest structure - the latter in particular is somewhat arbitrary. Whilst the absolute reflectances obtained by different workers for the same material vary quite widely (which, of course, affects the magnitudes of the optical constants found by equations (ix) and (x)) good agreement is usually obtained on the type of structure and the energy at which it occurs. Thus, as pointed out above, the positions of the absorption edges are consistent, although their magnitudes need not necessarily be, between different experiments.

Another important difficulty lies in assigning the observed edges to the various direct transitions which can take place by equation (viii) on the energy band scheme. Both experiment and theory must combine in order to interpret such spectra. The usual procedure is to calculate a band structure knowing only the fundamental gap, a theoretical analysis showing whether this is direct ($\Gamma_{15v} \rightarrow \Gamma_{1c}$) or indirect ($\Gamma_{15v} - L_{1c}$ or Δ). The approximate values of the other gaps are then compared with the experimental ones, with symmetry considerations helping in the analysis. For example, the L_{3v} level is

spin-orbit split (Δ_1) by approximately 2/3 Δ_o. More refined calculations can then be performed to make the band structure fit the experimental results better. Other types of measurements also assist in this process, magnetoresistance for example being capable of giving the relative levels of the three conduction band minima, together with their location in $\underline{k}$ space. The sizes of the absorption edges can sometimes be of assistance, and can be found from reflectance results

Practical evidence of the correlation between structure in the reflectance spectrum and absorption edges has been obtained, notably by Cardona and Harbeke (C 3, C 23).

3 3 REVIEW OF REFLECTANCE RESULTS.

This review only covers work published up to the end of 1963 when this project was started. Such an approach is necessary in order to make the reasons for attempting the work sound plausible, because some work of a similar nature was done concurrently, but independently.

The first measurements of the reflectance of a semiconductor at energies higher than the fundamental edge were made by Philipp and Taft in 1959 on Ge (P 4) and in 1960 on Si (P 5). The spectrum of Ge is shown in Fig 6, with the imaginary part of the index of refraction calculated by Kramers - Krönig relations (P 4). The relationship between the structure in R and k can be seen quite clearly. The first explanation of these results was given by Phillips (P 6). He proposed that the absorption edge corresponding to the 2 2eV peak was due to $L_{3'} - L_1$ transitions between the valence and conduction bands in the (111) directions The edge corresponding to the 4.4eV peak was allocated to the $X_4 - X_1$ transitions in the (100) directions. This interpretation was made more acceptable by Tauc and Antonick's report (T 1) of a splitting of the 2 2eV peak by an amount approximately equal to 2/3 Δ_o.

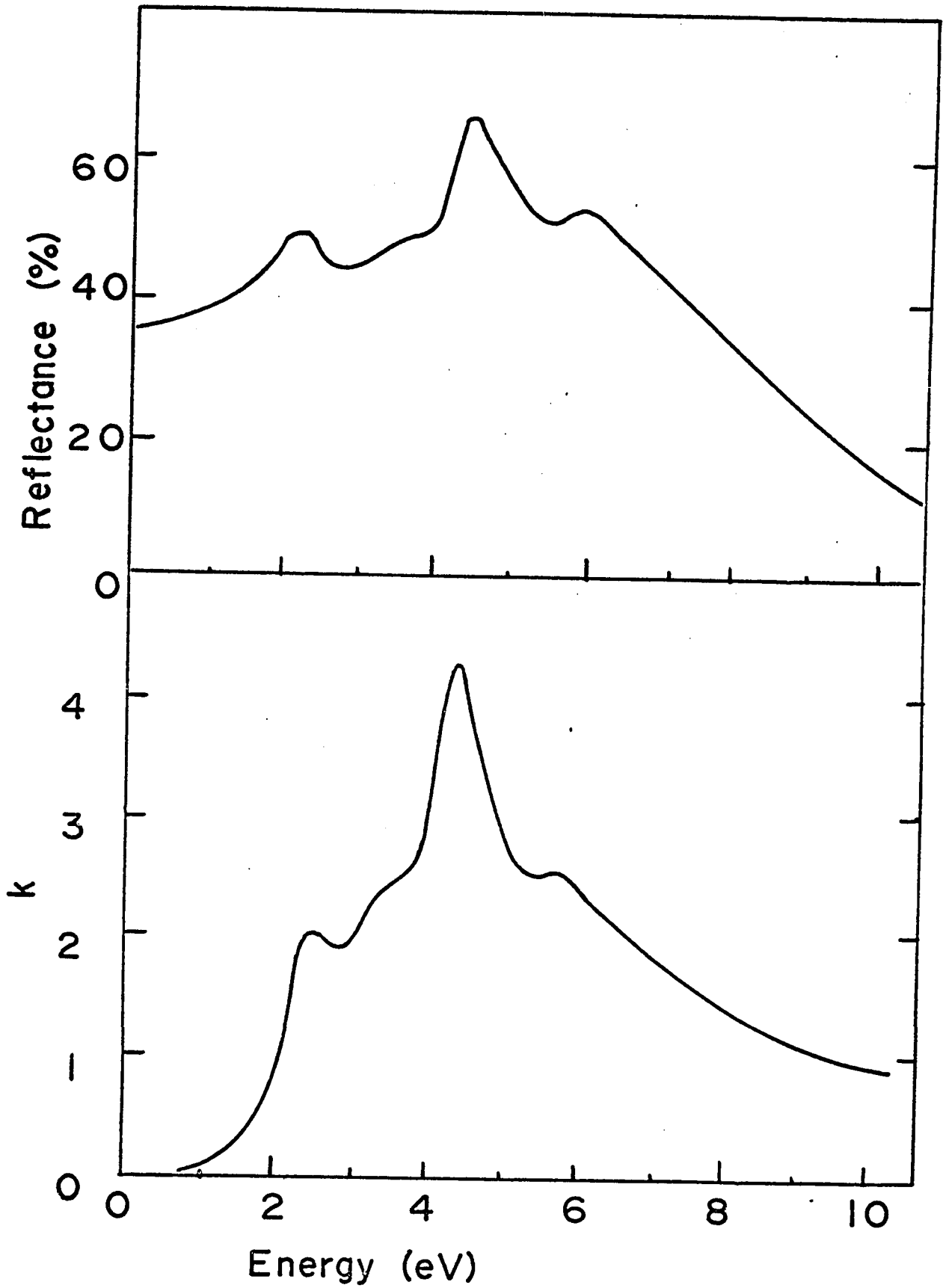

FIG 6 The Reflectance Spectrum for Ge, and the imaginary part of the Refractive Index derived from it (P 4)

The spectrum of Si (P 5) was found to be similar to that of Ge, but no splitting of the first reflectivity peak at 3.4eV was observed, discouraging an $L_{3'} - L_1$ assignment. The reflectance spectrum of gray Sn (C 2) shows the same characteristic structure as Ge. Measurements on the III - V compounds followed very shortly after, Tauc and Abraham giving the spectra of InSb, InAs, GaSb and GaAs (T 2), whilst Cardona measured GaSb (C 7), GaP and AlSb (C 8) and InP (C 5).

Work on the reflectance of semiconducting alloys started with the Ge - Si system (T 3), and showed that the 3.4eV transition in Si occured at a different place in $\underline{k}$-space from the 2.2eV doublet in Ge; it was postulated that the latter were $L_{3'} - L_1$ transitions (Later shown to be $\Lambda_3 - \Lambda_1$ transitions), but the single peak in Si was due to a $\Gamma_{25'} - \Gamma_{15}$ transition. Fig. 7 shows the various levels in Ge, Si and their alloys; the circled energies in the pure elements indicate levels which are fixed absolutely relative to $\Gamma_{25'}$, the top of the valence band, and which were obtained by combining direct and indirect absorption and photoemission data, as well as reflectance data (see P 36).

The reflectance spectra of the III - V alloy systems InSb - GaSb and InAs - GaAs were measured by

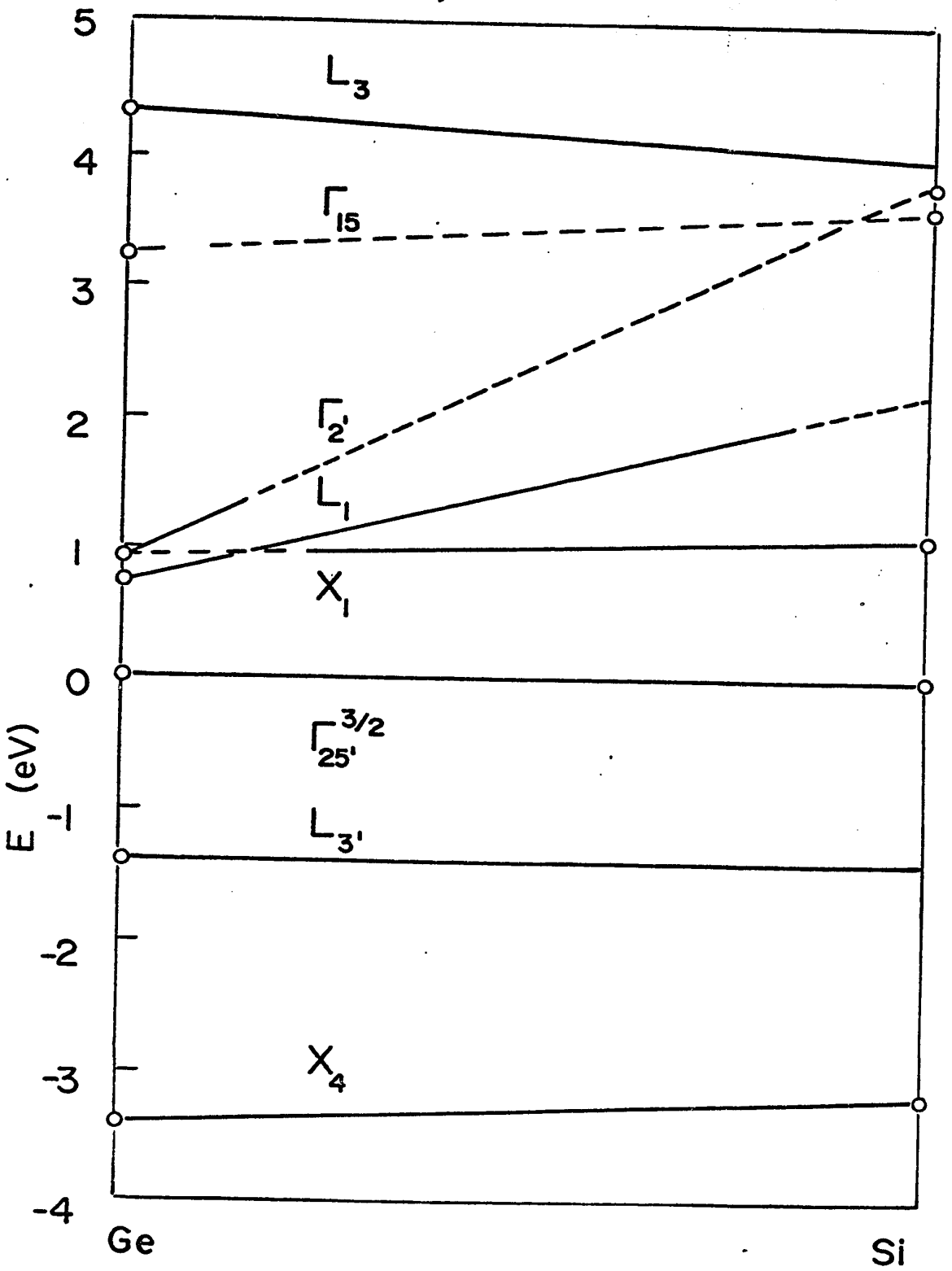

FIG 7 The Band Edge Energies for Ge-Si Alloys. (P 36) The solid lines indicate observed edge shifts and the dashed lines are interpolated. Circled energies in the elements indicate energy levels which are fixed relative to $\Gamma_{25'}$ (see text) .

Woolley and Blazey (B 49) between 1.5 and 5.5eV. They found a linear variation of all transitions with alloy composition within experimental error, as predicted by the virtual crystal model. No breaks were observed, as had been in the Ge - Si system, so the transitions invclved were the same for the two constituents of each system. This "following through" of properties in an alloy from one substance to another is an excellent example of the utility of alloy investigations

The reflectance spectrum of GaAs at 80°K is shown in Fig 8, reproduced from G 2. Additional structure sometimes appears when spectra are taken at low temperatures. The assignments of the various peaks at the time of commencement of the following work are given below, in order of ascending energy in eV.

1.4
1.75 } Fundamental direct gaps E_o and $E_o + \Delta_o$. (N.B. care must be taken when interpreting these since reflection from the specimen holder is possible, because the absorption is small below the edge)

$\Gamma_{15v} - \Gamma_{1c}$. Confirmed by absorption measurements (P 3, S 55).

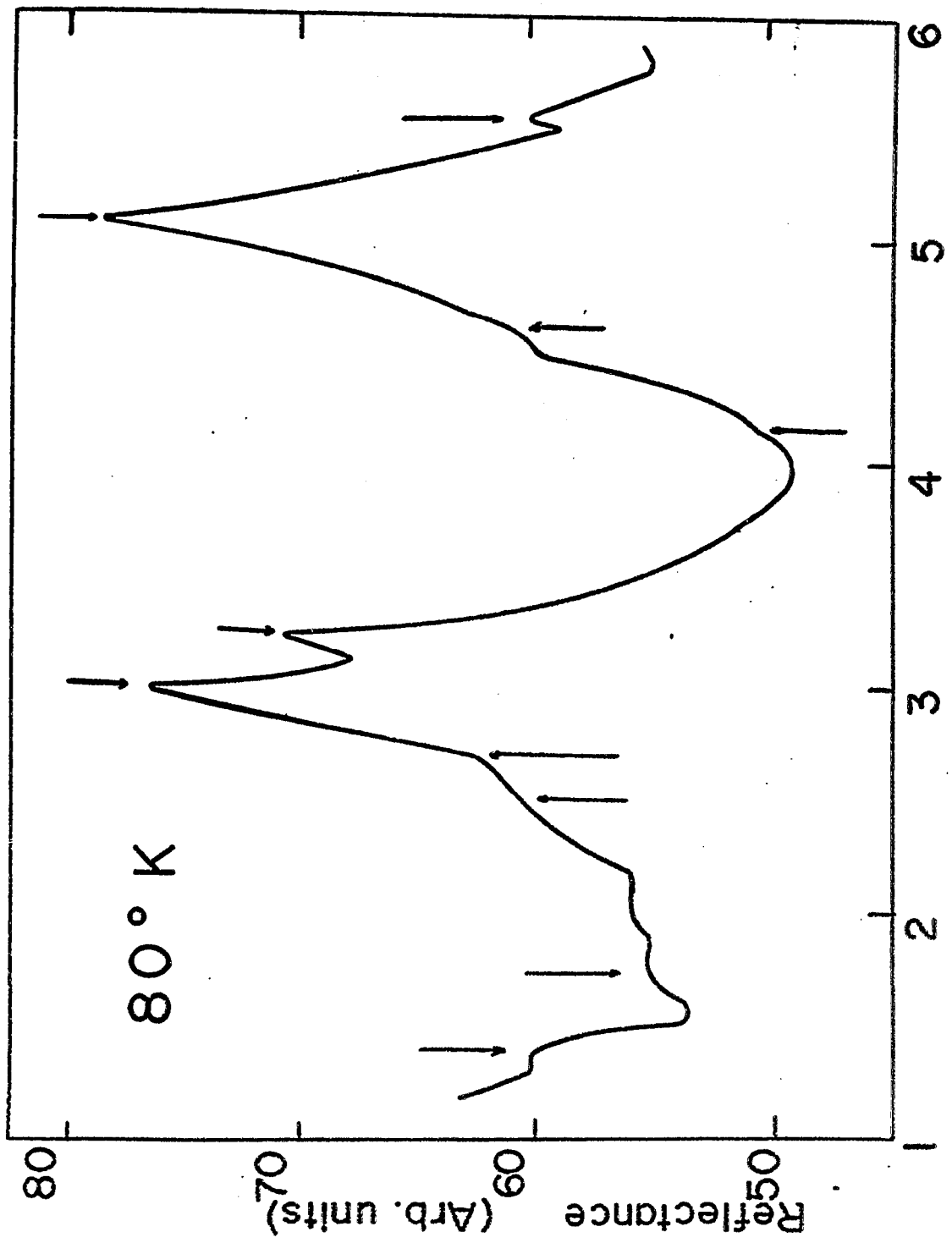

FIG 8 The Reflectance Spectrum of GaAs at 80° K (G 2). The transitions referred to in the text are indicated by arrows .

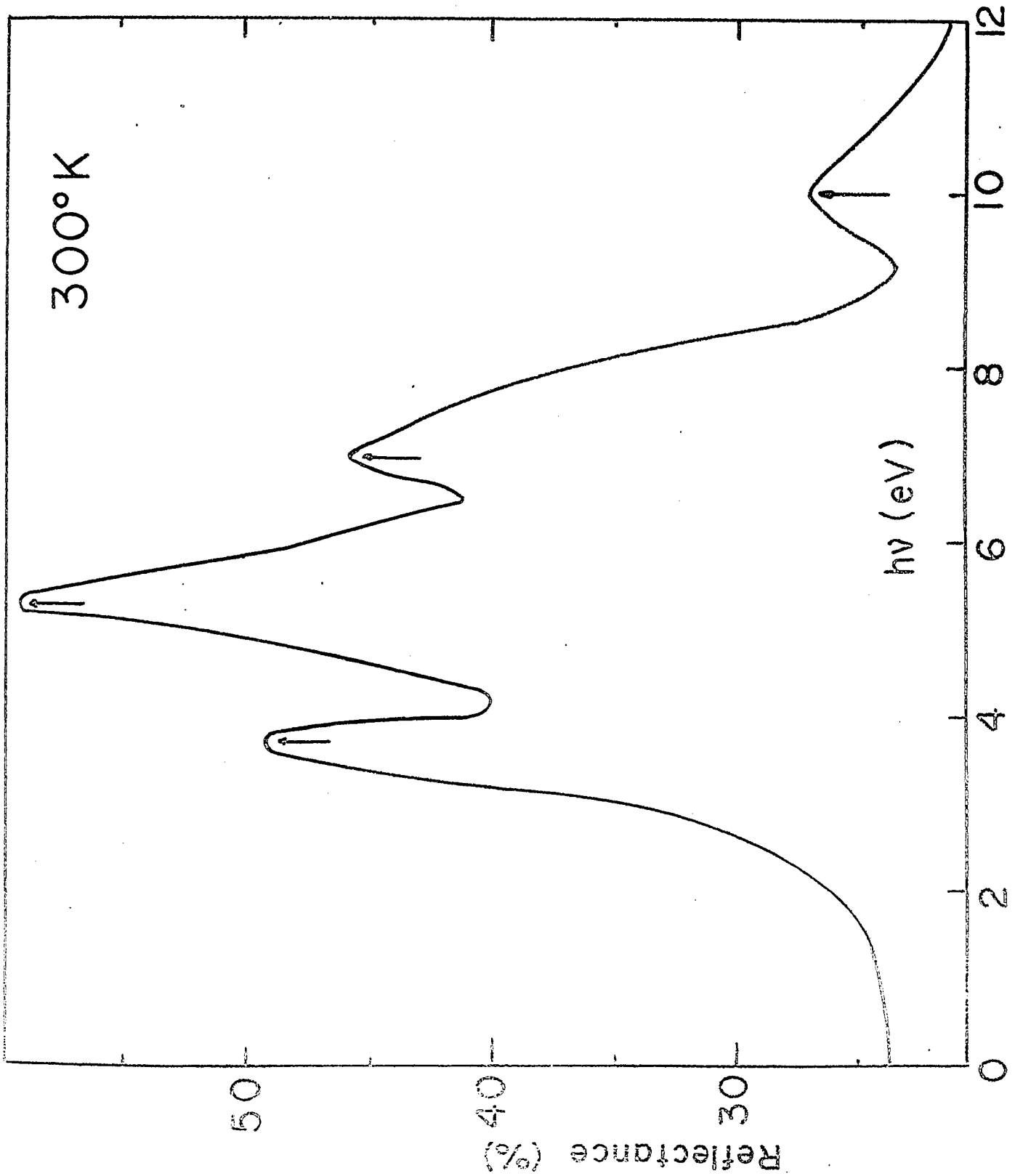

FIG 9 The Reflectance Spectrum of GaP at 300° K (E 2) .

2.3
2.6 } e_1 and $e_1 + \Delta_1$, $L_{3v} - L_{1c}$; small, occuring et edge.

2.99
3.23 } E_1 and $E_1 + \Delta_1$, $\Lambda_{3v} - \Lambda_{1c}$; strong transition since it occurs between saddle point edges.

4.2
4.52 } E_0' and $E_0' + \Delta_0$, $\Gamma_{15v} - \Gamma_{15c}$; small.

5.12
5.55 } E_2 and $E_2 + \Delta_2$, $X_{5v} - X_{1c}$ and X_{3c}

The E_1 and E_2 peaks were confirmed by other work (B 49, E 2, T 2), and the second of these also reported a higher transition -

6.6
6.9 } E_1' and $E_1' + \Delta_1$, $L_{3v} - L_{3c}$

The E_0' is at variance with Woolley and Blazey's work on InAs - GaAs alloys (B 49), where only the 4.5eV peak is observed in GaAs, going to 4.6eV in InAs, corresponding to the only peak observed by Greenaway in this region (G 2).

The e_1 doublet is also doubtful, as the structure is very small, and theoretical work puts the L edge values considerably closer to the E_1 doublet (see Section 3.6).

Δ_1 (0.24eV) is approximately 2/3 Δ_o (0.36eV) as expected, and Δ_2 (0.43eV) is in reasonable agreement with estimates by Paul (P 3) of 0.3eV.

The reflectance spectrum of GaP from E 2 is shown in Fig 9. The various peak energies are as follows (in eV).

3.7 ... Single peak with a temperature coefficient different from other E_1 peaks in III - V compounds, but the same as Si (C 8) Therefore presumably E_o', $\Gamma_{15v} - \Gamma_{15c}$

5.3 ... E_2, $X_{5v} - X_{1c}$, no splitting reported

6.9 ... E_1', $L_{3v} - L_{3c}$, no splitting reported.

With the above facts in mind, the reflectance spectra of GaAs, GaP and their alloys were measured as a function of alloy composition and temperature. The main point of interest was the correct interpretation of the 3.7eV peak in GaP, and the location of either the $L_{3v} - L_{1c}$ or $\Gamma_{15v} - \Gamma_{15c}$ transition in GaP, whichever one of these did not correspond to the 3.7eV peak. In addition this work formed part of a general investigation into alloys of the semiconducting III - V compounds.

3.4 APPARATUS

The reflectance of a material is the ratio of reflected to incident light intensities (= $\frac{I_r}{I_o}$). The problem of measuring it reduces to two separate measurements unless a standard is available. Whilst such standards are available in the infra-red (e.g. Al) none is in the visible and ultra violet, and the two measurements therefore have to be done separated by time. The first requisite then is a stable source of monochromatic light capable of covering the energy region of interest, and these are readily available. The next is a suitable detector, and for this energy range photomultipliers, run from a stable power supply, are a logical choice, having a high gain with low noise. The manner in which the measurement of the two quantities was to be undertaken was thoroughly investigated, three schemes being considered.

(i) See Fig 10 (a) For a particular wavelength, I_r is measured The specimen is then moved out of the way, and the detector moved around to measure I_o (more complex schemes have been devised which use essentially the same principle, see e.g. B 50, C 7). It was found with this method that the combined uncertainty in resetting the specimen and detector for each wave-

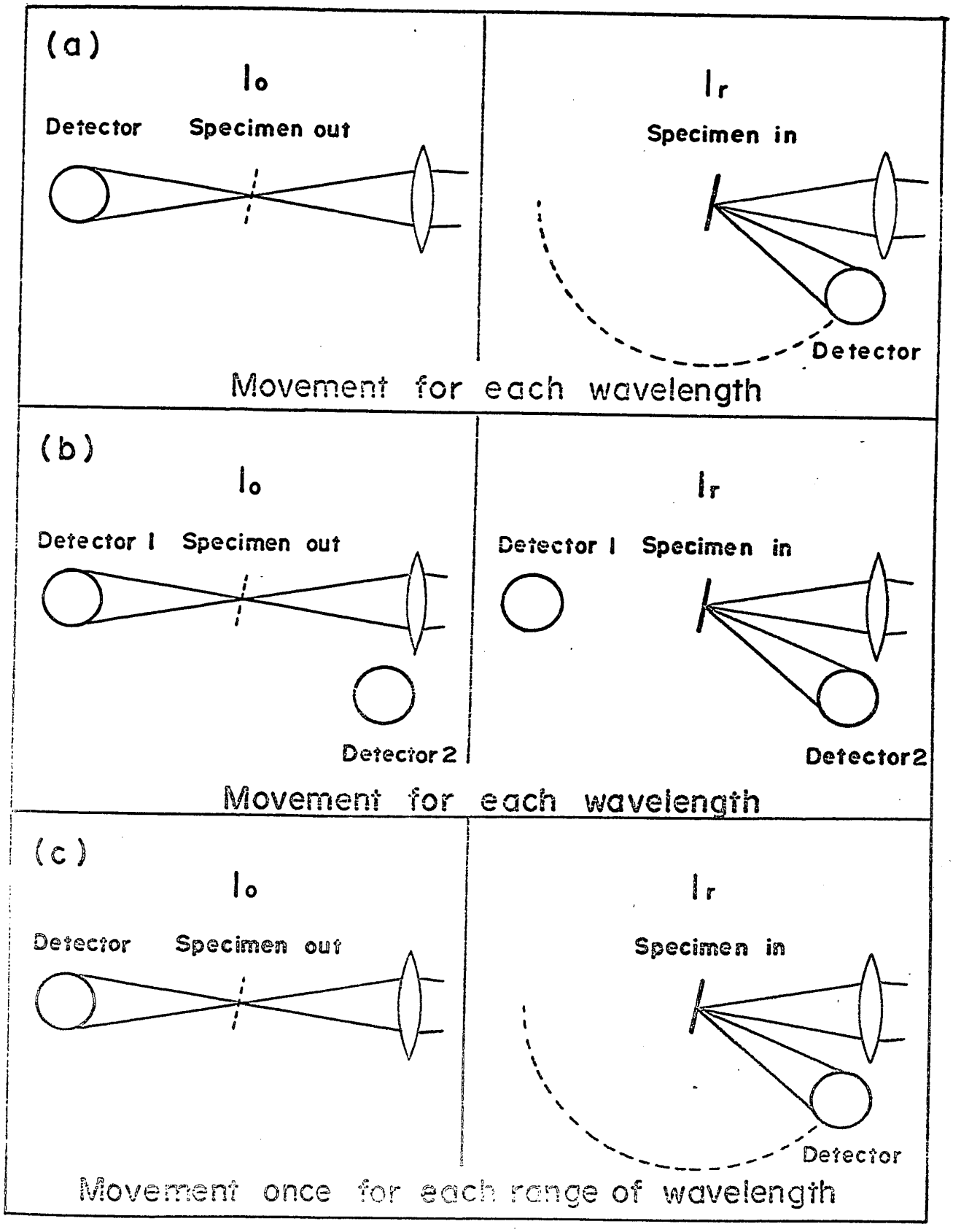

FIG 10 Experimental Layouts tried for Reflectance .

length was higher than could be tolerated, particularly for small specimens of the size to be used.

(ii) See Fig. 10 (b) Two detectors of the same type were used, so only the specimen had to be moved. Procuring a calibration curve between the detector responses proved difficult, and since it varied with time would have had to have been done after each short series of measurements.

(iii) See Fig 10 (c). One detector was used, but I_o was measured for the range of wavelength required. The specimen was then inserted into the beam, the detector moved, and I_r measured for the same range of wavelength. The stability of the lamp + detector + amplifier was found to be very good after a warm-up period of an hour for the instrument on trial (see next section). No resetting errors occurred for either the specimen or the detector as they were only moved once for any series of measurements.

The last method was adopted, and found to work satisfactorily. One drawback concerned the direction of the monochromator output beam which varied slightly in the ultra violet. Data taken several times for the same specimen showed that whilst the absolute value of reflectance varied, the position of the peak did not,

within the error of estimating it from a graph. The usual procedure was to take two runs, one in the visible for the E_1 and Ecp peaks (see section 3 6), and one in the ultra violet for the E_0' and E_2 peaks. This division corresponds to changing lamps (see below). The specimen and detector were realigned for each case at the wavelength at which the main peak occurred

The experimental layout is shown in Fig 11. The dark box was found to be necessary to reduce detector noise caused by room lighting etc , to an undetectable level with a 1 sec. time constant on the amplifier/indicator unit. The room was air conditioned, which further improved the stability of the apparatus.

Radiation from a low voltage tungsten lamp (1.0 to 4 5eV) or a stabilised deuterium lamp (3 5 to 6 0eV) was chopped on entering a Zeiss M40III prism monochromator at 120 c/s. The monochromatic output beam was focussed to an image approximately 1mm x 5mm by a quartz lens, and then either reflected from the specimen or allowed to continue straight through on to the RCA photomultiplier type 1P28 (see Fig. 11). The H.T. supply for the photomultiplier of approximately 800 volts was supplied by a Zeiss amplifier/indicator unit, and the 120 c/s output was amplified, converted

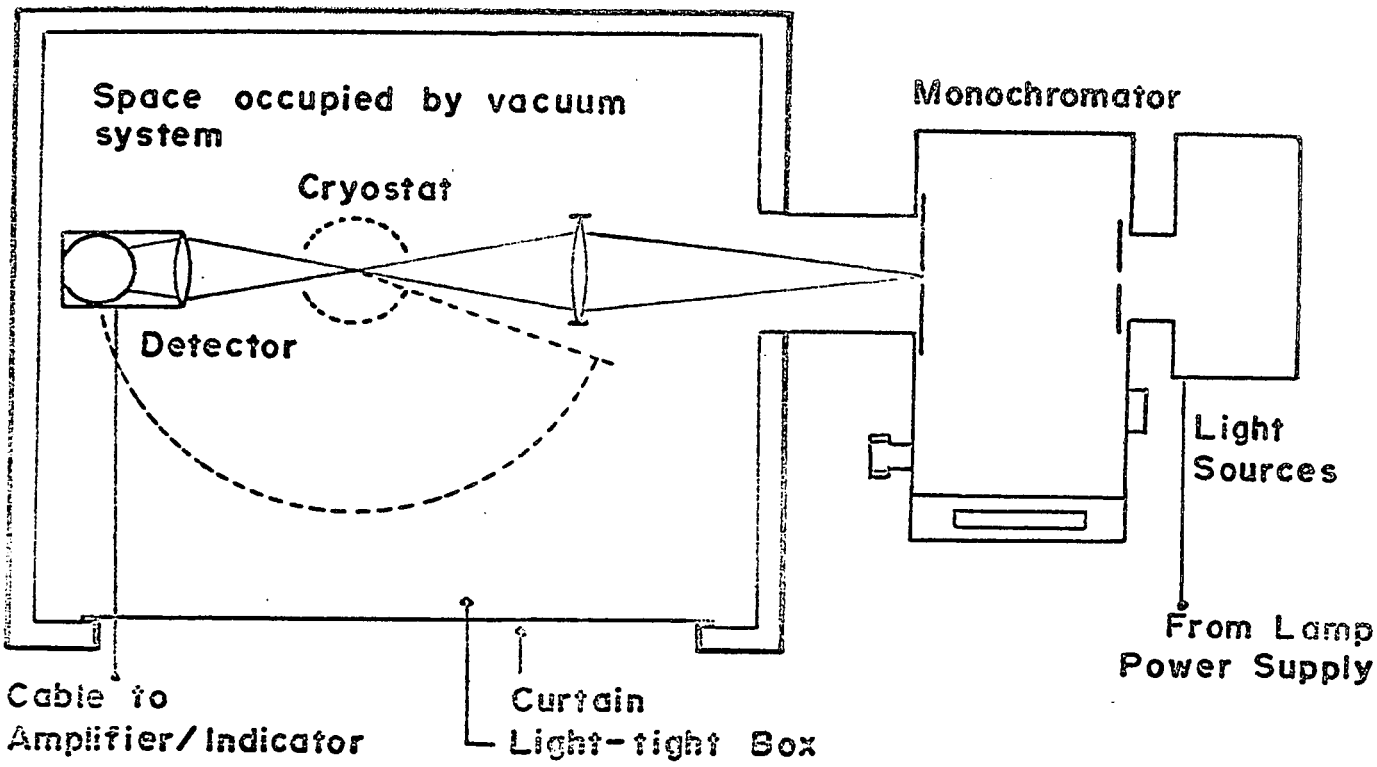

Fig. IIa) Apparatus Layout and Optical Path

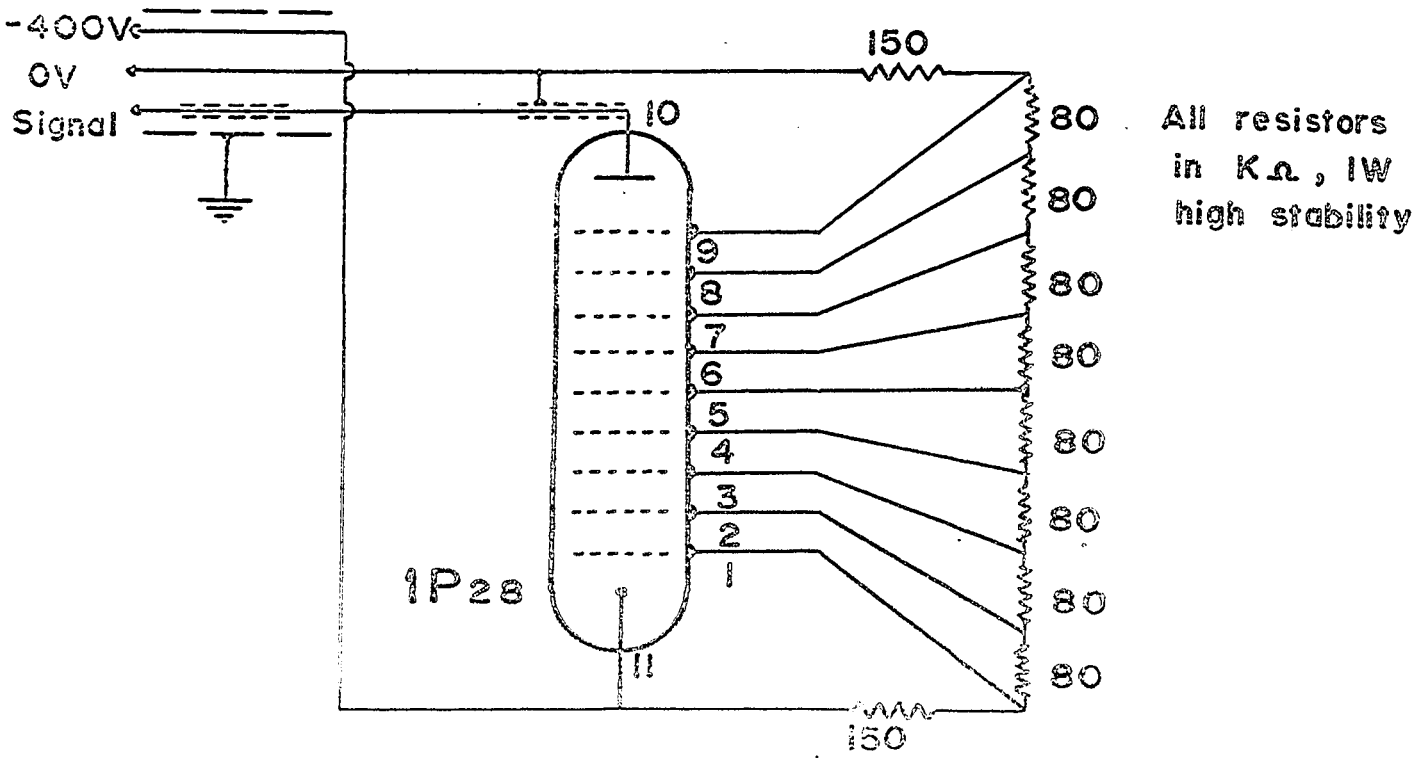

Fig. IIb) Detector Circuit

to d.c with a phase-sensitive detector, and displayed on the built-in galvonometer in the same instrument The galvonometer could be read to 0 05 to 0.2 on a scale of 110.0 units, depending on the noise level, which was in turn dependant on the wavelength in use, since the lamp intensity and detector response fell off in the far ultra-violet, necessitating a higher amplifier gain.

The cryostat shown in Fig. 12 was designed and built since low temperature spectra had been shown to yield extra structure when compared to room temperature spectra, and temperature coefficients were of interest It was initially intended to use both liquid nitrogen ($77^{o}K$) and liquid helium ($4^{o}K$) in the inner container, but the radiation heating proved to be too great for the size of holes that had to be used in the radiation shield (and hence the size of windows) for liquid helium. Before these holes were drilled, it held 1 litre of helium for 3 hours The associated vacuum system used a CVC 2" oil diffusion pump and a Balzers DUO 5 rotary back pump. A large cold trap just before the cryostat prevented oil entering the specimen chamber.

In use, the outer chamber was filled with liquid nitrogen when the vacuum fell below approximately 5×10^{-6} mm

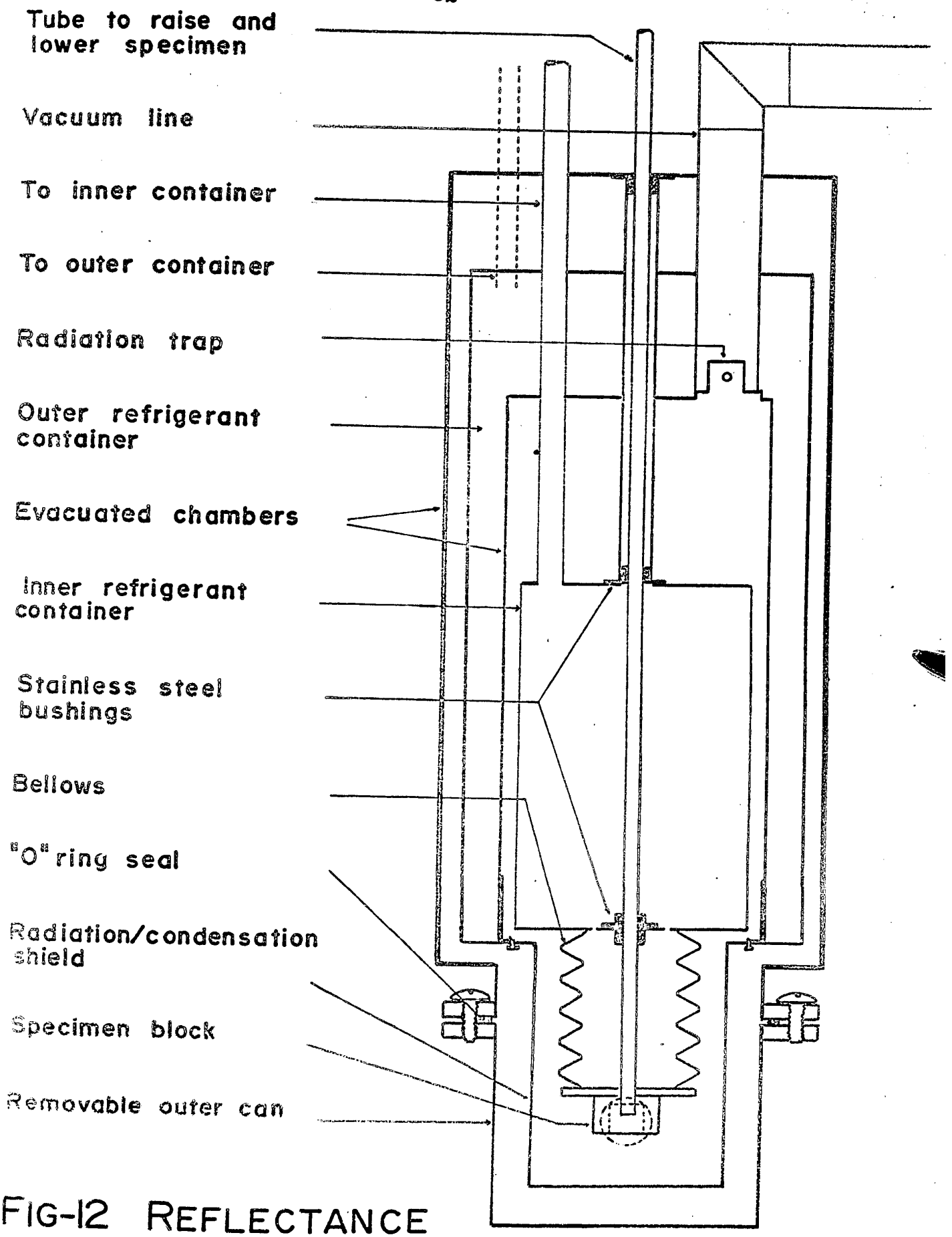

FIG-12 REFLECTANCE CRYOSTAT

Hg, which reduced the vacuum to the limit of the gauge, approximately 10^{-7}mm Hg After half-an-hour, any condensible matter in the cryostat should have condensed on the radiation shield or the walls of the outer liquid container, and the inner chamber was filled with liquid nitrogen. The fist I_o run was then commenced, so that by the time the I_r run was to be started the specimen had cooled to 2 to 4°C above liquid nitrogen (as measured by a differential thermocouple on the surfaces of several dummy specimens). The importance of keeping a clean surface on the specimen has been stressed by several authors (eg C 10, L 7), which was the reason for taking the above precautions.

The room temperature runs were taken immediately after etching (see next section) but without the radiation shield or outer can in place. As soon as this run was finished (1 to 2 hours), and if the specimen etch had proved satisfactory, the shield and can were replaced, and pumping started, 24 hours being needed to attain a sufficiently high vacuum for the low temperature run.

3.5 SPECIMENS

The GaAs specimens used were both polycrystalline and single crystal, whilst the GaP specimens were polycrystalline only. The alloy specimens were prepared by Dr. M. Rubenstein of Westinghouse Laboratories, using a sealed tube iodine transport method, which is fully described by him in R 8. They were more homogeneous than alloys of this system produced previously (K 4, P 52), and were polycrystalline, although some had large grains. They were received in either platelet or boule form, from which specimens of typically 4mm x 8mm elliptical, and 1/2 to 1mm thick could be obtained. The resulting slices were lapped on one side, and then lapped and mechanically polished on the other side, using carborundum paper followed by alumina powder down to 0.05μ grain size on cloth covered wheels.

Just before use, the specimens were etched for a few seconds, the best time and type of etch being judged from the reflectance spectra obtained. GaAs and the GaAs-rich alloys were etched in HNO_3 : HCl : CH_3COOH (1 : 7 : 8, "Wolsky" etch), whilst GaP and the GaP rich alloys were etched in HNO_3 : HCl (1 : 1). Specimens in the range x = 0.5 to = 0.8 inclusive (where x is the mol. fraction of GaP present) were etched with

either, and no detectable difference in peak positions or type of structure was observed Both etches were used at room temperature and were followed by washing in distilled water, acetone, and ethyl alcohol in that order The specimen was then mounted on the copper block in the cryostat with a thin smear of vacuum grease between the copper and the lapped side.

Measurements were taken as described in the previous section at room and liquid nitrogen temperatures At least two specimens at each composition were investigated, and the results are shown in the next section.

3 6 RESULTS AND DISCUSSION

The first specimens tried were Si, InSb, InAs and GaAs, at room temperature: the spectra obtained agreed well with those published in the literature, and so measurements were started on the GaAs - GaP alloys. The first few spectra taken were on epitaxial materials supplied by Dr F Williams of Monsanto Ltd., and Dr P.I. Pollak of Merck, Sharp and Dohme Labs. These specimens were etched in the same manner described in the previous section, except the polishing procedure was unnecessary This preliminary work served to show that the project was feasible and that the apparatus worked well The cryostat was designed and built, and the solid specimens obtained from Dr Rubenstein

Measurements were then made on these alloys at room and liquid nitrogen temperatures, as well as on the compounds GaAs and GaP Some typical spectra are shown in Fig 13, including the high energy data described in sections 3 7 and 3 8 Good agreement was obtained for GaAs and GaP with the literature (C 8, E 2, G 2, T 2, Z 2) except that a new transition was seen at 4 8eV in GaP. This peak was also seen by Williams (B 21, W 63) in his work on the same alloy system Whilst the

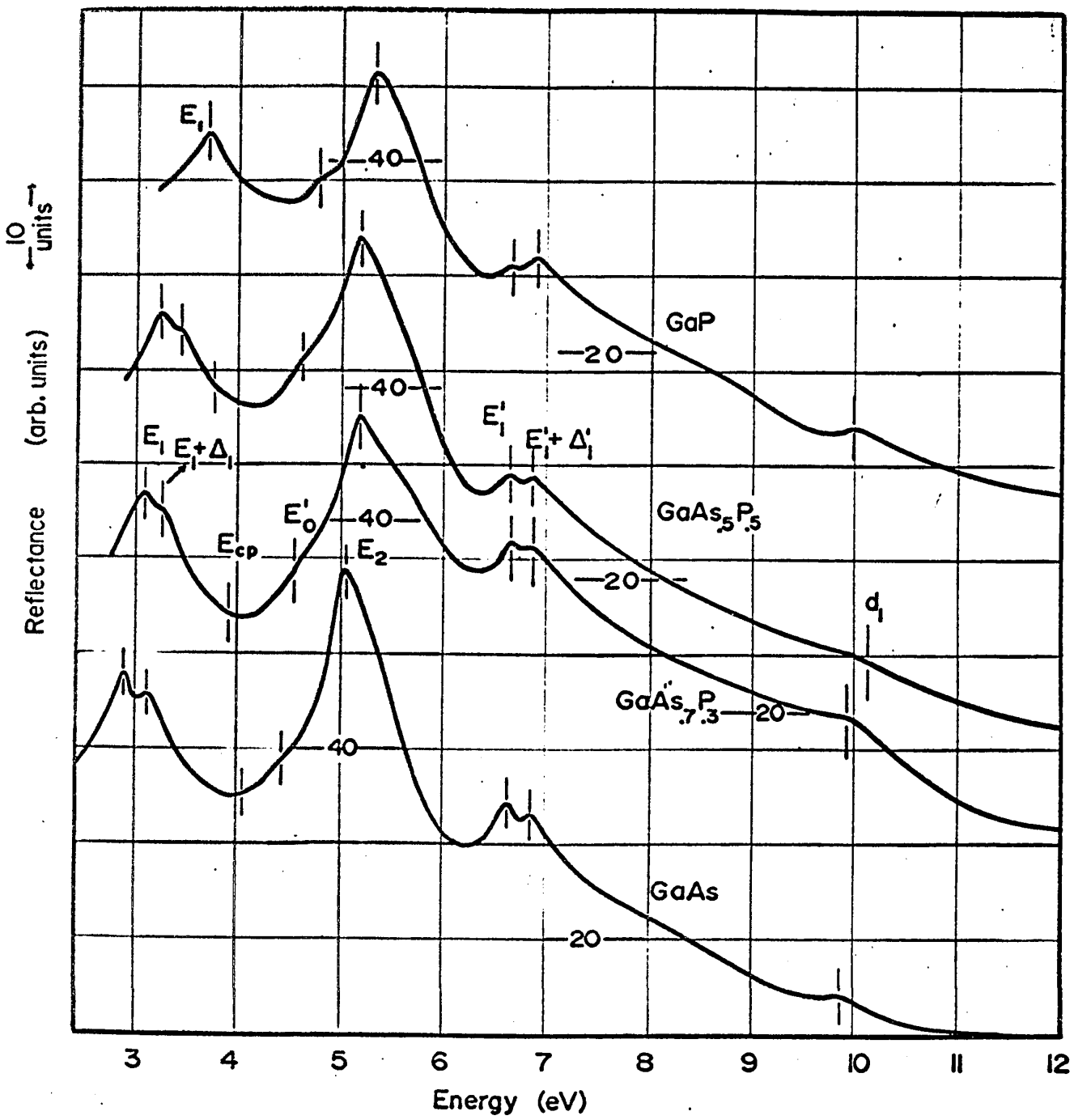

FIG 13 Some Typical Reflectance Spectra for GaAs, GaP, and the alloys, at Room Temperature (see text) .

peak positions and general form of the curves agree well with other work the value of the reflectance for a given energy varies quite widely from one author to another, due in part to instrument errors, but mainly to the different methods of surface preparation

The lowest energy peaks are shown in detail for the compounds and some of the alloys at room and low temperatures in Figs 14 and 15 It can be seen that the doublet in GaAs appears to narrow and the higher energy component decreases in intensity relative to the other component a combination of the two results in a single peak in GaP The splitting was not observed beyond x = 0 6 at 295°K or beyond x = 0 8 at 80°K, although the x = 0 7 peak at 295°K does have a very slight possible asymmetry (Reminder: x = mole fraction of GaP and alloy formula is Ga $(As_{1-x} P_x)$).

The next "peaks" were very slight departures from otherwise smooth curves and were not observed beyond x = 0 5 They were included in the results because their position was reproducible and they increased in energy with decreasing temperature like the other peaks The only other observation of this peak is by Greenaway (G 2) in GaAs at low temperatures

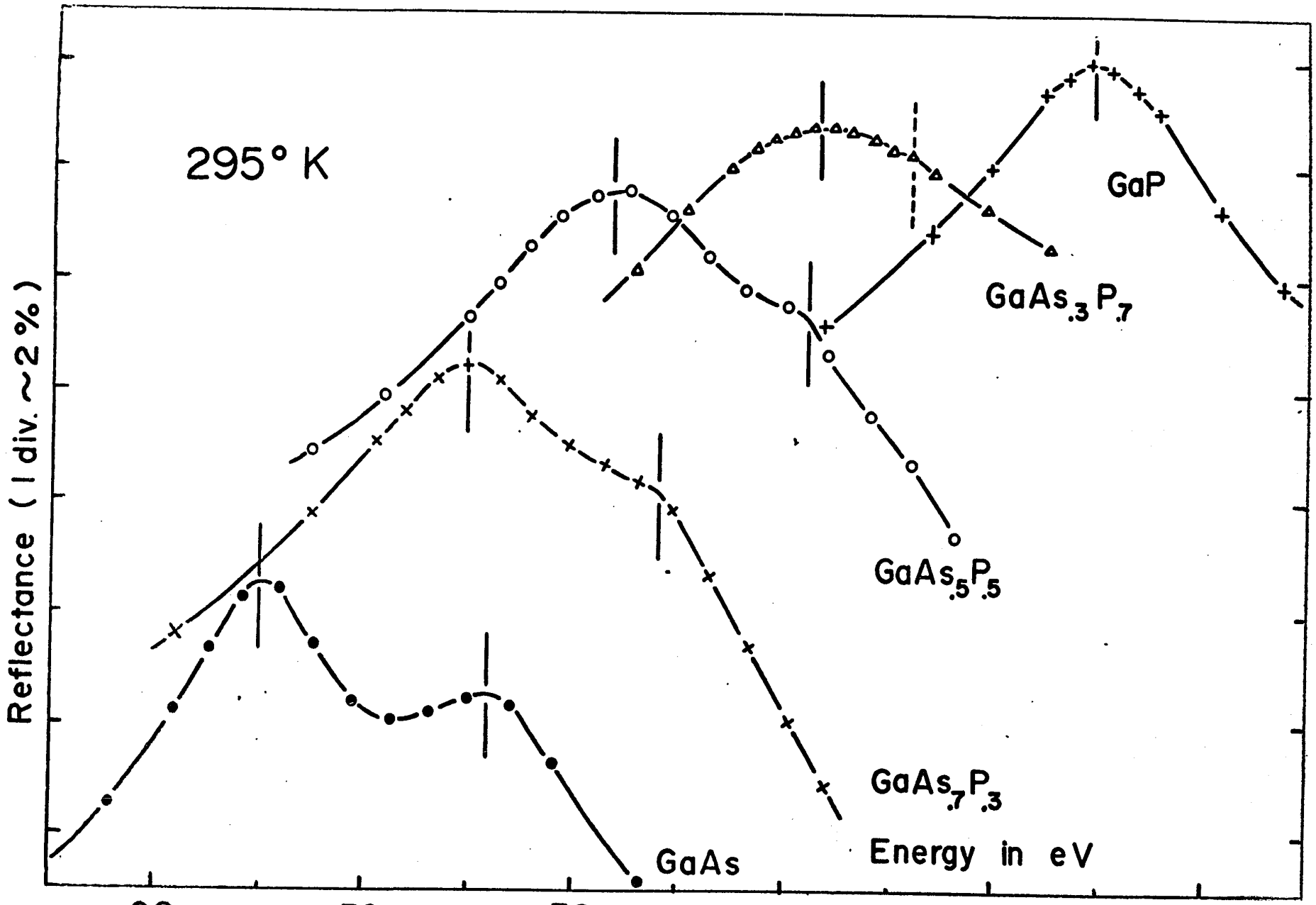

FIG 14 Detail of the E_1 peaks in $GaAs_{x-1}P_x$ at 295° K

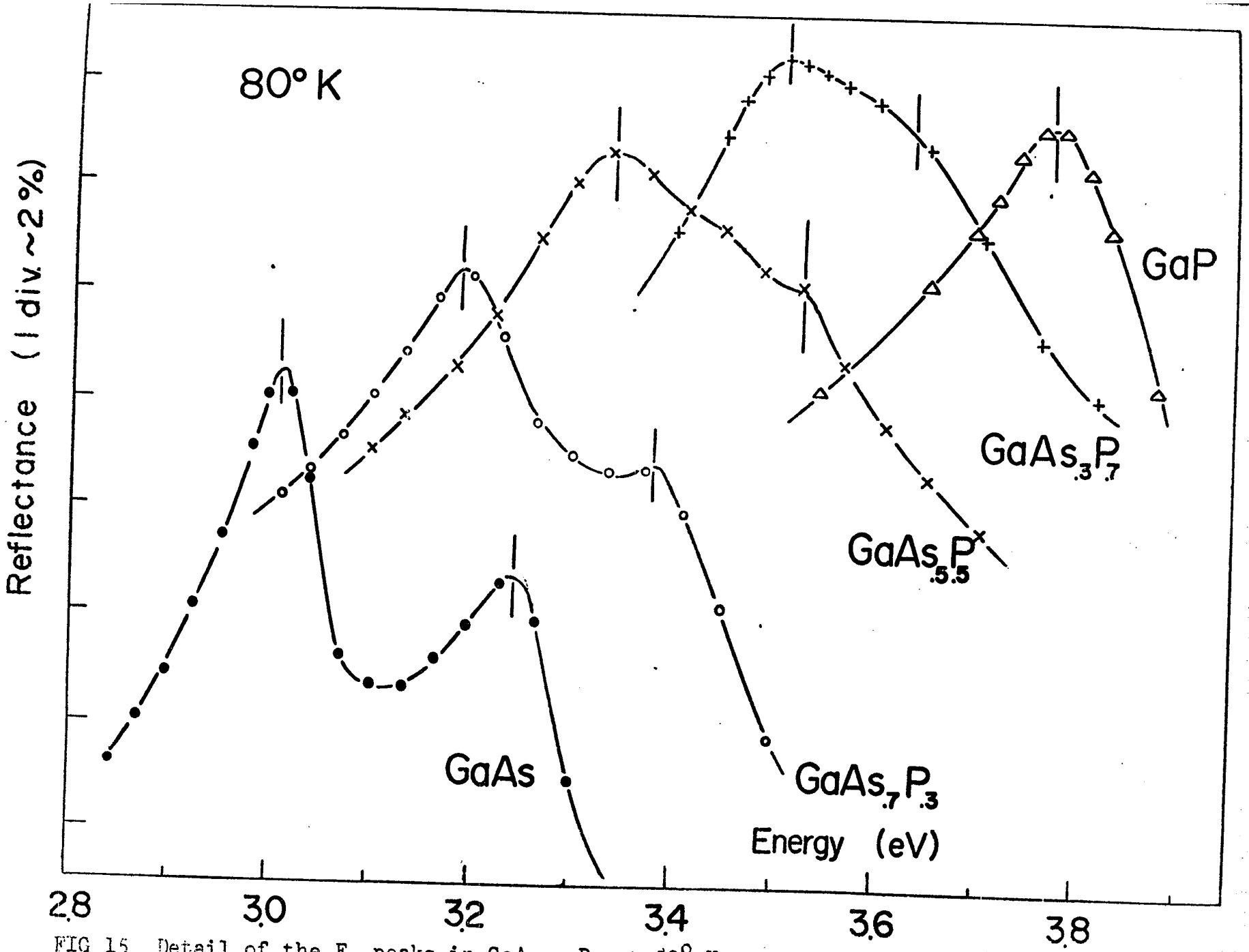

FIG 15 Detail of the E_1 peaks in $GaAs_{1-x}P_x$ at 80° K .

Just before the strong peak above 5eV, another departure from a smooth curve was noticed. This was stronger than the one mentioned in the previous paragraph, and takes the form shown in Fig. 16. Whilst this graph is for GaP, similar structure was also observed in GaAs and all the alloys. Unlike the preceding one, this transition increased in intensity with decreasing temperature (see Fig. 16). As mentioned earlier, this peak had not been seen previously in GaP, although it had in GaAs (G 2).

The large peak at 5.0eV in GaAs was also observed throughout the alloy range and in GaP (see Fig. 16), and formed the dominant feature of the spectra, as had been reported for the III - V compounds in general (C &, T 2).

The manner in which the energies of the above transitions vary with alloy compositions is shown in Figs. 17 and 18 for room and liquid nitrogen temperatures respectively, together with their transition assignments. The transitions marked by x instead of o are the results of measurements on the epitaxial specimens performed as part of the initial investigations. They are included for the sake of completeness, but were not included in the computer analysis of the results. This analysis took the form of curve-fitting to a straight

Fig 16 The Variation of Reflectance with Photon Energy for GaP showing the E_o' and E_2 peaks at 80°K and 295°K. The insets are the result of subtracting the E_o' structure from the smooth curve drawn.

Fig 16 The Variation of the Observed Transition Energies with Alloy Composition at 295°K for $GaAs_{1-x}P_x$

o - Vapour transport specimens.

x - Epitaxially grown specimens.

The lines shown are the computer fits to the averaged points shown, the epitaxial results not being included The reasons for assigning the transitions shown on the figure are given in the text (section 3 6).

Fig 18 The Variation of the Observed Transition Energies with Alloy Composition at 80°K for $GaAs_{1-x}P_x$ The points are the average of results for each value of x, the lines are computer fits to these points (see text, sections 3 5 and 3.6).

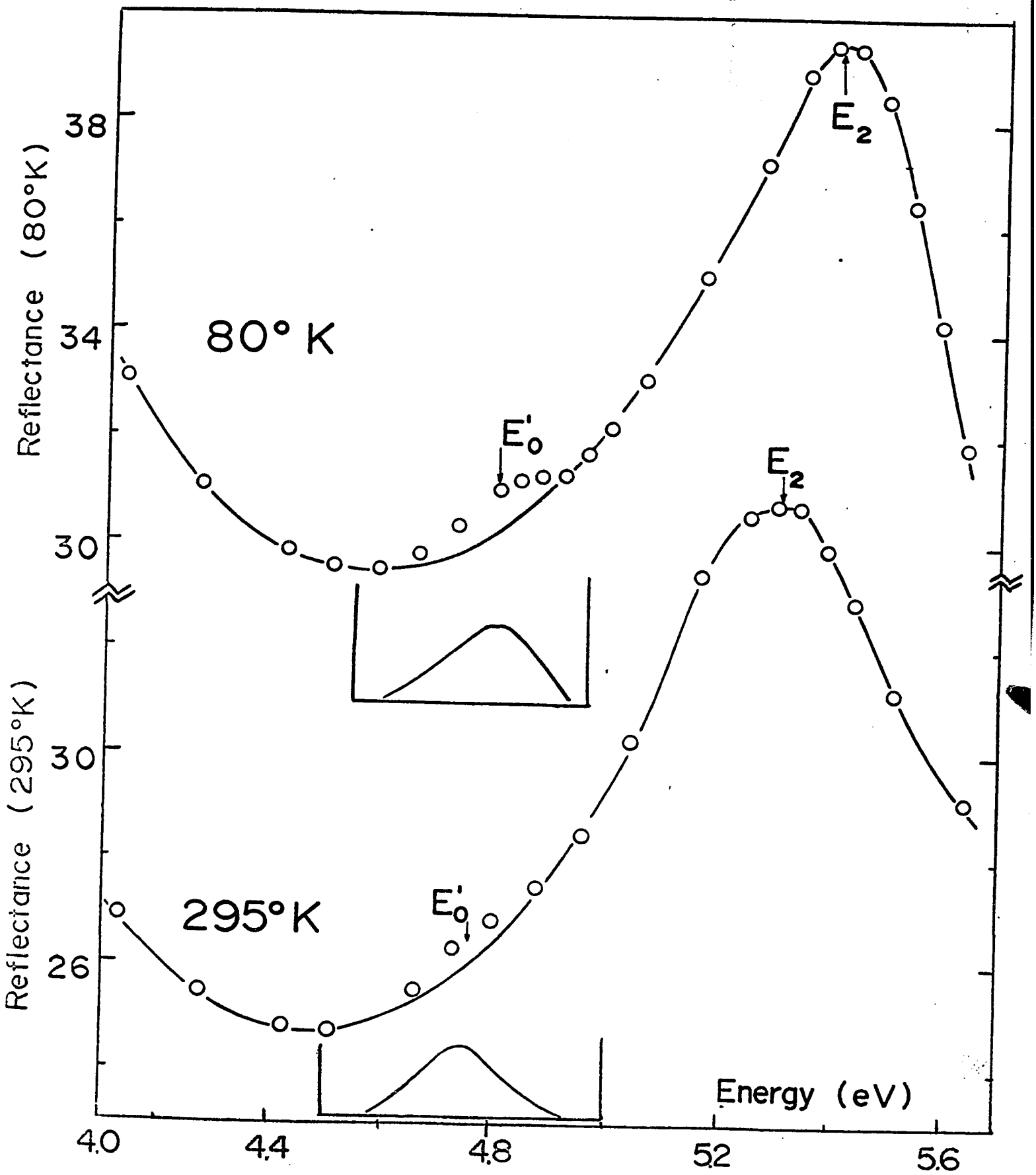
Reflectance (80°K)
38
34
30
80° K
E'0
E2
Reflectance (295°K)
30
26
295°K
E'0
E2
Energy (eV)
4.0
4.4
4.8
5.2
5.6

FIG 16

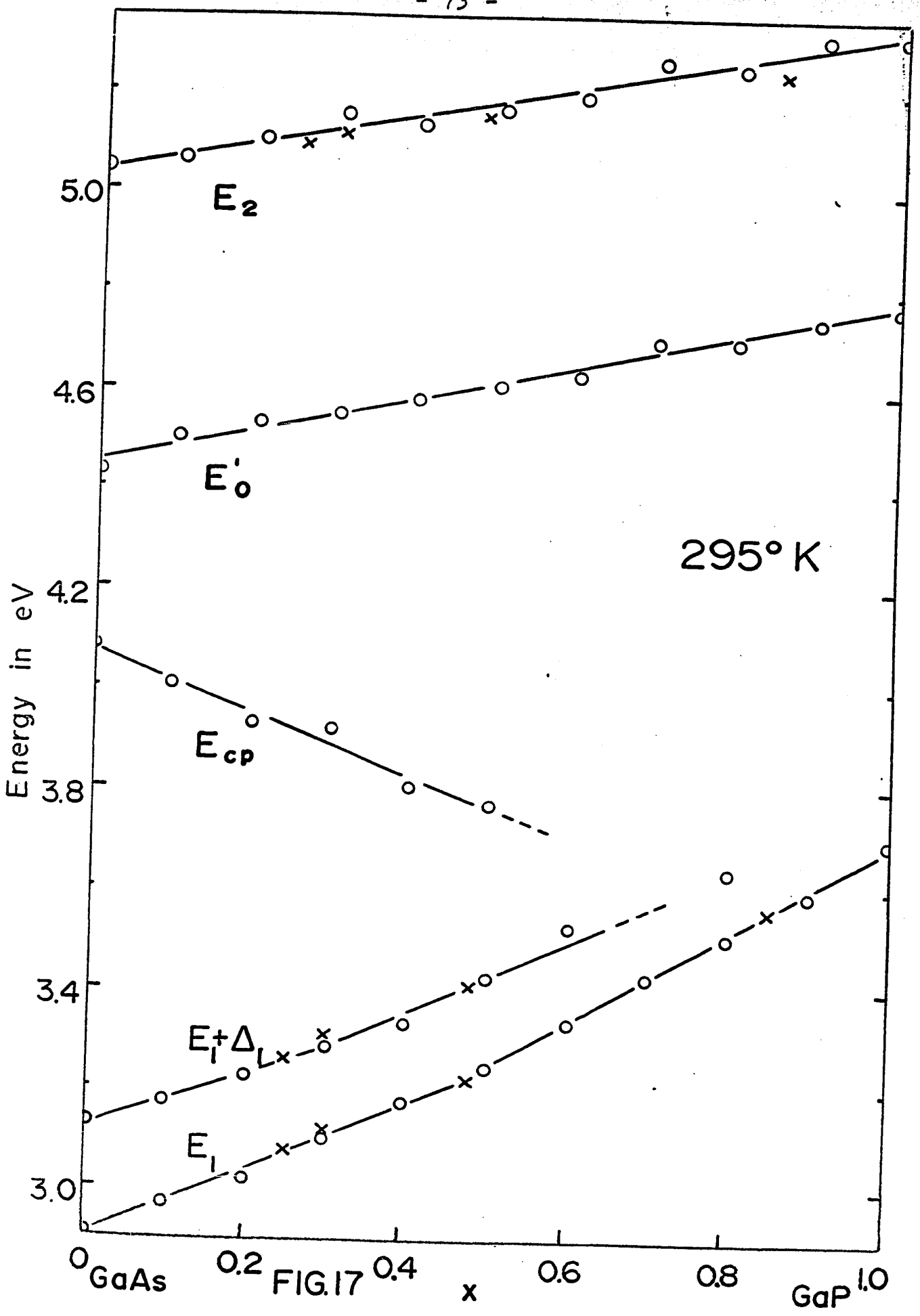
5.0
4.6
4.2
3.8
3.4
3.0
Energy in eV
E_2
E_0'
295° K
E_{cp}
$E_1+\Delta_{L_x}$
E_1
0 GaAs
0.2
0.4
0.6
0.8
1.0 GaP
x

FIG. 17

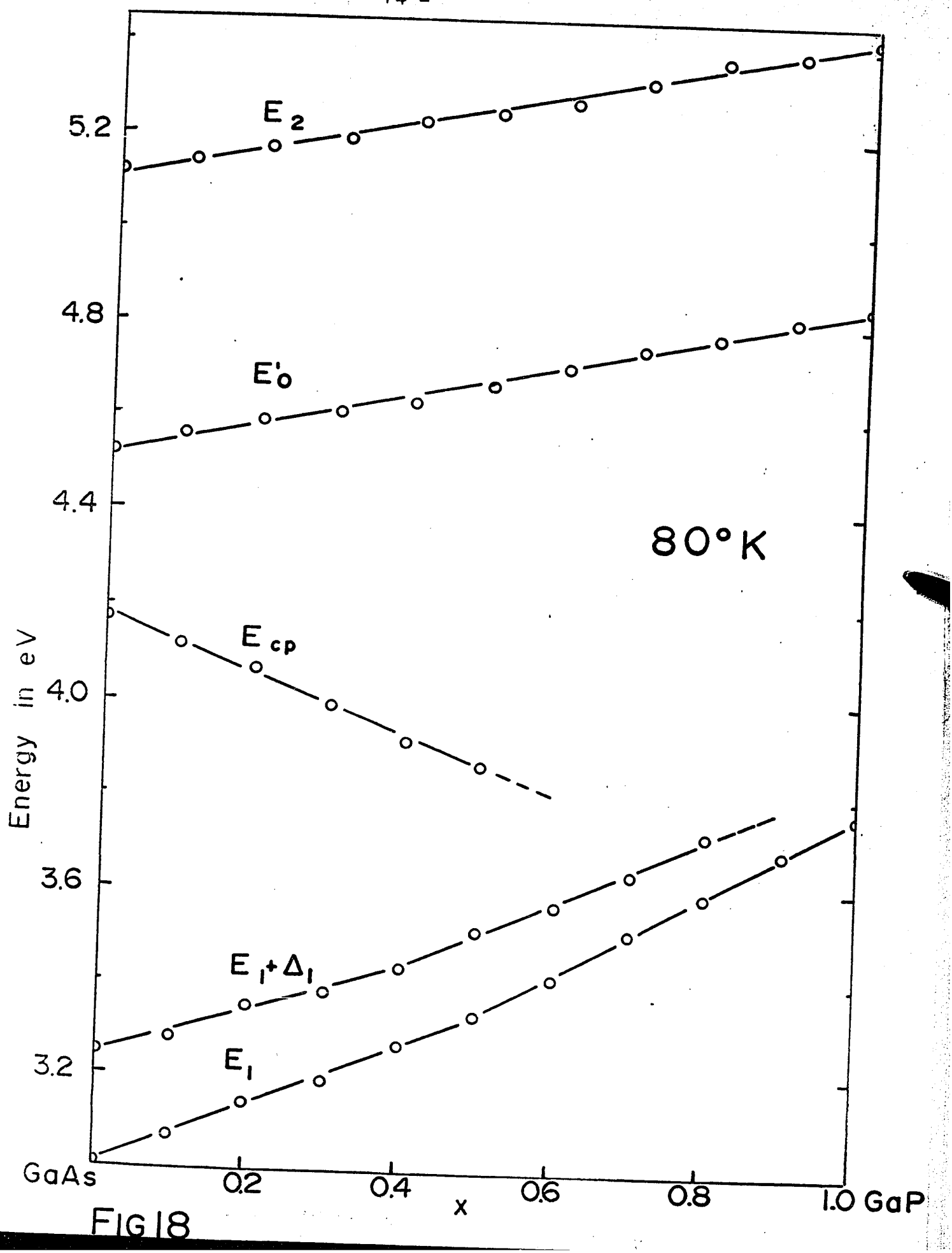
5.2
4.8
4.4
4.0
3.6
3.2
Energy in eV
E2
E'0
Ecp
E1+Δ1
E1
80°K
GaAs
0.2
0.4
0.6
0.8
1.0 GaP
x

FIG 18

line or parabola each of the transitions shown in Figs. 17 and 18 by using standard deviation techniques. The assignments of the various transitions will now be discussed.

E_1 and $E_1 + \Delta_1$:- The computer fitting favoured two linear parts with a break at x = 0.47 for T = 80°K and x = 0.45 for T = 295°K, rather than a parabolic variation over the entire alloy range, although the difference in standard deviations was difficult to judge as the straight lines each had fewer points than the parabolae. Each of the points shown in Figs. 17 and 18 for this transition is the mean of at least two separate measurements done on different specimens with slightly different surface treatments. Typical results varied over a range of approximately 0.04eV or less; when a larger variation was observed measurements were repeated on the same specimens after repolishing and re-etching. The break would seem to indicate that a different mechanism is responsible for the peak in GaP from that in GaAs. As was shown in section 3.3, the peak in GaAs is due to $\Delta_{3v} - \Delta_{1c}$ or E_1 transitions, and this is supported by the observed splitting Δ_1 being approximately 2/3 Δ_o, and the temperature coefficient data agrees with

other observations, (C 8, L 7). The peak in GaP was postulated as being either E_o' ($\Gamma_{15v} - \Gamma_{15c}$) or E_1 ($\Lambda_{3v} - \Lambda_{1c}$). However, the 4.8eV peak in GaP is assigned unequivocably to the former (see below) so that the latter must be the transition involved at 3.7eV in GaP (N.B. all others are accounted for by reflectance or absorption measurements). The observed break is postulated to be the result of the E_1 transition moving to a different place in $\underline{k}$ - space, but still in the [111] direction The continued observation of the splitting Δ_1 beyond the break, plus the fact that projection of the computer fits to GaP for both sets of straight lines gives values of 0.07 to 0.09eV, which is roughly 2/3 Δ_o, (see Table 2) both lend weight to this theory The smaller temperature coefficient in GaP (see table 4) suggests that this movement in Λ may be towards the Γ point

E_{cp} :- This peak decreases in energy with increasing GaP content, and its position in $\underline{k}$ space remains a mystery. Cohen and Phillips (C 2&) have suggested that a cluster of critical points occurs between 4 0 and 4 2eV in the region of $\underline{k}$ space around Γ, and it is possible that one or more of these could result in the structure observed. Further theoretical work on GaAs

and the alloys is necessary for a stronger identification. The fact that its temperature coefficient (see Table 4) is too high, and that it diverges from the next higher transition, both suggest the tentative assignment of E_o' placed on it by Greenaway is wrong. A linear projection to GaP leads to an energy approximately 0.2eV below the 3.7eV E_1 peak, so presumably in the range $0.5 < x < 1.0$ it is completely overshadowed by the strong E_1 and $E_1 + \Delta_1$ saddle point transitions.

$\underline{E_o'}$:- This transition varies linearly with alloy composition within experimental error, as is expected from the virtual crystal model. Its assignment was supported by photoemission experiments on GaAs (C 28) and GaP (F 19, F 20), and by theoretical calculations (B 21, C 37). Also, its temperature coefficient (Table 4) is close to that expected for E_o' transitions (C 8).

$\underline{E_2}$:- The transition energy of this peak also varies linearly within experimental error, a parabolic fit showing an insignificant improvement. The location of this peak as being a $X_{5v} - X_{1c}$ transition has been accepted for a long time, as it is a strong peak in all group IV and III - V materials. Recent theoretical work (C 33, P 36) has shown that it may be due to an $\Sigma_{5v} - \Sigma_{1c}$ (at $\underline{k} = \frac{2\pi}{a}(\frac{1}{4}, \frac{1}{4}, 0)$) transition, or possibly both,

TABLE 4 Transition Energies and Temperature Coefficients for GaAs and GaP from the low energy Reflectance data.

Peak	GaAs Transition Energy (eV) 295°K	GaAs Transition Energy (eV) 80°K	GaAs Temp. Coeff. $\times 10^{-4}$eV/°C.	GaP Transition Energy (eV) 295°K	GaP Transition Energy (eV) 80°K	GaP Temp. Coeff. $\times 10^{-4}$eV/°C	$\frac{dE}{dx}$ (295°K) eV/mole frac.
E_1 (GaAs rich)	2.90	3.01	-4.8 ±0.4	(3.56)	(3.65)	(-4.2)	0.66
E_1 (GaP rich)	(2.80)	(2.90)	(-4.8)	3.69	3.77	-3.5 ±0.4	0.89
$E_1 + \Delta_1$ (GaAs rich)	3.13	3.24	-5.4 ±0.4	(3.64)	(3.72)	(-3.5)	0.52
$E_1 + \Delta_1$ (GaP rich)	(3.09)	(3.17)	(-3.7)	(3.79)	(3.85)	(-2.9)	(0.70)
E_{cp}	4.07	4.18	-4.9 ±0.8	(3.46)	(3.55)	(-4.4)	-0.62
E_0'	4.45	4.52	-3.0 ±0.4	4.77	4.84	-3.2 ±0.4	0.32
E_2	5.04	5.11	-3.3± 0.6	5.32	5.42	-4.5 ±0.6	0.32

Table 4: The energies of transitions occuring in GaAs and GaP derived from computer fits, using linear relationships, on the reflectance data of the compounds and their alloys. Also given are the temperature coefficients calculated from the computer fits and assuming that all levels vary linearly with temperature in the range 80°K to 295°K, and the rate of change of energy as a function of composition at 295°K. The energies are reduced to 3 s.f., and the accuracy of dE/dx is given to a corresponding accuracy. Energies and temperature coefficients not directly observed are shown in parentheses.

bearing in mind the fact that the bands are approximately parallel going from X to Σ and Kane's suggestion (K 30) that large regions of $\underline{k}$ - space with approximately parallel bands may be necessary for a strong transition probability at saddle point edges.

Other reflectance work on GaAs - GaP performed concurrently with the above work was done by Subashiev et al (A 9, S 30) and Williams et al (C 37, W 43). The former observed the E_1 and E_2 peaks in three alloy specimens, but did not see the splitting of E_1 even at $x = 0.44$. The latter measured the E_1, E_0', and E_2 transition energies at room temperature on epitaxial specimens, observing the splitting of E_1 up to the break at $x = 0.5$. The results obtained by the above two groups agree within the combined experimental errors with the results shown in Fig. 17.

Mention should also be made here of Sobolev's group's results on GaP (S 21, S 23). They claimed a splitting of E_1 at 0.1ℰeV in the reflectance spectrum, but this is incompatible with the alloy work (T 16, W 42), detailed work on GaP itself (C 8, Z 2) including pressure measurements, and theoretical considerations (see also section 4.).

The transition energies and temperature coefficients for GaAs and GaP derived from the linear computer fits, are listed in Table 4. The difference in values resulting from fitting parabolic rather than linear relationships is quite small. Since the virtual crystal model predicts linear variations of energy for transitions between non-sensitive levels to a first approximation, the linear fits were preferred when the parabolic fit was only insignificantly better.

3.7 HIGH ENERGY APPARATUS.

It was decided to extend the above measurements above 6eV, which was the cut-off of the prism monochromator, other optics and photomultiplier, in order to attempt a Kramers-Krönig analysis of the alloy reflectance spectra. After obtaining the low energy measurements it was realised that the reflectances of the different alloys varied far too widely, even for the same composition, due to the differing surface qualities and treatments, for such an analysis to be meaningful. The positions of the peaks were given accurately from the reflectance spectra, any difference from the actual absorption edges being small (C 29) and either a constant or very slowly varying function of alloy composition. However, the high energy reflectance measurements were still made in order to look at the higher transitions, and to see if the general form of the curves varied smoothly from one compound to the other through the alloy range. The work described below was done in the Physics Department of Brown University (Providence, Rhode Island) at the invitation of Professor M. Cardona.

The spectrometer used was a McPherson vacuum

ultra-violet grating instrument in windowless operation, using a Tanaka air-cooled arc with hydrogen gas for measurements down to 1000Å, and neon and helium giving strong lines at 733Å and 581Å respectively (C 10). The reflectometer used was similar in principle to that described in section 3 4 (i), giving absolute measurements as long as the specimen size exceeded that of the beam falling on it (the grating focusses on the exit slit, so the exit beam diverges). The specimen could be raised out of the beam, and the sodium salicylate coated 1P28 photomultiplier detector could be rotated on an arm to measure I_r and I_o. Various filters were placed in front of the exit slit; these were sapphire (2000Å to 3500Å) and SnO_2 coated glass (3500Å to 5000Å) to cut out higher orders from the grating, and LiF (below 1000Å) to measure stray light. The detector was supplied by a stabilised power supply with 500 to 750 volts, and the signal current was detected by a Keithley model 150A electrometer.

Measurements were made of the two intensities at each wavelength, adjusting the photomultiplier H.T. to obtain a reading of 100 on the electrometer scale with the detector in the I_o position, so that the I_r reading equalled the reflectance R. The usual stray light

precautions were taken for the two He and Ne points below 1000Å. The spectrum of the lamp with hydrogen was continuous down to 1650Å, below which point peaks became apparent superimposed on a continuum. In this region (1650 - 1000Å), only wavelengths corresponding to peaks were used in order to cut down on stray light and because the band width was relatively large compared to the peak separations. A zero correction found from the white light maximum (straight through position = 0Å) was applied to all the wavelengths measured.

Specimen preparation followed that used for the low-energy measurements, using one specimen at each 0.1 mole fraction composition as well as the compounds. Due to the small size of some of these specimens, some very small reflectances were observed, being as much as 5 times smaller at the E_2 peak compared to the value measured with the low-energy apparatus for the same peak. Because such a procedure had to be used, besides the surface conditions mentioned earlier, a Kramers - Krönig analysis of the reflectance results was not attempted.

3 8 HIGH ENERGY RESULTS.

The results took similar forms to those shown in Fig 13, from approximately 4 5eV upwards The E_2 peak was measured in order to correlate the values of reflectance and to ensure that the etching was reasonable. A small doublet was observed between 6.5 and 7 OeV, but in some cases only a singlet could be resolved. Most spectra gave indications of an absorption edge around 10eV, being a slight departure from a smooth curve for most cases and a small peak in some specimens. The reflectance at 21eV was higher for all specimens than at 17eV, showing evidence of a peak above 17eV.

The inaccuracy due to returning both specimen and detector to the same positions at each wavelength was approximately a magnitude greater than for the low-energy apparatus, and so in some cases peaks were seen which might have been due to this uncertainty. Unfortunately, due to lack of time and a limited number of specimens, these measurements could not be repeated and checked Doubtful results have been indicated by + rather than o in Fig 19, which shows the variation of E_2 and E_1' with alloy composition A linear relationship was fitted to the three definite sets of points

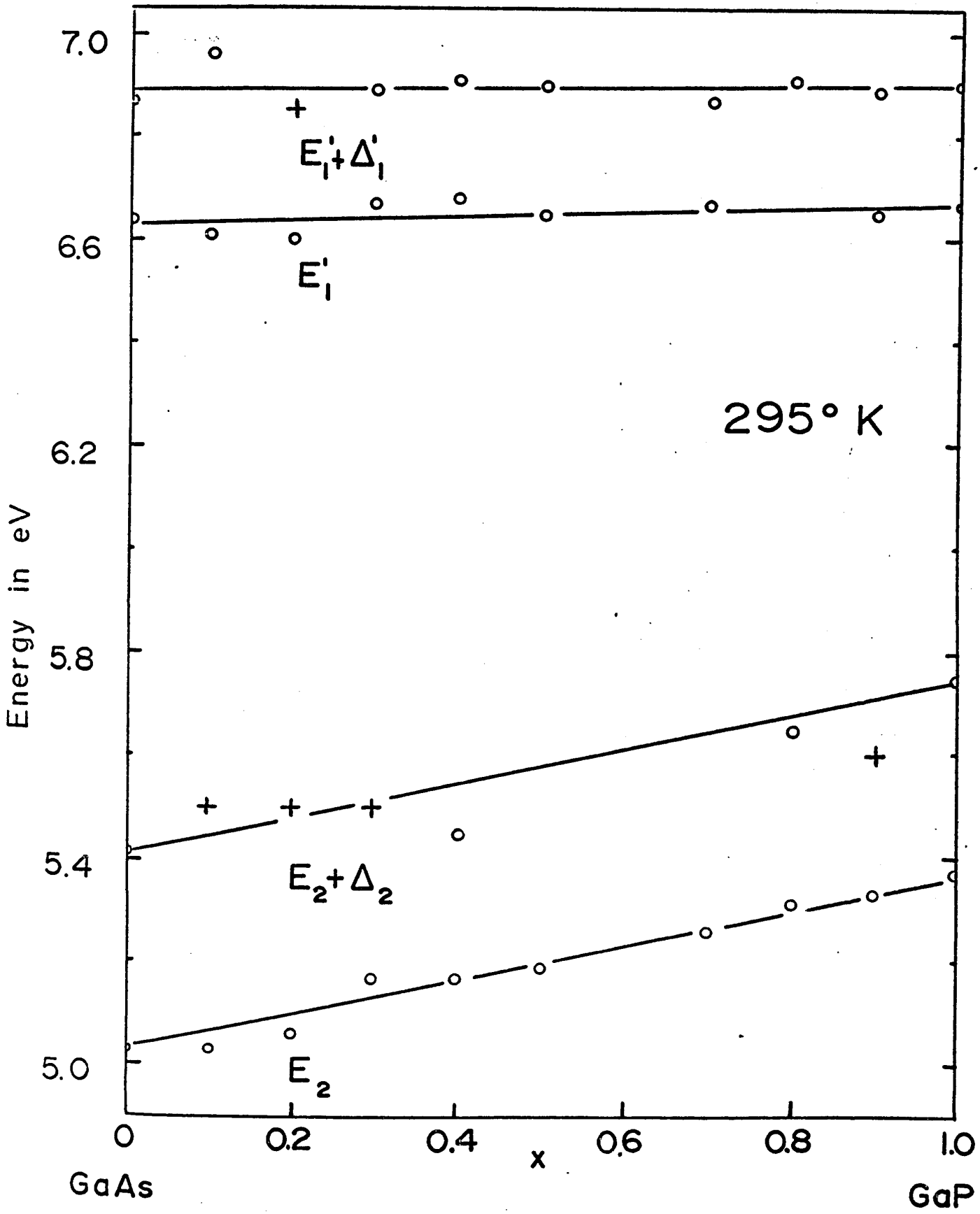

FIG 19 Variation of the High Energy Reflectance Peaks in $GaAs_{1-x}P_x$ with x .

in the same manner outlined in section 3.6, and the values of the transition energies for the compounds are given in Table 5.

E_2 and $E_2 + \Delta_2$:- The energies obtained agreed quite well with those obtained with the low energy apparatus, (compare Figs 17 and 19, Tables 4 and 5), although there was more scatter, as might be expected from the greater inaccuracy in determining R and the use of a single set of specimens The indications of $E_2 + \Delta_2$ were slight, but the values of Δ_2 in the compounds (GaAs = 0 38eV, GaP ~ 0.4eV) agree reasonably with Greenaway's reflectance value of 0.43eV for GaAs (G 2) and Zallen and Paul's estimate of 0.4eV for GaP (Z 2).

E_1' and $E_1' + \Delta_1'$:- This peak seems to be a doublet, as is expected, since theory places these transitions at the L edge in the [111] direction i e $L_3' - L_3$. The splitting Δ_1' should be approximately 2/3 Δ_o, which it is for GaAs, being 0.26eV (compared tc 0.23eV), but it is not for GaP, the value of 0 23eV disagreeing with 0.08eV (see Table 5). However, GaP has a low cationic number, and, like InP, may not necessarily obey the "2/3 rule", which is after all only an approximation (C 8, H 30, P 53). Ehrenreich and Philipp (E 2) observed a doublet for GaAs (6.6 and 6.9eV) but only

TABLE 5 Transitions Energies and Temperature Coefficients for GaAs and GaP from the low energy Reflectance data

Transition	Energy (eV)		$\frac{dE}{dx}$
	GaAs	GaP	eV/mole fraction
E_2	5 02	5 37	0.35
E_1°	6 63	6 67	0.04
$E_1^{\circ} + \Delta_1^{\circ}$	6 89	6 90	0.01

Table 5

The energies in eV of the E_2 and E_1° transitions at 295°K for the compounds, derived from computer fitted linear relationships to the high energy results shown in Fig 19

a singlet in GaP (at 6.9eV).

Now $\Delta_1^?$ should equal Δ_1 approximately, unless the E_1 transitions take place far from the L edge and the region of almost parallel valence and conduction bands. The above evidence seems to suggest that in GaAs the E_1 transitions take place at Λ near enough to L for $\Delta_1^? = \Delta_1$, but move toward Γ as x, the concentration of GaP in the alloys, increases. Thus Δ_1 decreases also, since it must vanish at Γ, but the experimental evidence shows that the splitting at the L edge remains approximately constant. However, other than a qualitative explanation could not be found with the above evidence. With this in mind electroreflectance experiments were done at Brown University concurrently with the high energy measurements in an attempt to shed further light on the E_1 transitions in particular. These are described in the next section.

d_1:- This small peak or departure from a smooth curve was seen for many of the specimens, but not all. Its position was constant at 10.0 ± 0.5eV, and is presumably due to $L_{3v} - L_1$ transitions (P 14).

d_2:- The rise in reflectance at 21eV compared to 17eV mentioned earlier does not warrant the accuracte location

of a peak; it does prove the existence of a peak in this region however. More detailed results on the compounds show a peak at approximately 19eV for the In compounds and 22eV for the Ga compounds. The alloy results agree with this inasmuch as they suggest a peak above 18eV. The dependance of the peak energy on the anion, plus the lack of such a peak in the group IV materials, strongly suggest that the d_2 peak is due to transitions from the d electrons of Ga (or In for the In compounds) to the lowest conduction band.

SECTION IV

THE ELECTROREFLECTANCE OF GaAs - GaP

4.1 THE THEORY OF ELECTROREFLECTANCE

The influence of an electric field on the optical absorption edge of a semiconductor was first studied by Franz (F 22) and Keldysh (K 31) independently. Their results were improved and extended to indirect transitions and energies higher than the fundamental edge by Callaway (C 46, C 47), Chester and Fritsche (C 27), Tharmalingam (T 15) and Yacoby (Y 3). The expression for the absorption coefficient in the presence of an electric field F, was given by Tharmalingam;

$$\alpha(\omega,F) = \theta_F^{1/2} \int_{\left(\frac{\omega_1 - \omega}{\theta_F}\right)}^{\infty} C \;\; Ai(t)^2 \, dt$$

where Ai (t) is the Airy function, $\theta_F^3 = \frac{e^2F^2}{2\mu\hbar}$, C includes n and ω, $\hbar\omega_1 = E_g$, the energy of the band gap, μ = the reduced mass of the electron-hole pair, e = the charge on an electron and $\hbar$ = Planck's constant.

Let $\frac{\omega - \omega_1}{\theta_F} = \beta$. Then for $\omega > \omega_1$, but near the edge,

$$\Delta\alpha(\omega, F) = \alpha(\omega, F) - \alpha(\omega, 0)$$

$$\approx C\theta_F^{1/2}\left[\int_0^\infty Ai(t)^2\,dt + \beta^{1/2}\right] \qquad \text{(xi)}$$

where $\int_\beta^\infty \left|Ai\ (t)\right|^2 dt = \left|\frac{d\ Ai\ (\beta)}{d\beta}\right|^2 - \beta\left|Ai^2\ (\beta)\right|$

Now $\Delta k = \left(\frac{\lambda}{4\pi}\right)\Delta\alpha$ (xii)

so Δk can be found from the calculated $\Delta\alpha$.

The refractive index n also varies since it is coupled to the absorption coefficient α by the Kramers - Krönig dispersion relation.

$$n(\omega, 0) - 1 = \frac{c}{\pi}\int_0^\infty \frac{\alpha(\omega_1', 0)}{\omega'^2 - \omega^2}\,d\omega' \qquad \text{(xiii)}$$

so $$\Delta n(\omega, F) = \frac{c}{\pi}\int_0^\infty \frac{\Delta\alpha(\omega_1', F)}{\omega'^2 - \omega^2}\,d\omega'$$

Thus Δn can be calculated from a knowledge of $\Delta\alpha$ as a function of frequency.

The quantity of interest here is the reflectance and its behaviour with n and k changing due to α being changed by the electric field.

$$R = \frac{(n-1)^2 + k^2}{(n+1)^2 + k^2}$$

By taking the total differential and dividing by R we obtain,

$$\frac{\Delta R}{R} = a(n, k, \omega)\,\Delta n + b(n, k, \omega)\,\Delta k \qquad \text{(xiv)}$$

Changing n and k to ϵ_1 and ϵ_2 by equation (vi)

$$\frac{\Delta R}{R} = \frac{4(\epsilon_1 - 1)}{(\epsilon_1 - 1)^2 + \epsilon_2^2}\,\Delta n + \frac{4\epsilon_2}{(\epsilon_1 - 1)^2 + \epsilon_2^2}\,\Delta k \qquad \text{(xv)}$$

which is more convenient for the purposes of calculation.

The integrals given above usually only have to be evaluated over a small energy interval, as other transitions occur too far away to have any real influence. Such calculations have yielded reasonable values of $\frac{\Delta R}{R}$, and have shown that the approximation of considering only energies around the edge is a reasonable one (S 28). It is necessary, however, to assume the coupling of n and k through equation (xiii) as the variation of k alone by equation (xii) gives values of $\frac{\Delta R}{R}$ two orders of magnitude too small.

The above calculations based on the work of Tharmalingam involve a number of approximations. Equation (xi) is derived from the weak-field expression for absorption, the effective mass approximation is used, the field is assumed parallel to a symmetry axis, and the results only apply to normal or parabolic

thresholds of the M_o type. Aspnes (A 20) has recently generalised the theory to apply to an arbitrary orientation of field in an anisotropic solid, and he derived the change in absorption coefficient $\Delta\alpha(\omega)$ for the saddle point edges M_1 and M_2, as well as for the M_o and M_3 edges.

Preliminary calculations by Callaway (C 47), extended by Seraphin and Bottka (S 28) showed that the absorption coefficient at E_g should have a tail below the edge, and oscillations above the edge, whose period depended on the electric field strength. Phillips duality theorem (P 33) showed that for a saddle point edge, the reverse of the situation for a parabolic edge should apply i.e. oscillations in α or ϵ_2 precede the edge (see Fig. 20a). The corresponding changes in ϵ_1 can be calculated using the Kramers - Krönig relations.

The identification of an edge from its electroreflectance response is complicated by the fact that although Δn and Δk may be calculated, and shown to be oscillatory with photon energy, the change in reflectance is a complex expression (equation (xiv)) involving the quantities a and b, themselves dependent on n, k, and ω. It has been shown (S 38) for the group IV

materials, that a predominates strongly at the fundamental gap E_o, is of the same order as b at E_1, and at higher energies is smaller than b. This variation is shown in Fig. 20(b) for GaAs, where the values of ϵ_1 and ϵ_2 were taken from the data of Philipp and Ehrenreich (P 2), and it was assumed that a liquid having n = 1.33 (water) covered the semiconductor face (see sections 4.3 and 4.4). It can be seen that the conclusions drawn by Seraphin for Ge and Si also apply to GaAs, and the other III - V's are expected to behave similarly.

Aspnes' results (A 20) agreed with those obtained by the workers mentioned above for a critical point of the M_o type. For the M_1 and M_2 saddle point transitions the electroabsorption spectrum (or variation of $\Delta\alpha$ with ω) depends on whether the field is more nearly parallel or transverse to the symmetry axis of the reduced mass of odd sign (following Brust's notation, B 12). For orientations more parallel, the change in absorption due to the application of a field is similar to that in a normal edge; if the field is more transverse the oscillations occur on the other side of the absorption edge. The M_3 edge was found to be similar to the M_o edge.

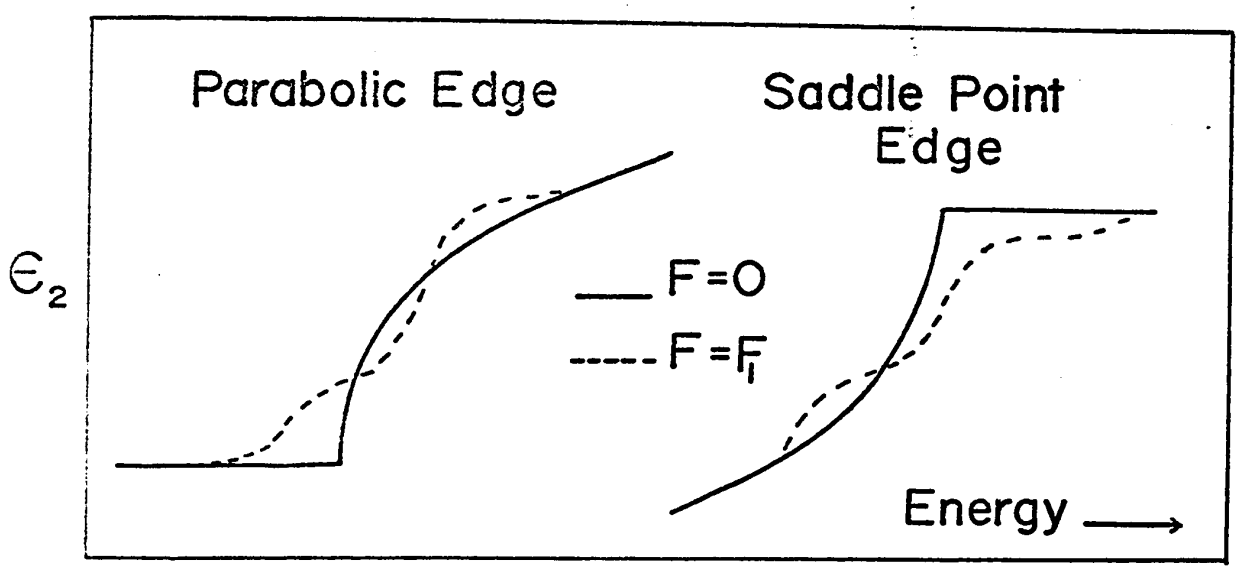

FIG 20 (a) The Effect of an Electric Field on Parabolic and Saddle Point Edges according to Phillip's Duality Theorem (P 33) .

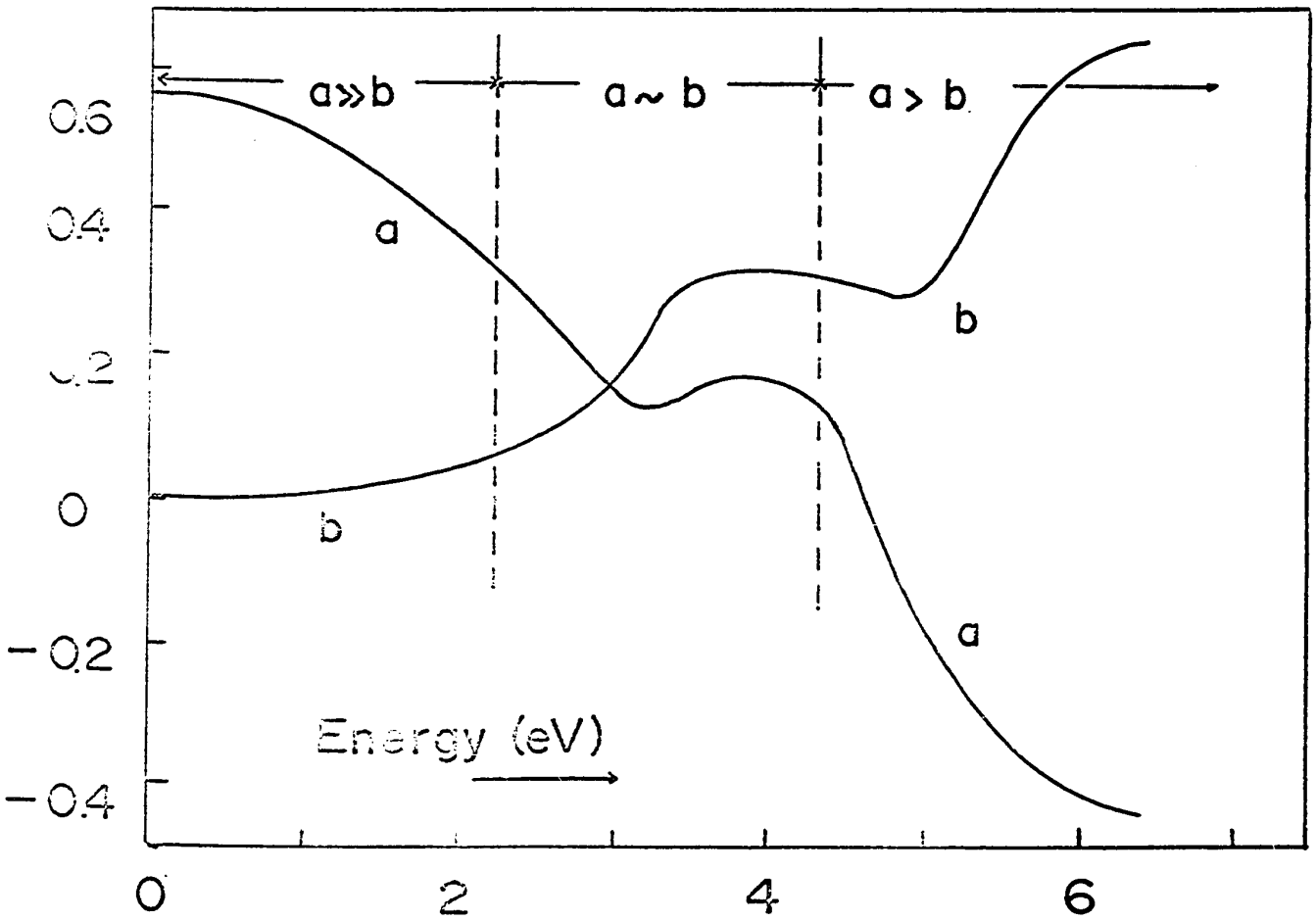

FIG 20 (b) Variation of **a** and **b** with Energy for GaAs (see text) .

Aspnes points out that since all the edges have different $\Delta\alpha(\omega)$ dependencies on field orientation and photon energy, it should be possible to identify the nature of any direct optical transitions by measuring the electro-absorption effect. For the reasons expounded earlier, transferring conclusions of the above nature to the electroreflectance effect is difficult. Firstly, n and k, or ϵ_1 and ϵ_2 have to be known accurately so that a and b can be found. Then Δn and Δ k have to be calculated from $\Delta\alpha$, with several integrations that have to be handled carefully. Only then can a comparison between theory and experiment be made.

4.2 COMPARISON OF NORMAL- AND ELECTRO-REFLECTANCE

As shown in the previous section, the electro-reflectance spectrum should, after a careful analysis, be capable of indicating the type of critical points involved in a transition. However, it is interesting to note that a knowledge of the optical constants is required, and this can only be found with any degree of precision from reflectance measurements. The derivation of these constants from band structure calculations is not yet very accurate (see P 36).

The structure expected in an electroreflectance spectrum should be of an oscillatory nature, which involves sharp changes of the derivative type in the quantity to be measured, $\frac{\Delta R}{R}$. This fact should enable much more precise location of E_g and higher edges, being especially useful where two transitions are located close to one another, such as when a spin-orbit split level is involved. No comparison methods are necessary for electroreflectance since the two quantities ΔR and R may be measured simultaneously by modulating the electric field and hence ΔR (see section 4.4). Measuring such a ratio means that the incident beam can overlap the specimen, or the detector need only look at part of the reflected beam, without the results being

seriously affected. This is in direct contrast to reflectance measurements where the measurements have to be done separately and no light losses can be tolerated Since ΔR is modulated, sensitive a.c. techniques can be used for detection, and the output $\frac{\Delta R}{R}$ can be directly presented without the need for computation.

The disadvantages of electroreflectance are therefore in the complexity of the apparatus, but the availability of commercial devices allays this problem to a large degree Also, it is necessary to maintain a high field at the surface of the specimen; the ways of satisfying this last requirement, some of which are rather ingenious, will be dealt with in the next sub-section.

4.3 PREVIOUS WORK AND TECHNIQUES

There have been numerous observations of the exponential tail on the fundamental absorption edge of a semiconductor predicted by Franz and Keldysh. The results for Si (K 32, V 4) GaAs (M 1), CdS (W 61) and others (W 62), were usually interpreted in terms of a shift of the fundamental edge. Since these materials already have an exponential edge, the transition from a sharp, direct, interband absorption edge to the exponential edge predicted by theory was not explicitly demonstrated. The first use of a.c. techniques by Frova and Handler (F 21) and by Seraphin (S 19) in electroabsorption and electroreflectance respectively, showed more structure than had been predicted by Franz and Keldysh in their original theory.

Frova's group found the variation of the absorption coefficient at the direct edge in Ge p - n junctions, which were reverse biased in order to produce electric fields of the order of 10^4 to 10^5 V/cm. Since the absorption tail from the direct edge obscured the indirect transition edge at high fields, lower fields had to be used to investigate the latter. This work was extended (F 11, F 14, F 16) and also applied to Si (F 16), and much detail, including the various phonon energies associated with indirect transitions was investigated. This group also obtained

good agreement with theoretical calculations (F 16, H 25) as to the shape and position of the structure resulting from the Franz - Keldysh effect in electroabsorption.

In order to attain the high electric field needed at the surfaces of a semiconductor for electroreflectance, Seraphin made use of the field-effect configuration (S 18). In this, the specimen is used as one of the plates of a condenser, the other being a transparent conductor. Seraphin used SnO_2 on a quartz plate (Nesa glass), separated from the polished and etched semiconductor surface by a thin dielectric film (Mylar or Saranwrap). The d.c. bias voltage and a.c. modulating voltage are then applied across the "plates" in order to modulate the surface field. The whole system is bonded together with suitable optical cements and oils to avoid internal reflections, interference effects, and the mechanical vibrations produced by the high alternating fields. For this type of construction the semiconductor surface must be very accurately plane. Such an assembly effectively prevents the changes induced by the electric field on the optical constants from being calculated. There is also a high energy cut-off at about 4.5eV due to the dielectric and conducting film absorption edges. In later papers Seraphin and co-workers measured the electroreflec-

tance of Ge (S 18, S 19, S 28, S 31), Si (S 29, S 38) and GaAs (S 37, S 46), at energies around and higher than the fundamental edge (see also S 48).

Cardona's group also reported electroreflectance measurements, but their technique of obtaining the high internal fields at the semiconductor surface differs from Seraphin's. The specimen is immersed in an electrolyte and biassed in the blocking direction, causing most of the voltage to be dropped in the space-charge layer in the semiconductor surface (W 61). With this method, fields typically of the order of 10^5 V/cm. are produced with a bias of 1V for a wide range of materials and carrier concentrations (C 49, T 12). Advantages of this method over Seraphin's include a higher photon-energy cut-off (~7eV for water) and lack of mechanical vibration troubles, since the capacitor is formed only by the semiconductor/liquid interface; also, the evaluation of optical constants is facilitated by the lack of reflecting surfaces other than that of the specimen itself. In addition, whilst this surface should be "clean" in an atomic sense, this can be achieved with irregularly shaped surfaces without affecting the field or results. Disadvantages include the difficulty of estimating the field and measuring dependences of various effects on the field in other than a qualitative sense, a

temperature limitation (although ethanol with a few drops of H_2SO_4 is capable of cooling to 180°K), and a low energy limit of about 1eV due to electrolyte absorption. This group has worked on the group IV, III - V and II - V materials, including Ge, Si (C 49), Gray Sn (C 50), InP, InSb, GaAs, GaSb (C 49, S 34, S 39), GaP (C 49, S 39), AlSb (C 49, S 34). They have also worked on the GaAs - GaP alloys (this thesis, T 12) and the Ge - Si alloys (C 48).

Other techniques reported up to the present time have used stress as the modulating agency in piezo-absorption (A 13, C 34, G 10, W 45, Y 1) and piezo-reflectance (A 19, E 7, E 8), temperature as the modulating agency in optical absorption (B 52) and current in reflectance (B 55). Use has also been made of the high resolution inherent in the above techniques in such measurements as the variation of the energy gaps with stress (P 43), hydrostatic pressure (P 55) and magnetic field (A 19). The results are, of course, of great interest to those involved in semi-empirical band calculations (C 33, C 35, P 42, P 53).

4.4 APPARATUS.

The apparatus described below is that set up by the author at the University of Ottawa Physics Department The GaAs - GaP electroreflectance spectra was taken at Brown University Physics Department, at the invitation of Professor M. Cardona. Since the apparatus set up at Ottawa is similar to that used at Brown, and because the writer is more familar with the former, it is described. Essential differences between the two will be detailed after the main description.

The experimental layout is shown in Fig 21. Since the signal-to-noise ratic of photomultipliers is proportional to the square root of the light intensity, a strong source and efficient monochromator were required. Also, the d.c. level involved is large, so the dark current is usually negligible Hence a Bausch and Lomb 50cm grating monochromator was used, with a Hanovia 600W Xenon d c. arc for the entire energy range. A 500W quartz iodine incandescent lamp, Sylvania type DWY, running from a d c. supply, was also found to be suitable between 1.5 and 4eV. The detectors used were an EMI 6255S photomultiplier between

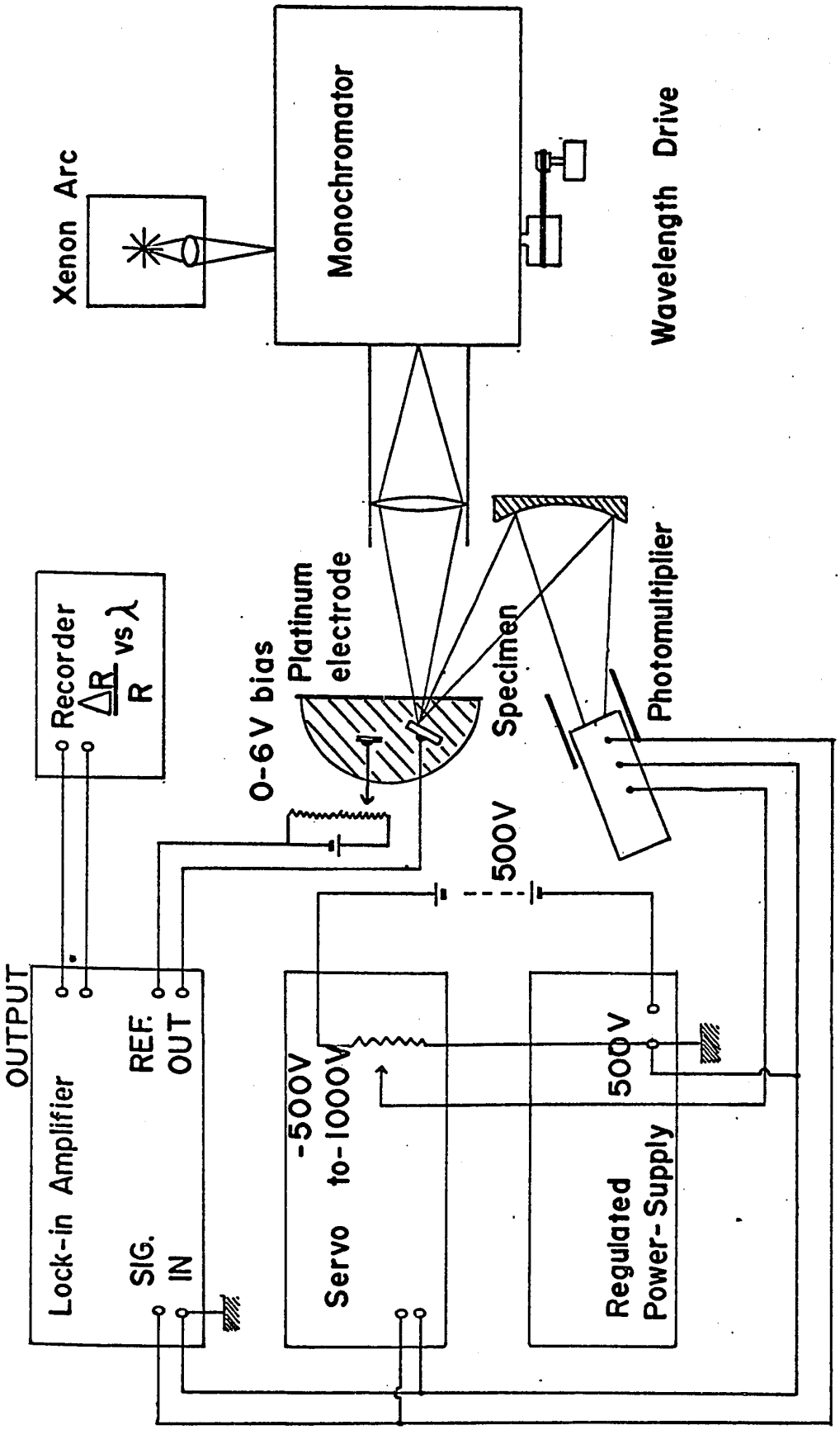

FIG. 21 ELECTROREFLECTANCE APPARATUS

2 and 6eV, and a DUMONT 6911 for the 1 to 3eV region.

Due to the lamp intensity and photomultiplier sensitivity falling off above 5eV, an effective cut-off of approximately 6eV was obtained. Use of higher quality optics, such as suprasil or LiF, for lenses and windows, together with nitrogen flushing, should extend the measurements to 7eV, the cut-off of the aqueous electrolyte. The infra-red cut-off was determined by a combination of the S1 response of the 6911 falling off and the water cut-off, and was approximately 1eV.

The electrolytic cell had a thin quartz window, the two electrodes being the specimen and a piece of platinum foil. The specimen was mounted on a brass rod with silver paint (GC # 21-1) to form an ohmic contact, and then insulated except for the polished face with liquid tape (GC #176-2). A bias of 0 to 6V d.c. was supplied by the battery/potentiometer combination and the modulating voltage of 2 to 5V peak-to-peak was supplied by the PAR model JB-6 lock-in amplifier. Higher modulating voltages, when required, were taken from a Hewlett-Packard 200AB AF oscillator, with the lock-in on the external mode of operation. The

output signal from the photomultiplier consisted of two parts; the one proportional to the reflectance R was d.c. and kept constant at 1V by means of a Heathkit Recorder operating as a servo. The off-balance signal was amplified and adjusted a helipot across the stabilised power supply to vary the photomultiplier voltage until the d.c level again reached 1 volt. The other part of the output signal was proportional to ΔR and varied at the modulation frequency; it was amplified by the JB - 6 which uses phase sensitive detection The output was displayed on a Heathkit chart recorder, and since R was kept constant, took the same form as $\frac{\Delta R}{R}$. The wavelength control of the monochromator was motor driven, so the chart represented a $\frac{\Delta R}{R}$ vs. λ plot, wavelength intervals being manually marked every 100°.

Differences between the Brown and Ottawa set-ups are: Osram 450 W Xenon arc; EMI 6255 B photomultiplier; two lenses instead of one lens and one mirror; PAR JB - 5 lock-in amplifier; modulating voltage in excess of 5V obtained by amplifying JB - 5 output with Heathkit audio amplifier; R signal kept at 1V by external source instead of internal mercury cell of Heathkit Recorder/ Servo

Measurements were taken by mounting the specimen as described above, and then placing it in the electrolyte bath which contained a 0.1N to 1N aqueous solution of KCl. After applying a bias of 1V and aligning the optical system, the spectral region in which structure was expected was searched. By experimentation, the best bias, modulating voltage, amplifier gain, and phase setting were determined, and $\frac{\Delta R}{R}$ measured as a function of wavelength. The phase and gain settings were sometimes changed when covering different regions of the spectrum (i.e. for different peaks), maximum signal with least noise being the aim. A wavelength drive speed of 50Å/min. at a chart speed of 2"/min., with a time constant of 1 or 3 secs, provided spectra with ample resolution and quietness, except in the extreme ultra-violet when the noise level increased.

4.5 RESULTS

All the GaAs - GaP results were taken at room temperature (~25°C) with a d.c. bias of 1.5V and a modulation frequency of 70 c/s. Typical spectra for GaAs, GaP and four of the nine alloy specimens measured are presented in Figs. 22, 23 and 24. The general shape and position of the structure in GaAs is the same as had previously been reported (S 34, S 35). Later measurements on both GaAs and GaP agreed well with these results (GaAs; C 49, S 39, S 46 : GaP; C 49, S 39). The alloy spectra represented a smooth change between the two compounds, except that the signal strength was lower for several of the specimens and thus was usually recovered through the use of higher modulating voltages. The spectra can each be divided into three energy regions, one group of peaks corresponding to the direct gap E_o, the next to the E_1 complex, and in the ultra violet the structure generated by the E_o' and E_2 transitions. The reasons for these assignments will be given in the next sub-section.

Plots of the various peak energies with alloy composition are shown in the next three figures. In Fig. 25, the variation of E_o, $E_o + \Delta_o$, and Δ_o is shown, together with the computer-fitted parabolae for the first two and a straight line for Δ_o. The choice of a parabola for E_o

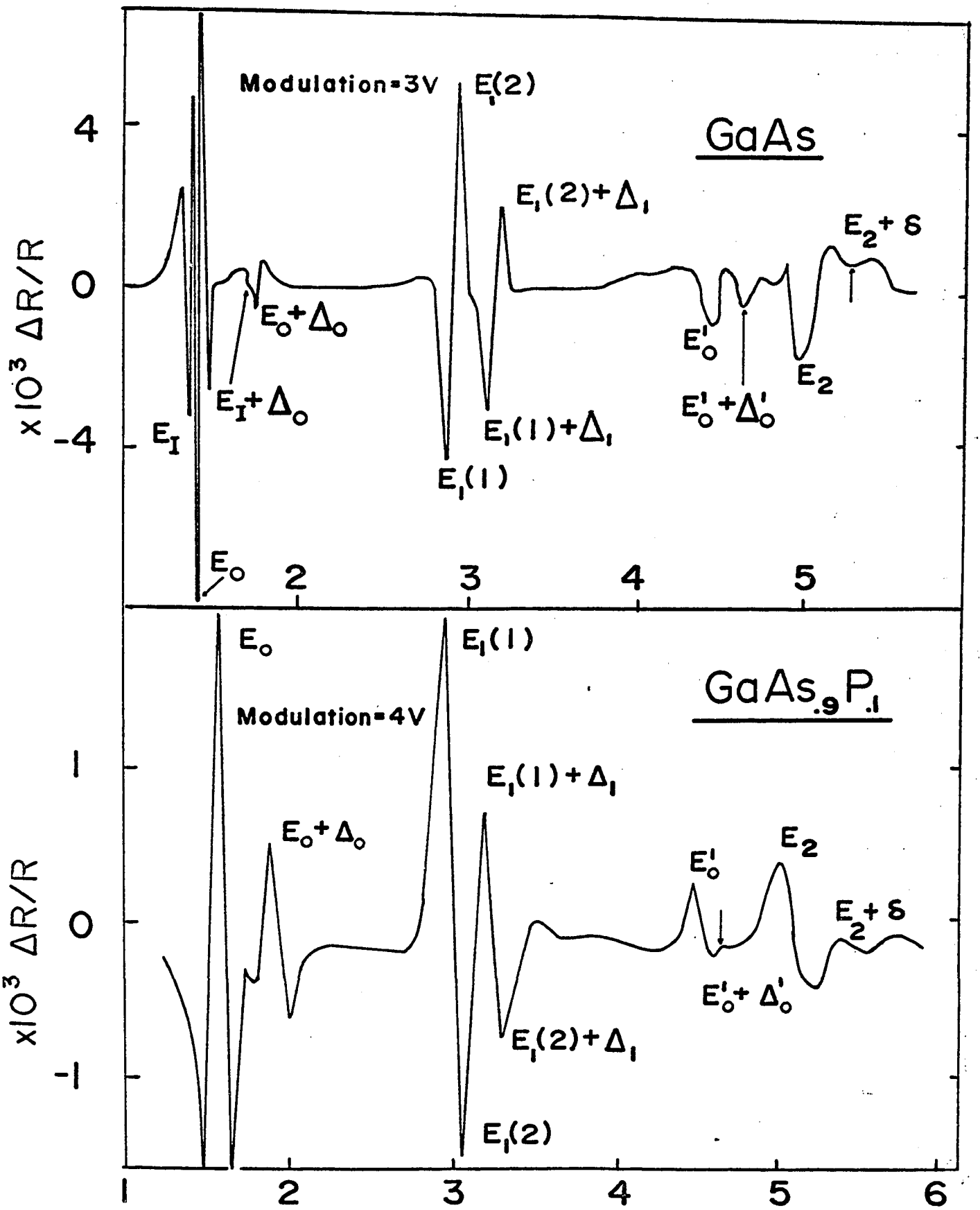

FIG 22 Electroreflectance Spectra of GaAs and $GaAs_{.9}P_{.1}$

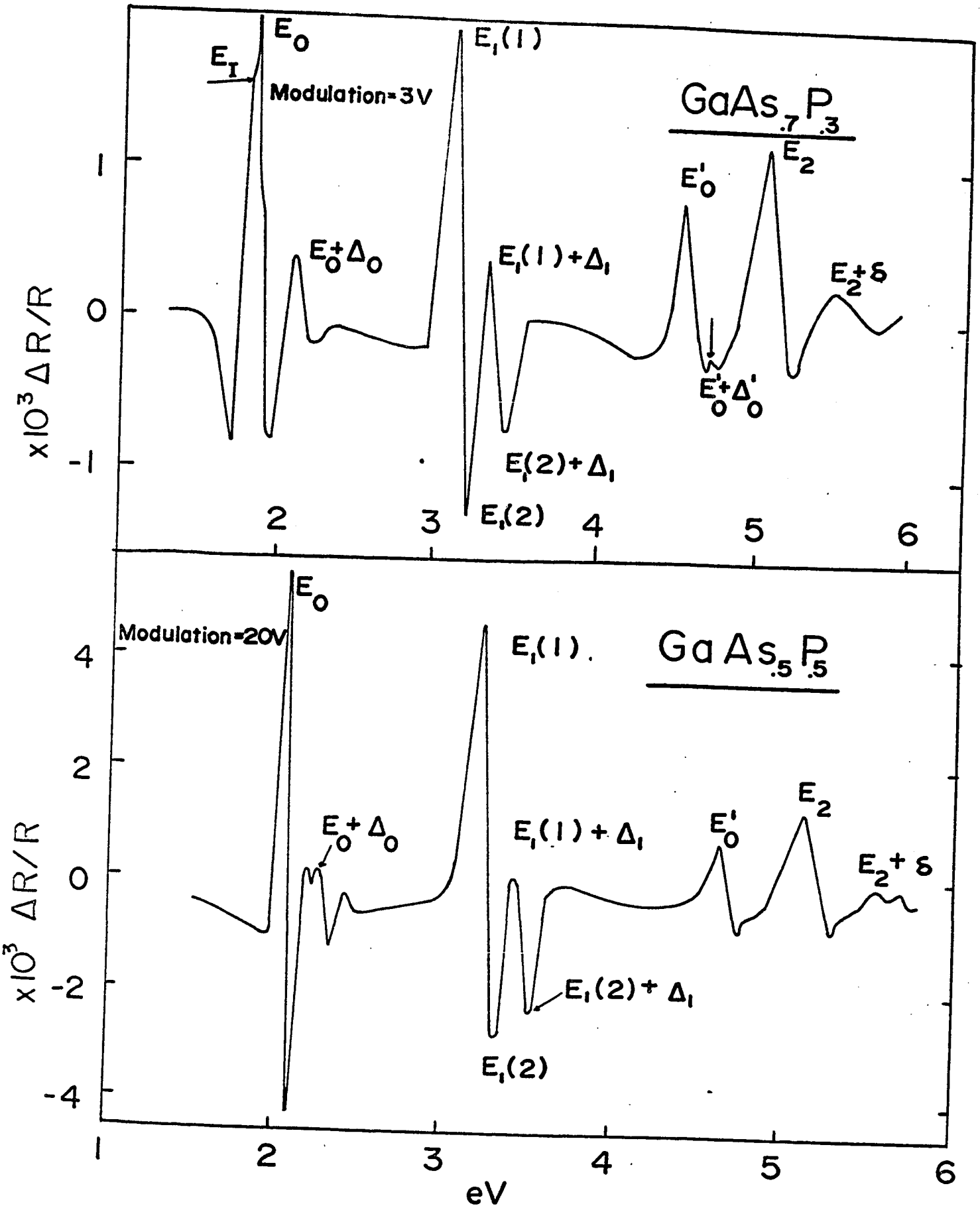

FIG 23 Electroreflectance Spectra of $GaAs_{.7}P_{.3}$ and $GaAs_{.5}P_{.5}$.

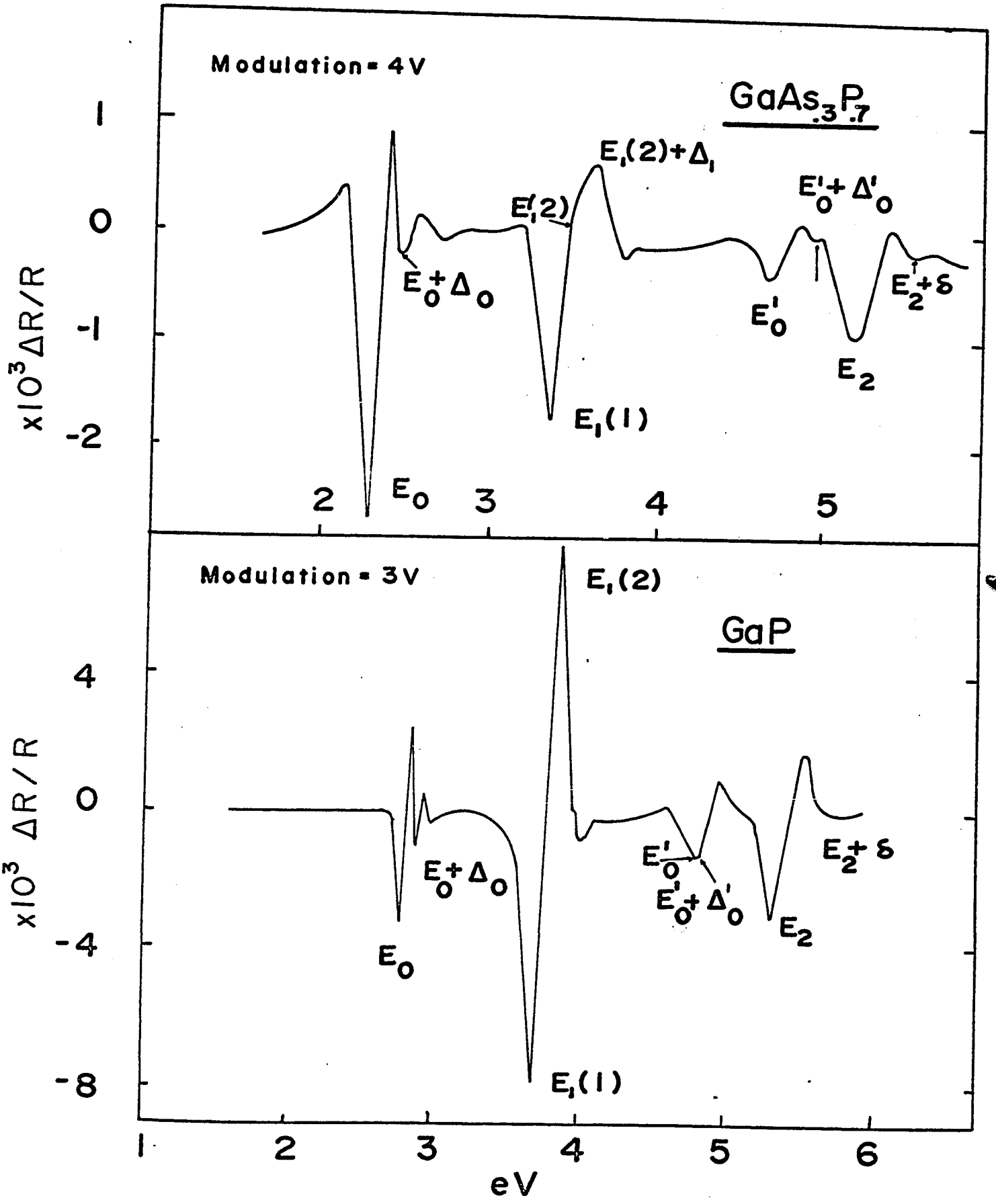

FIG 24 Electroreflectance Spectra of $GaAs_{.3}P_{.7}$ and GaP .

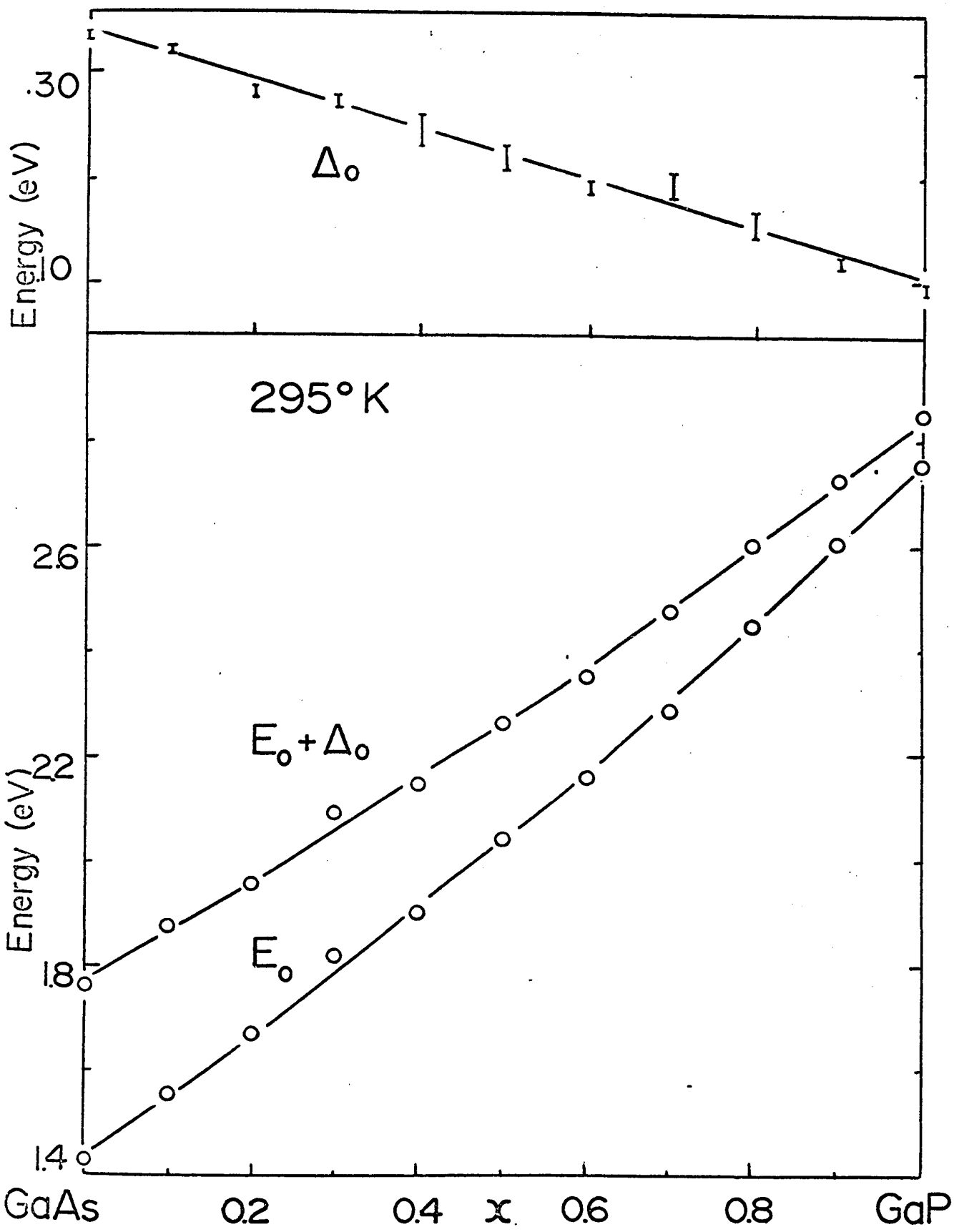

FIG 25 Variation of the E_o and $E_o + \Delta_o$ peaks, and Δ_o,, with Alloy Composition for $GaAs_{1-x}P_x$.

and $E_o + \Delta_o$ was made because it was significantly better than a linear fit. The error bars on the Δ_o graph represent solely the inaccuracy of estimating the difference of the E_o and $E_o + \Delta_o$ peak energies; no attempt was made to estimate additional errors arising from slightly different surface treatments etc. The fitted equations are, where x is the mol. fraction of GaP present, and all energies are in eV:-

$$E_o = 1.441 + 1.091x + 0.210x^2$$

$$E_o + \Delta_o = 1.776 + 0.684x + 0.182x^2$$

$$\Delta_o = 0.339 - 0.236x$$

The variation of the E_1 peaks with alloy composition is shown in Fig. 26. The notation here is that $E_1(1)$ and $E_1(2)$ are the first and second peaks of the complex for increasing energy, and $E_1(1) + \Delta_1$ and $E_1(2) + \Delta_1$ are the next two peaks. In addition it can be seen that $E_1(1)$ and $E_1(1) + \Delta_1$ always have the same sign of $\frac{\Delta R}{R}$ as the E_o and $E_o + \Delta_o$ peaks. The two values of Δ_1 result from $[E_1(1) + \Delta_1] - [E_1(1)] = \Delta_1(1)$ and similarly for $\Delta_1(2)$, and are also shown in Fig. 26. The (1) components of E_1 can be seen to follow the corresponding peaks in the reflectance quite closely, if Fig. 17 is consulted.

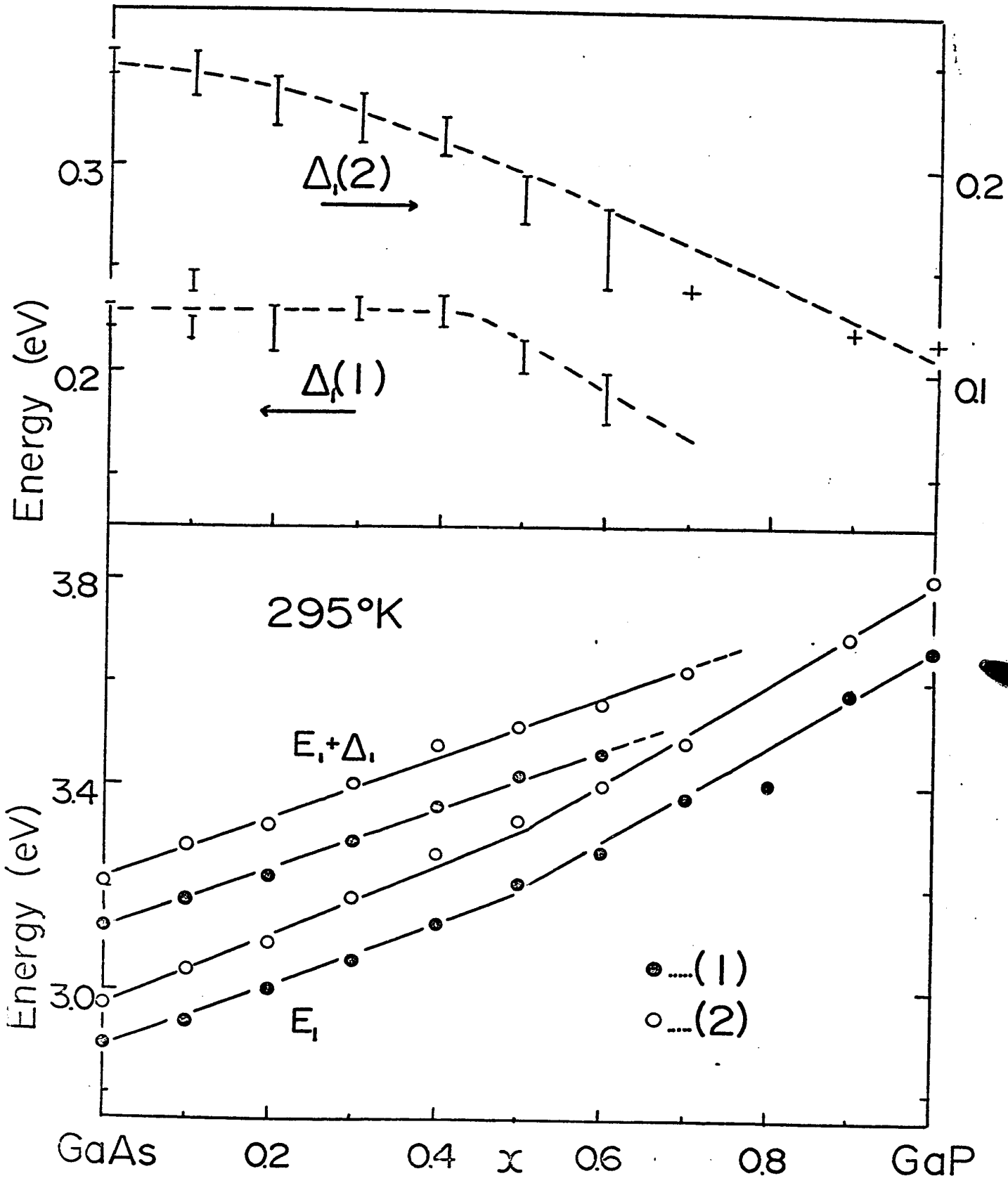

FIG 26 Variation of the E_1 peaks, and Δ_1 (see text) with Alloy Composition for $GaAs_{1-x}P_x$.

The variation of the E_o', $E_o' + \Delta_o'$, E_2, and $E_2 + \delta$ peak energies with alloy compositin is shown in Fig. 27, and all are seen to be linear within the experimental accuracy. Missing points indicate that the transitions were either very weak or not definitely observed, as happened for several specimens in the ultra-violet.

In Figs. 22, 23 and 24 it can be seen that some of the E_c (and hence $E_1(1)$, E_o' and E_2) peaks have a negative value of $\frac{\Delta R}{R}$ whilst others have a positive value. The spectra were observed to change phase in this way if the specimen majority carrier type changed, and the convention used here is that negative-going peaks correspond to n-type material, positive-going to p-type material. All specimens were later checked for carrier type and found to follow the sign observed in the electroreflectance spectra This effect has been fully analysed for Ge (C 49), and enables conclusions to be drawn about the position of the Fermi level if the doping level positions are known.

The reasons for choosing the above assignments for the various peaks, and conclusions that can be drawn from the reflectance and electrcreflectance data combined, will now be given

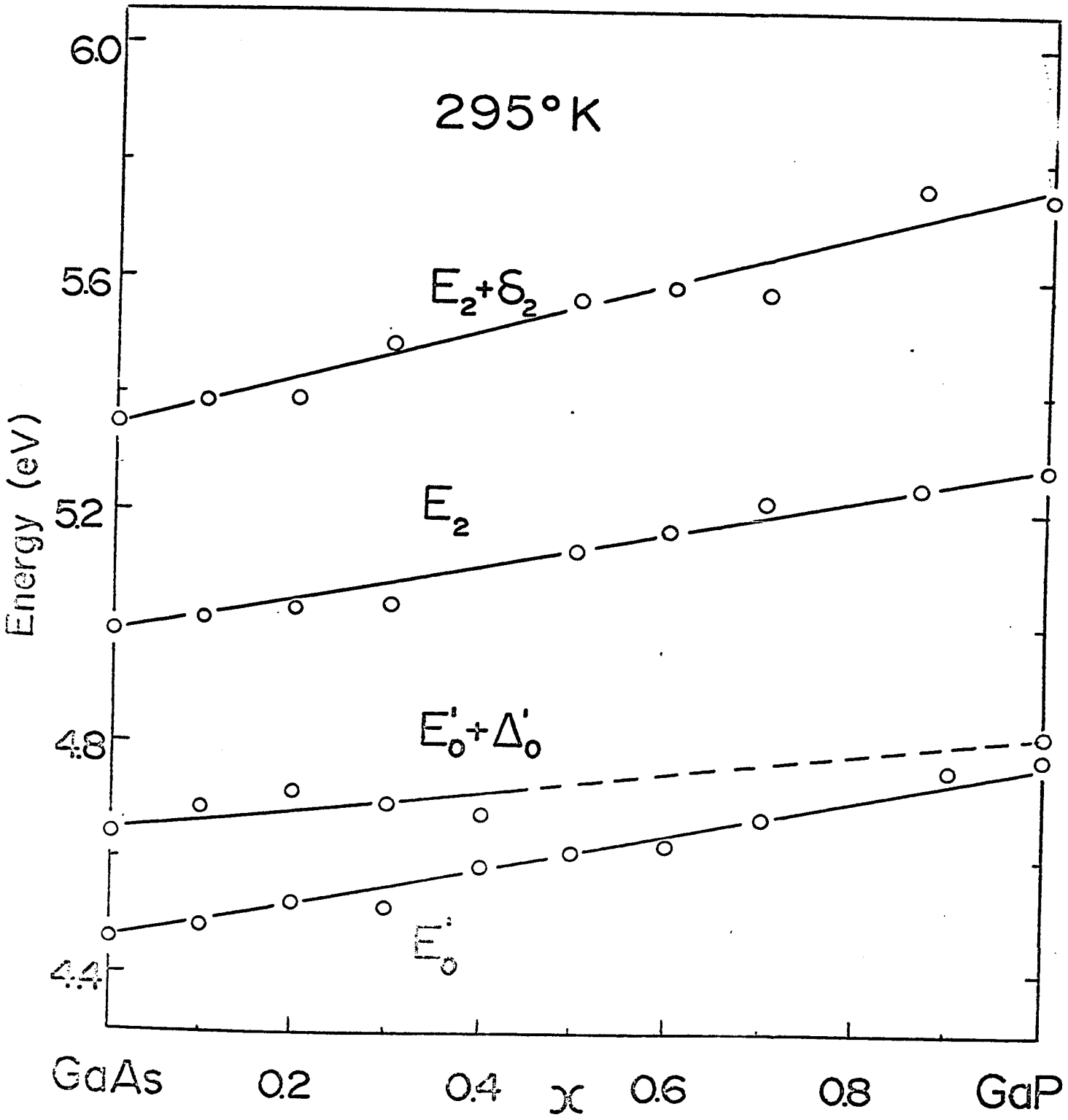

FIG 27 Variation of the E_0' and E_2 peaks with Alloy Composition for $GaAs_{1-x}P_x$.

4.6 DISCUSSION

Lowest Direct Absorption Edge.-

The peaks labelled E_o and $E_o + \Delta_o$ correspond very closely to the lowest direct edge observed in absorption spectra for the compounds, and are not normally observed in reflectance due to the small density of states. In GaAs, the E_o peak at 1.441eV compares with Sturge's value of 1.436eV at the same temperature (S 55), whilst the spin-orbit splitting at Γ_{15v}, Δ_o = 0.339eV, compares with Hodby's value of 0.33eV from infra-red absorption and Sturge's value of 0.35eV from the absorption edge (S 55). The peaks labelled E_I and $E_I + \Delta_o$ are believed due to an impurity level, since they have a different dependence on both the d.c. bias and a.c. modulating voltage from all the other peaks (C 49). From the observed behaviour with doping on several specimens, it is shown that this level lies close to the bottom of the conduction band. For the specimen of GaAs used in this study, the ionisation energy $E_o - E_I$ is approximately 0.04eV. Seraphin's results on the electroreflectance of GaAs (S 35, S 46) showed values of 1.42 and 1.77eV for E_o and $E_o + \Delta_o$ respectively. In GaP, the E_o peak energy of 2.742eV agrees with values of 2.77eV in absor-

ption (S 36) and 2.78eV in reflectance (since E is large, the density of states is large enough to produce a small response in R^4, see Z 2). The magnitude of Δ_o = 0.103eV agrees with absorption data at the edge, 0.09 ± 0.01 (S 36), but not with the alloy infra-red absorption data of Hodby, 0.127eV (H 2).

The above energies were all taken from the fitted curves shown in Fig. 25, as these values are considered more representative than those obtained from the compounds alone. In practice, the differences were very slight.

A parabolic variation of the lowest direct energy gap in semiconducting alloy systems has been observed previously, and noted by Cardona (C 20) and Woolley and Warner (W 34). This parabolic deviation from the expected linear relation is fully discussed for the III - V alloy systems in general in Section VI. The linear variation of Δ_o is expected as non-sensitive levels are involved, and had previously been observed by Hodby (H 2) in the infra-red absorption spectra of p-type GaAs - GaP alloys. However, due to the approximations used to derive a value of Δ_o from the various peaks involved, his value for Δ_o in GaP is too high (see above).

The E_1 peaks:-

In GaAs and some of the alloys, four peaks are seen which correspond to the structure in the reflectance in the same energy region. These are denoted E_1 and are believed due to transitions in Λ between the uppermost valence band and lowest conduction band. Due to the splitting of the valence band by spin-orbit interaction, two transitions are expected to take place. In the analysis of this work, $E_1(1)$ and $E_1(1) + \Delta_1$ were chosen as being representative of the transitions, whilst $E_1(2)$ and $E_1(2) + \Delta_1$ were considered as oscillations following the edge. This viewpoint was held because the (1) components closely followed the reflectance results (see section 3.6 and Fig. 17), and because their phase was the same as all the other peaks, some of which (eg. E_2) were also due to saddle point edges. Also, in Ge where only two E_1 peaks are observed, they have the same phase as the E_0 peaks (S 18). Seraphin chose to take the (2) components in GaAs (S 46), arguing that by Phillips duality theorem (P 33, P 54), if oscillations follow a parabolic edge they should precede a saddle point edge. A full analysis by Cardona et al (C 49) using Aspnes' theory (A 20) on GaAs shows that the best fit of the experimental curves to the theory is obtained if it

assumed that the E_1 peaks are due to a M_1 transverse-field critical point, whose edge occurs just below 2.9eV. This substantiates the above argument that the (1) peaks correspond more closely to the actual edge than the (2) peaks.

The splittings $\Delta_1(1)$ and $\Delta_1(2)$ do not vary linearly with alloy composition (Fig. 26). In the following discussion $\Delta_1(1)$ will be considered (see above paragraph) but $\Delta_1(2)$ takes a similar form. The splitting appears to be approximately constant at 0.23eV (the value in GaAs) out to x = 0.45; it then starts to fall, projecting to approximately 0.1eV in GaP. The break in Δ_1 occurs at the same composition as the breaks in E_1 in both the reflectance and electroreflectance data. However, by fitting linear relations to E_1' and $E_1' + \Delta_1'$, it was found that Δ_1' decreases from 0.26eV in GaAs to 0.23eV in GaP i.e. Δ_1' stays approximately constant with alloying. Now Δ_1' represents the splitting of the valence band at L, since the splitting of L_{3c} is small in comparison (C 33).

This enables us to construct a picture of the upper valence band for GaAs, $GaAs_{0.5}P_{0.5}$ and GaP (see Fig. 28). The splitting at L varies from 0.26 to 0.23eV as x varies from 0 to 1.0. In GaAs and the alloys

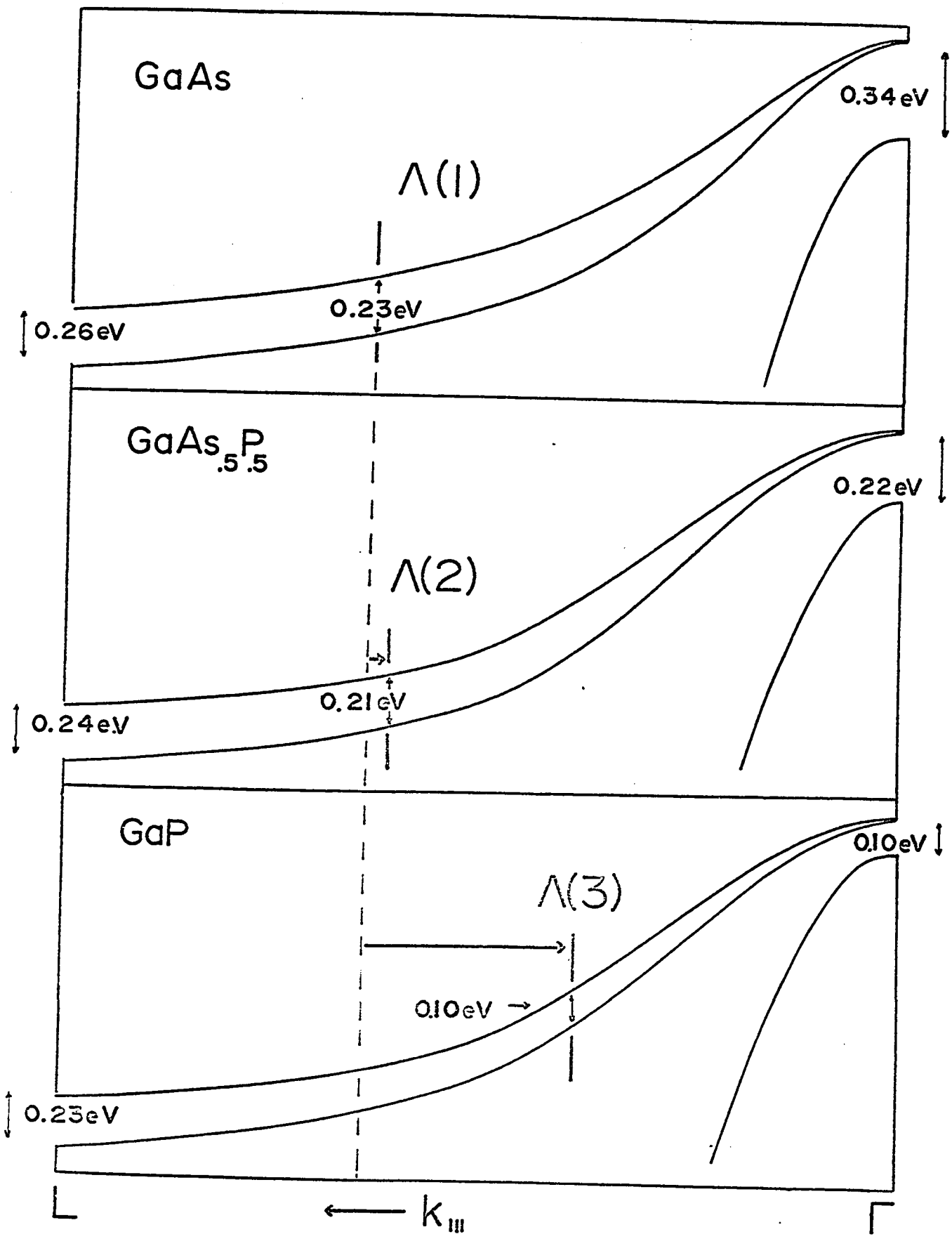

FIG 28 Postulated Valence Band Structures of GaAs, $GaAs_{.5}P_{.5}$ and GaP, showing the Δ_o, Δ_1 and Δ_1' splittings (see text) .

out to $x \sim 0.45$ the E_1 transition stays in approximately the same position in $\underline{k}$-space, at $\Lambda(1)$. As x continues to increase, the slope of the conduction band starts to increase because Γ_{1c} is rising faster than Λ_{3c}, relative to the valence band, (i.e. E_o increases faster with x than E_1, see Figs. 25 and 26). Therefore the transition moves to the steeper part of the valence band (i.e. toward Γ, at $\Lambda(2)$ for $x = 0.5$) so that the condition of parallel valence and conduction band slopes given by equation (vii) will still be satisfied. As this movement commences, Δ_1 starts decreasing since the two valence bands have to converge in this region in order to become degenerate at Γ. There is always a limit on how near to Γ the E_1 transition can get since there is a maximum in the conduction band before Γ is reached. Presumably the proximity of the E_1 in GaP to Γ (i.e. $\Lambda(3)$) is responsible for the temperature coefficient of -3.5×10^{-4}eV/°C compared to -4.8×10^{-4}eV/°C for E_1 in GaAs and -3.2×10^{-4}eV/°C for E_o' in GaP (see table 4). (N.B. the Λ_{1c} level seems to be a less sensitive to alloying and temperature variations than the Γ_{1c} level).

Since the slopes of the two Λ_{3v} valence band branches are unlikely to be parallel in GaP for the transition point ($\Lambda(3)$), the possibility arises of

having the centres of the regions of k-space responsible for the E_1 transitions lying at different values of Λ. Whilst this could be capable of explaining the apparently different transition strengths of E_1 and $E_1 + \Delta_1$ before and after the $x = 0.45$ break, it also introduces another variable parameter into the analysis. The situation then becomes unduly complex until more detailed band structure calculations become available.

The above results and conclusions give rise to some general information about the III - V compounds, and this will be considered at the end of this section.

The E_0' peaks:- The peak attributed to E_0' follows the corresponding reflectance transition very closely, and varies linearly with alloy composition within experimental error. It is shown much more strongly in electroreflectance however, being about the same magnitude as the E_2 peak, since the general conditions about parabolic and saddle point edge transition strengths, (section 3.2) no longer apply. A small component is also seen at higher energies whose intensity in comparison to E_0' decreases with increasing x, and it draws closer to E_0' at the same time. It was not resolvable in the GaP-rich alloys, but was seen in a good specimen of GaP as a slight break in the main peak (see Fig. 24). This transition is labelled

$E_o' + \Delta_o'$ and is thought to occur with E_o' not at Γ but in the Δ region slightly away from Γ (S 39). The splitting Δ_o' then corresponds to the splitting of the valence band at Δ; agreement between its magnitude and that found by $\underline{k}.\underline{p}$ calculations (P 53) is good for most III - V compounds. Its proximity to Γ ensures that E_o' still represents the $\Gamma_{15v} - \Gamma_{15c}$ gap accurately. Also the photoemission results that confirmed the E_o' assignment in the reflectance work (section 3.6) are still correct since they can only specify the positions in $\underline{k}$-space of the transitions approximately. The difference in levels is too small to be detected by this method, being less than 0.2eV lower than the corresponding Γ levels.

The E_2 peaks:- The transition labelled E_2 is also linear within experimental error, and again follows the corresponding reflectance transition, but at an energy approximately 0.05eV lower. The higher energy transition $E_2 + \delta$ confirms the small structure seen in the high energy reflectance as being real and associated with the E_2 peak. The splittings in the compounds of 0.36eV and 0.46eV in GaAs and GaP respectively agree reasonably with the low temperature reflectance results for GaAs of 0.43eV (G 2)

and the infra-red absorption estimate for GaP of 0.4eV (Z 2), as well as the aforementioned high energy reflectance results (0.38eV and 0.40eV respectively).

The conclusions drawn in section 3.6 regarding the possibility that the E_2 transitions are due to Σ or Σ and X rather than X alone still apply here. Recent k.p calculations (P 53) have shown that the saddle point in the [110] direction ($\Sigma_2 - \Sigma_1$) correspond much more closely to the observed E_2 peak energy for both GaAs and GaP rather than the $X_5 - X_1$ transition. The latter seems to be degenerate with E_o' for these compounds. The splitting observed is therefore still due to the X_1 splitting (since zinc-blende lacks an inversion centre) and will be approximately equal to the $X_3 - X_1$ gap, but it occurs in the Σ region. It is hoped that piezo-electroreflectance studies will clarify this point (P 43)

Other Transitions:- The energy region in which E_{cp} occurred in the reflectance spectra was diligently searched using a high amplification, but no trace of any structure was seen. A response approximately 100 times smaller than that of the E_1 transitions would have been detectable. Also, the region in which Greenaway reported e_1 transitions (2.2 and 2.5eV, see section 3.3) and the regions where the indirect transition was lower than

E_o ($x > 0.5$) yielded no structure in the electroreflectance. Thus, as expected, no response was obtained for indrect transitions. The explanation of the e_1 and E_{cp} transitions is still lacking; the structure seems real in reflectance, but is not seen in the sensitive method cf electroreflectance.

Rehn (R 18) claims to have seen a small response in one ($x = 0.8$) of two $GaAs_{1-x}P_x$ specimens he measured, using Seraphin's apparatus, at 2.2eV, which had a temperature coefficient of $< -1 \times 10^{-4}$ eV/°C. He claimed that this was due to either an e_1 transition or to an indirect transition. In view of the great number of results on the compounds (C 49), besides two alloy systems (C 48, T 12) which have specifically reported no e_1 or indirect transitions observed, together with the high noise level of his results and the strangely low temperature coefficient, such a response must be viewed as spurious until substantiated by similar responses on several other specimens under better conditions. (The electrolyte technique has an advantage here because of the lack of films, several interfaces, vibration problems, etc, any one of which might cause spurious peaks.).

The conclusions drawn above regarding the movement of the E_1 transitions have further consequences. One is that there is not necessarily any connection between the Δ_1 and Δ_1' splittings at Λ and L respectively. The 2/3 rule, which states that Δ_1 is approximately 2/3 Δ_o, was originally enunciated when Δ_1 was thought to be the splitting at the edge (C 8). It has been widely used with the exception of a few materials of low cationic number (GaP, InP, CdS). It now appears that any agreement with the rule where the Δ_1 splitting is concerned is somewhat fortuitous; the Δ_1' splittings certainly do not follow that rule. We will now consider the contributions of the anion and the cation at the zone edge (L) and centre (Γ) in the light of the experimental results.

Let y = the fractional contribution of Ga to the splitting of the L (or Γ) point in GaP.

Let x = the fractional contribution of Ga to the splitting of the L (or Γ) point in GaAs.

Then we can write.

$$\frac{\Delta_{III}^{y} + \Delta_V (1 - y)}{\Delta_{III}^{x} + \Delta_V (1 - x)} = \frac{\Delta_1' (GaP)}{\Delta_1' (GaAs)} \quad \text{for L}$$

$$= \frac{\Delta_o (GaP)}{\Delta_o (GaAs)} \quad \text{for } \Gamma \qquad \text{(xvi)}$$

where Δ_{III} and Δ_V are the atomic splittings of the respective group III and V elements. Using Cardona's values (C 8) for these atomic splittings, the electroreflectance results for Δ_o (T 12) and the high energy reflectance results for $\Delta_1^?$ (T 16) we obtain for the L and Γ points respectively.

$$\frac{.21y + .10(1 - y)}{.21x + .51(1 - x)} = \frac{0.23}{0.26}$$

and

$$\frac{.21y + .10(1 - y)}{.21x + .51(1 - x)} = \frac{0.10}{0.34} \qquad \text{(xvii)}$$

If the ratio of x to y is known, the proportion of anion to cation contribution to the splittings of the valence bands at L and Γ can be found. Normally one would expect x to be approximately the same as y; since GaP has such a small atomic number, the case of $y > x$ will also be considered (N.B. x and y must lie between 0 and 1). The terminal conditions are for $y = 1$ and $x = 1$, whilst a practical condition is $y \approx x$. The values of x and y are shown for a range of ratios in Table 6 for the L and Γ points of the valence band, found by the equations (xvii).

TABLE 6. Comparison of anion and cation contributions to the valence bands of GaAs and GaP.

		$y > x$	$y = x$	$y < x$
At L, (Δ_1')	y =	1.00	0.93	0.75
	x =	0.89	0.93	1.00
At Γ, (Δ_o)	y =	0.45	0.25	0
	x =	0	0.25	0.57

It can be seen that for reasonable values of y (> x), the cation mainly (~90%) determines the L_{3v} splitting, whilst the Γ_{15v} splitting is dependant mainly (~75%) on the anion. This conclusion should be applicable to the rest of the III - V compounds, and this is reasonably substantiated by Table 7, which shows Δ_o listed in cationic groups and Δ_1' in anionic groups. The agreement between Δ_1 and 2/3 Δ_o is shown to be quite good for most cases, so that if the ratio of $\frac{\Delta_1(A)}{\Delta_1(B)} = \frac{\Delta_o(A)}{\Delta_o(B)}$, the indication is that the Δ_1 splitting must be due to the same proportion of anion as the Δ_o splitting. Hence agreement between Δ_1 and Δ_1', when it does occur, is fortuitous, as one is determined mainly by the cation and the latter by the anion.

The values shown are all quoted from the electroreflectance data in C 49 except where otherwise indicated. The value of Δ_1' from GaSb is approximate since the photoemission data gave only a small indication of a doublet. Similarly Δ_1' for InP has been estimated from the single peak shown by Cardona, since this is very broad and could be a doublet. The other discrepencies between Δ_1' and Δ_1 (GaP, InAs, InSb) are quite definite.

TABLE 7. Comparison of the valence band splittings in the III - V Compounds.

Material	Δ_o, (eV)	Material	Δ_1' (eV)	Δ_1 (eV)	$2/3\Delta_o$ (eV)
GaP	0.10	AlSb		0.40	0.50
InP	0.10				
GaAs	0.34	GaP	0.23 (T16)	0.1	0.07
InAs	0.43 (M28)	GaAs	0.26 (T16)	0.23	0.23
		GaSb	~0.3 (C28)	0.46	0.52
AlSb	0.75	InP	~0.6 (C29)	0.15	0.07
GaSb	0.80	InAs	0.6 (E2)	0.28	0.29
InSb	0.82	InSb	0.7 (E2)	0.50	0.52

Further measurements on GaSb, InP, AlSb, and AlAs would be capable of testing the above reasoning, since AlSb and AlAs should both have $\Delta_1' \sim 0.04$eV and be seen as a single narrow peak at E_1', whilst $\Delta_o \sim 0.3$eV for the latter (and hence Δ_1 probably will be ~ 0.2eV) which should be easily detectable by electroreflectance.

The above conclusions indicate that the use of some experimental results in band calculations must be carefully reconsidered, as the values of the splittings are often utilised. If the few measurements mentioned in the preceding paragraph confirm these conclusions, a new look at the cation/anion role in III - V compounds and its effect on band structures will become necessary.

SECTION V

THE ELECTROREFLECTANCE OF InAs - GaAs

5.1 INTRODUCTION

References are made to the InAs - GaAs alloy system in Section II. Since the preparation of these alloys is of interest here, some of the pertinent literature will be reviewed in more detail.

The first proof of complete solid solution was obtained by Woolley and Smith (W 2) with an X-ray analysis of powder specimens, which showed that Vegard's law was satisfied within experimental error Solid specimens were later obtained by Abrahams et al (A 2) and Woolley et al, (W 15). The optical results of these two groups in these and later papers will be discussed in the next subsection.

Interest in this alloy system has increased recently because of its suitability for use in stimulated emission diodes (lasers). As pointed out previously, GaAs - GaP alloys are capable of such activity in the direct-energy gap part of the system ($0 < x < .45$) resulting in a range of 2.0eV to 1.5eV. Semiconductor lasers can therefore be made from alloys of this system which emit light in the range red ($x = 0.45$, $\lambda = 0.6\mu$) to the near infra-red ($x = 0$, $\lambda = 0.85\mu$), (see e g. A5, C22, F10, G16,

K5, N7, P29). In a similar manner coherently-emitting diodes made from InAs - GaAs alloys cover an energy range from 1.5eV to 0.4eV, extending out into the infra-red from the GaAs value (M5, M12). Diodes utilising the InSb - GaSb alloys are capable of covering the range 0.8eV to 0.2eV (R 10), whilst the InSb - InAs system, by virtue of the minimum exhibited in its energy gap versus composition curve (see section VI), should be able to extend the range down to almost 0.1eV (~10μ), which is well into the infra-red. No work on either spontaneous or stimulated emission from diodes of this last alloy system has yet been reported.

The materials used in the above and other studies on the physical properties of the InAs - GaAs system have been prepared by "fast" zone melting (see 5.3) (A 2, H 45), directional freezing (B 49, W15), flash evaporation (M 10), and vapour transport to produce both solid (M 12, S 26) and epitaxial (C 41, M 21, T 13) specimens

5.2 REVIEW OF THE ALLOY SYSTEM.

It was decided that the optical properties of the InAs - GaAs system above the edge warranted further investigation. The only previous investigations were by Woolley's group (B 49, W 30) and the Texas Instruments group (C 41, J 6). The former measured the reflectance spectra between 2.0 and 5.2eV of alloys prepared by directional freezing They found that the E_1, $E_1 + \Delta_1$, E_o' & E_2 transitions all varied linearly with alloy composition, within experimental error. The scatter was large for the E_o' peaks, as they appeared only as a small departure from the smooth curve near the large E_2 peaks (cf section III). The reflectance measurements of E_1 by Conrad et al. on epitaxial materials were made to study growth conditions, but quantitative measurements by Jones (J 6) yielded an E_1 curve that was linear for most of the range, but showed a concave behaviour near InAs. Although the values for the compounds appear good when compared with electroreflectance results (C 49), the etch used on the alloys was different from that used on these compounds, and gave poorer structure of the $E_1 + \Delta_1$ peaks than those obtained by Blazey (B 49).

The availability of the inherently higher resolution technique of electroreflectance brought new problems to the interpretation of the structure shown by the compounds.

Early measurements on InAs and GaAs (S 39) had assigned the doublets at 4.44 and 4.70eV and 4.45 and 4.64eV respectively to $E_o' + \Delta_o'$ transitions. Later measurements on InAs at higher energies showed that the 4.7eV peak was probably due to E_2 transitions, with a small peak at 5.2eV corresponding to $E_2 + \delta$. The alloy reflectance work of Blazey (B 49) showed that the 4.4eV peak in GaAs projected to ~4.5eV in InAs, whilst the 5.0eV (E_2) peak projected to ~4.6eV in InAs. Thus the $E_o' + \Delta_o'$ peak in InAs is obscured by the larger E_2 peak, and probably lies within 0.1eV of it, since this is near the resolution of the electroreflectance method (see e.g. section 4.5). Photoemission studies (C 28) showed E_o' at ~4.3eV, $E_o' + \Delta_o$ at ~4.7eV, with E_2 tentatively having an energy between these figures.

In order to confirm the above hypothesis, and to find the actual value of $E_o' + \Delta_o'$ in InAs, electroreflectance measurements were made upon the InAs - GaAs alloy system. It was also hoped that the linearity of the various transitions could be closely checked with such a high-resolution method, in view of the disagreement over the form of the E_1 versus composition curve mentioned above (J 6, W 30). The preparation of specimens of sufficiently high homogeneity to make such measurements is described in the following sub-section.

5.3 SPECIMEN PREPARATION.

The method of alloy preparation used in the past by this group was directional freezing (InSb - GaSb, W 6, W 12; InAs - GaAs, B 49, W 15, W 30), where a freezing surface is swept along the length of an initially molten charge by the simple expedient of slowly lowering the temperature of the furnace, which has a temperature gradient over the length of the ingot. Fast (comparatively) zone melting has been used for several of the III - V alloy systems (see e.g. W 57) including InAs - GaAs (A 2). With sweep rates ~1 - 2mm/hour, the resulting alloys are slightly inhomogeneous, but by making a large number of passes the central region of the ingot becomes reasonably homogeneous and of approximately single composition, which is useful if large specimens are required. If a large number of specimens of different compositions are required, and size is not critical, a single directionally frozen ingot is far less trouble.

The directional freeze (DF) technique worked quite well for the InSb - GaSb system with a freezing interface velocity ~ 3mm/day, but difficulties were encountered with the InAs - GaAs system, in spite of the fact that powered specimens reached equilibrium more quickly than InSb - GaSb specimens upon annealing (W 3).

For a reasonable initial charge of $x = 0.3$ ($In_{1-x}Ga_xAs$), which should yield an ingot with x varying from 0 to 0.8, the initial melting point is 1080°C. For a temperature gradient of 10°C cm^{-1}, the hot end of a 15cm ingot is at 1230°C, at which temperature commercial quartz begins to soften. Due to loss of As from the melt, excess As has to be added, and this has two effects. The As has a high vapour pressure, and attacks the quartz; because the quartz is soft these effects lead to a loss of vacuum and subsequent oxidation. Double sealing helped, but the production of ingots was still unreliable. Because small temperature gradients were used in an attempt to avoid high temperatures, constitutional supercooling occurred which resulted in inhomogeneous or two-phase regions centered around $x = 0.5$

The only reasonable directionally frozen ingot obtained by the author was the fourth attempt, and was slightly inhomogeneous over most of the length of the ingot (between 1 and 3%), with a two-phase region between $x = 0.5$ and 0.1. The furnace profile used in the production of this ingot is shown in Fig. 29, and the ingot composition as a function of length is shown in Fig. 30. Only a few specimens between $x = 0.82$ and 0.53 had a reasonable homogeneity The electroreflectance spectra obtained were not very good except for these specimens.

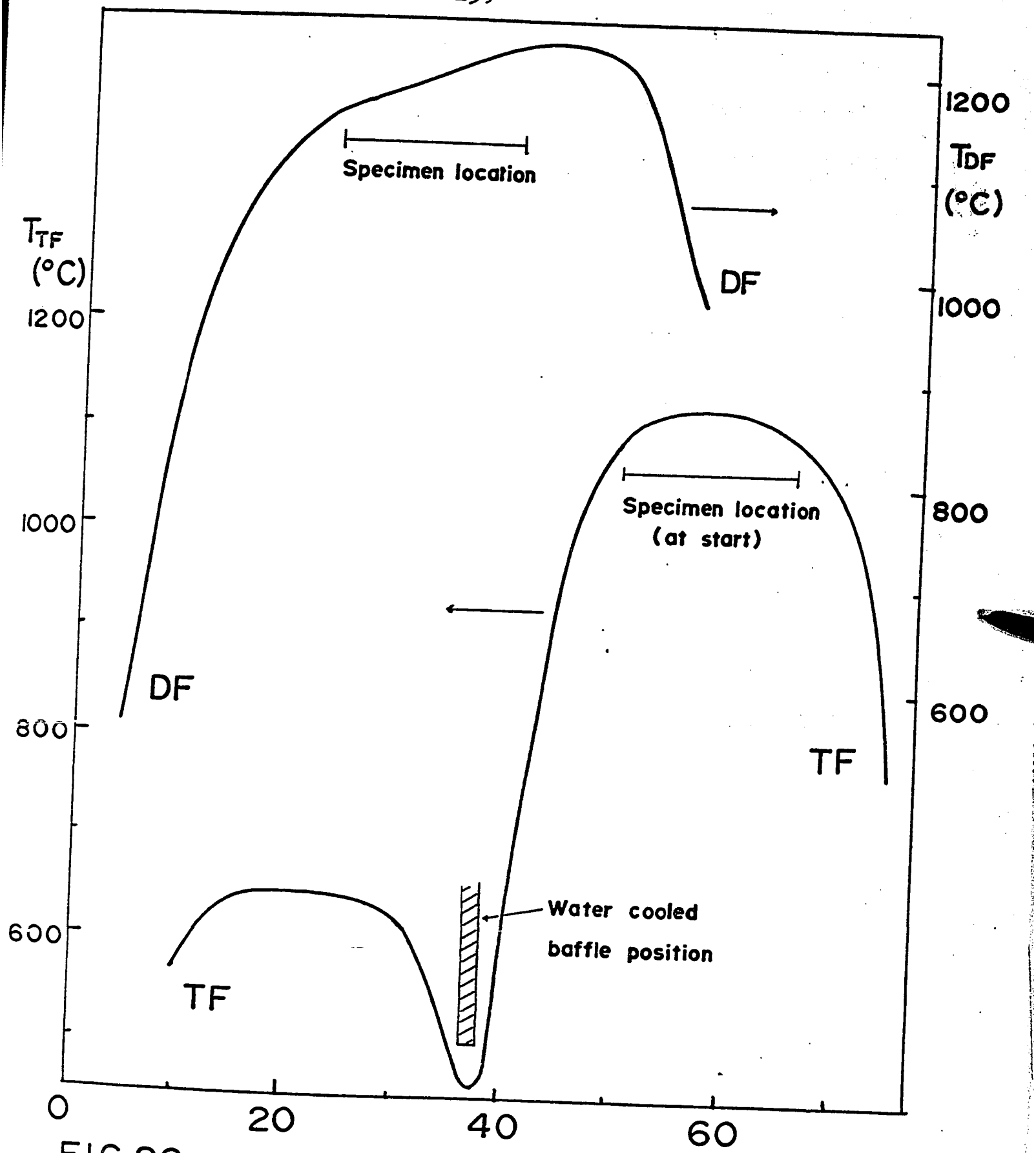

FIG. 29

Directional Freeze and Travelling Freeze Furnace Profiles .

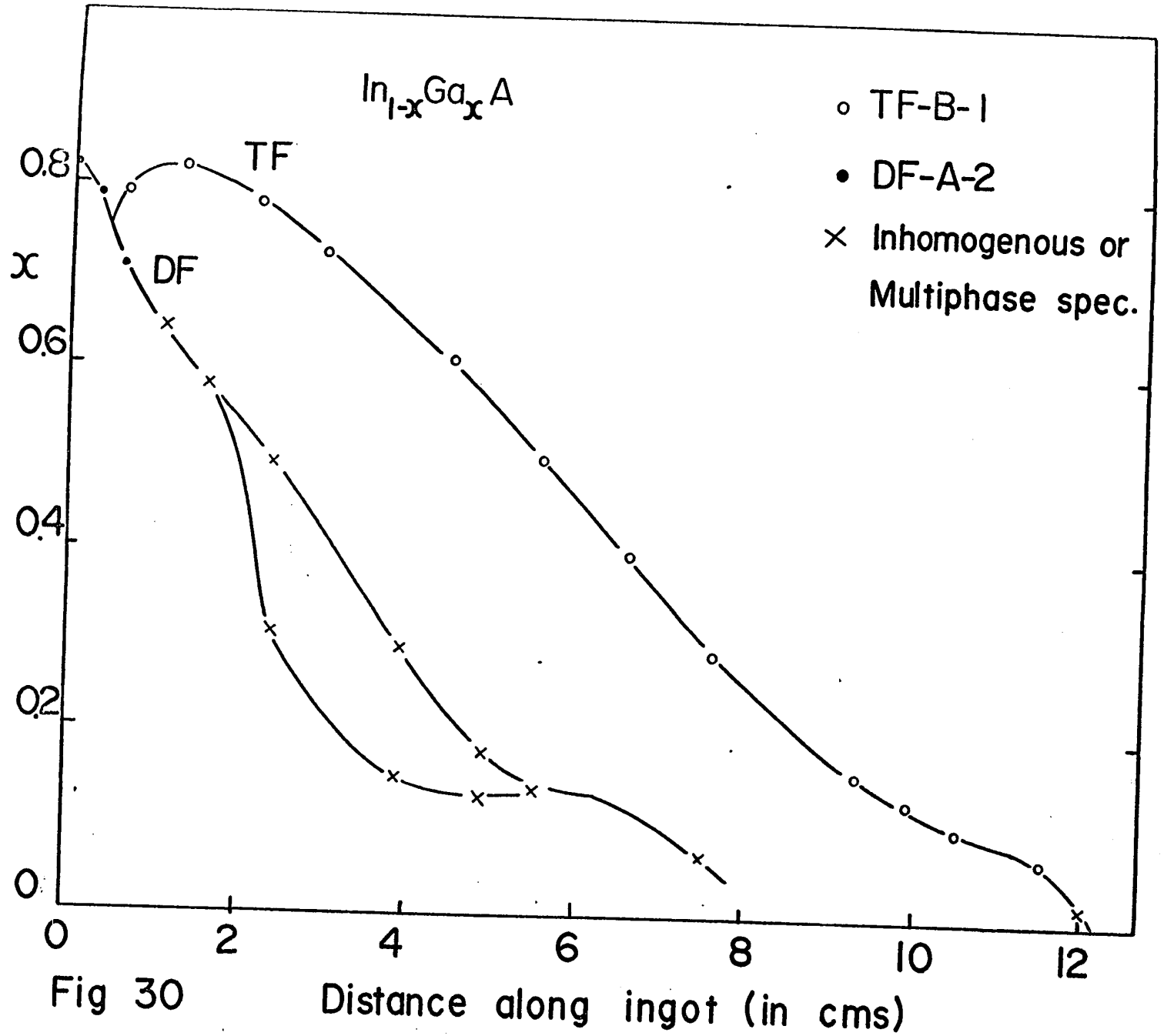

Fig 30

Variation of composition along the length of ingots prepared by directional freeze and travelling freeze techniques .

The two-phase regions produced by constitutional supercooling can be avoided by a steeper temperature gradient in the furnace, a vertical gradient being the ideal. This eliminates the directional freeze technique, and so a travelling freeze (TF) furnace was built. This had a hot zone, kept ~ 1120°C (for an x = 0.3 initial charge) with a proportional controller (to ± 0.1°C), and a cool zone, kept at ~ 650°C with a simple on-off controller (to ± 1°C), in order to maintain a reasonable As pressure over the ingot length. The furnace profile is shown in Fig. 29 with the ingot starting position marked. The initial charge (x = 0.3, 50 grm, with 0.2 grm of excess As) was sealed under vacuum in a quartz tube, and this was placed in another (long) quartz tube. The latter was supported by trolleys, and moved by a chain driven by a geared down motor at ~1.2cm/day This outer tube was continuously evacuated by a mechanical pump in case the ingot tube cracked.

The resulting ingot gave homogeneous (better than 1%) specimens between x = 0.04 and 0.82, with the back-reflection lines on the X-ray films showing no more blurring than the compounds. The composition as a function of ingot length is shown in Fig. 30, and can be seen to be a great improvement over the directionally frozen

ingot. Advantages of the travelling freeze method over the directional freeze method include:- faster in time (by a factor of 3), lower temperatures for a given starting composition (furnace construction simpler, lower As pressures, less danger of ingot tube blowing), more homogeneous ingots, and movement of freezing surface controlled mostly by the furnace rather than the phase diagram. The system built would stand temperatures ~ 100°C higher than were used for the first ingot, which would enable an x = 0.6 initial composition ingot to be used, yielding alloys having compositions up to x ~ 0.95.

This travelling freeze method has also been used with similar success by Coderre and Van Tongerloo of this laboratory on the InSb - GaSb system. In this case the variation of composition/unit length is improved, and ingots can be produced up to five times quicker than by directional freezing. The lack of a volatile component in this alloy system precludes the use of a background furnace, so only one furnace element has to be wound. The ingot moves from this hot zone into a room-temperature (water cooled) zone.

Specimens cut laterally from the ingot were ellipsiodal in shape (typically ~9 x 5 x 1 mm thick). Small pieces cut from the side of these specimens were powdered

and X-rayed to determine their homogeneity and composition (latter accurate to ± 1%). The variation of lattice parameter was assumed to be linear between the values for the compounds, as Vegard's law had previously been shown to hold within experimental error (~ 2). Both sides of the optical specimens were lapped, and one face was polished as described in section 3.5 They were mounted for the electroreflectance measurements in an identical manner to the GaAs - GaP specimens (section 4.4), and etched immediately prior to use in Wolsky etch for a few seconds.

Room temperature Hall effect measurements on three specimens showed that the ingot was n-type, with free carrier concentrations $\sim 1 \times 10^{18}$ cm^{-3} for $x = 0.8$ and $x = 0.5$ and $\sim 2 \times 10^{18}$ cm^{-3} for $x = 0.15$.

5.4 RESULTS.

Measurements were taken in the same way as for the GaAs - GaP alloys, with a modulation frequency of 75 c/s, a modulation voltage between 1.0 and 4.0 V peak-to-peak, and a d.c. bias of 1.0 to 1.5 V. Typical spectra for InAs and three of the alloys are shown in Figs. 31 and 32, GaAs having been shown in the preceding section (Fig. 22). It was found for all specimens that the surface discoloured quite quickly with modulations $\sim$ 4V, and for $x < 0.7$ the signal strength decreased rapidly with time. Small modulating voltages ($\sim$ 1.5V) lessened this problem enough to allow an hour or so of measurements, but the consequent small signal necessitated the use of the highest gain on the lock-in amplifier, so the noise level was higher than for the GaAs - GaP alloys and the InAs - GaAs alloys with $x > 0.7$. In many cases the ultra-violet structure was completely lost in noise. No measurements could be made between $x = 0.82$ and 1.00 (GaAs) because of the lack of specimens in this range.

As x is increased from o (InAs), the dip before $E_1(1)$ grows in size and finally becomes as large as $E_1(1)$, with a slight dip occasionally observable before it. As this happens, $E_1(1) + \Delta_1$ becomes small and $E_1(2) + \Delta_1$ quickly disappears. The dip before $E_1(1)$, labelled $E_1(d)$ for convenience, starts decreasing in intensity around

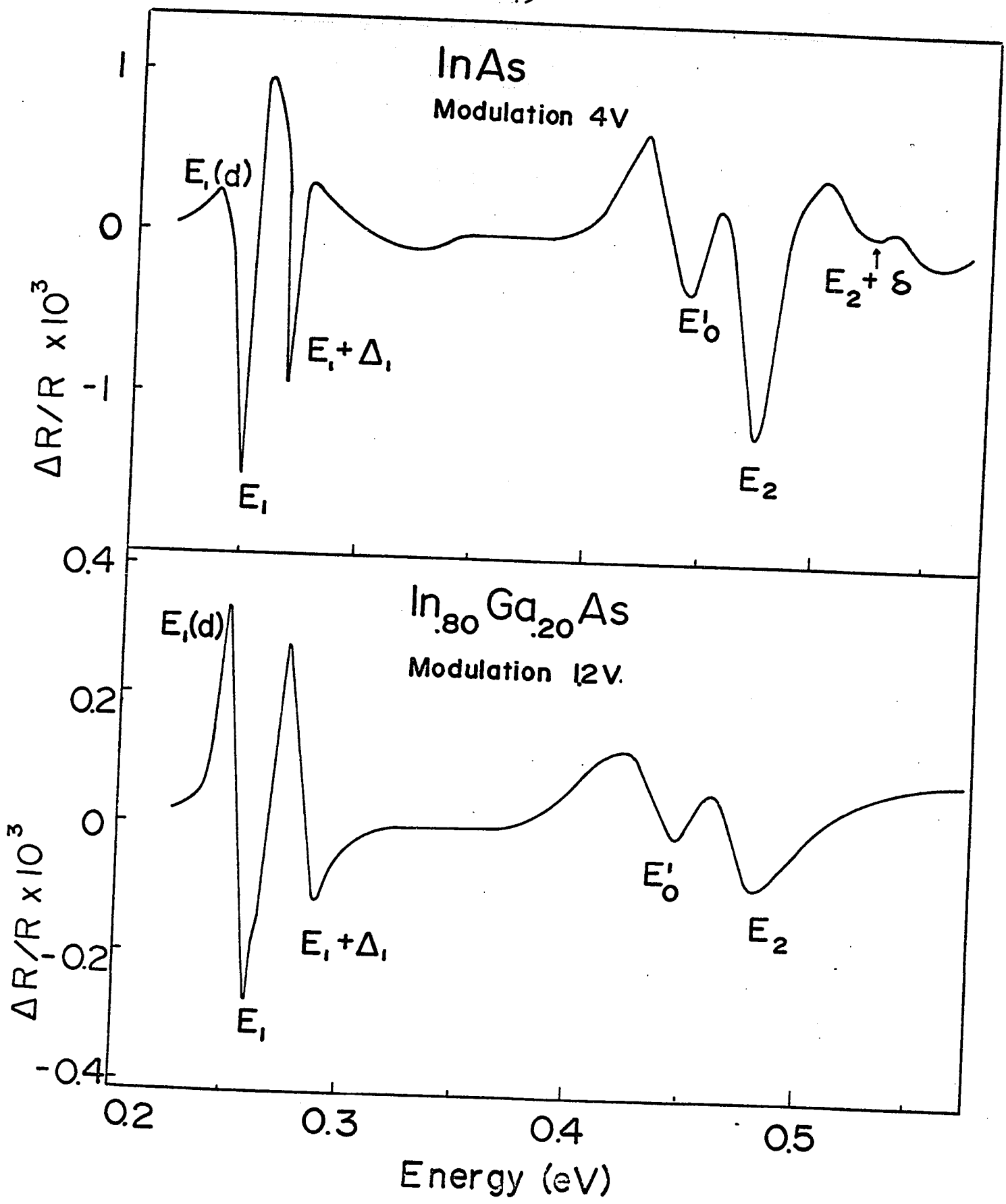

FIG 31 The Electroreflectance Spectra of $In_{1-x}Ga_xAs$ at room temperature for x = 0 and x = 0.20 .

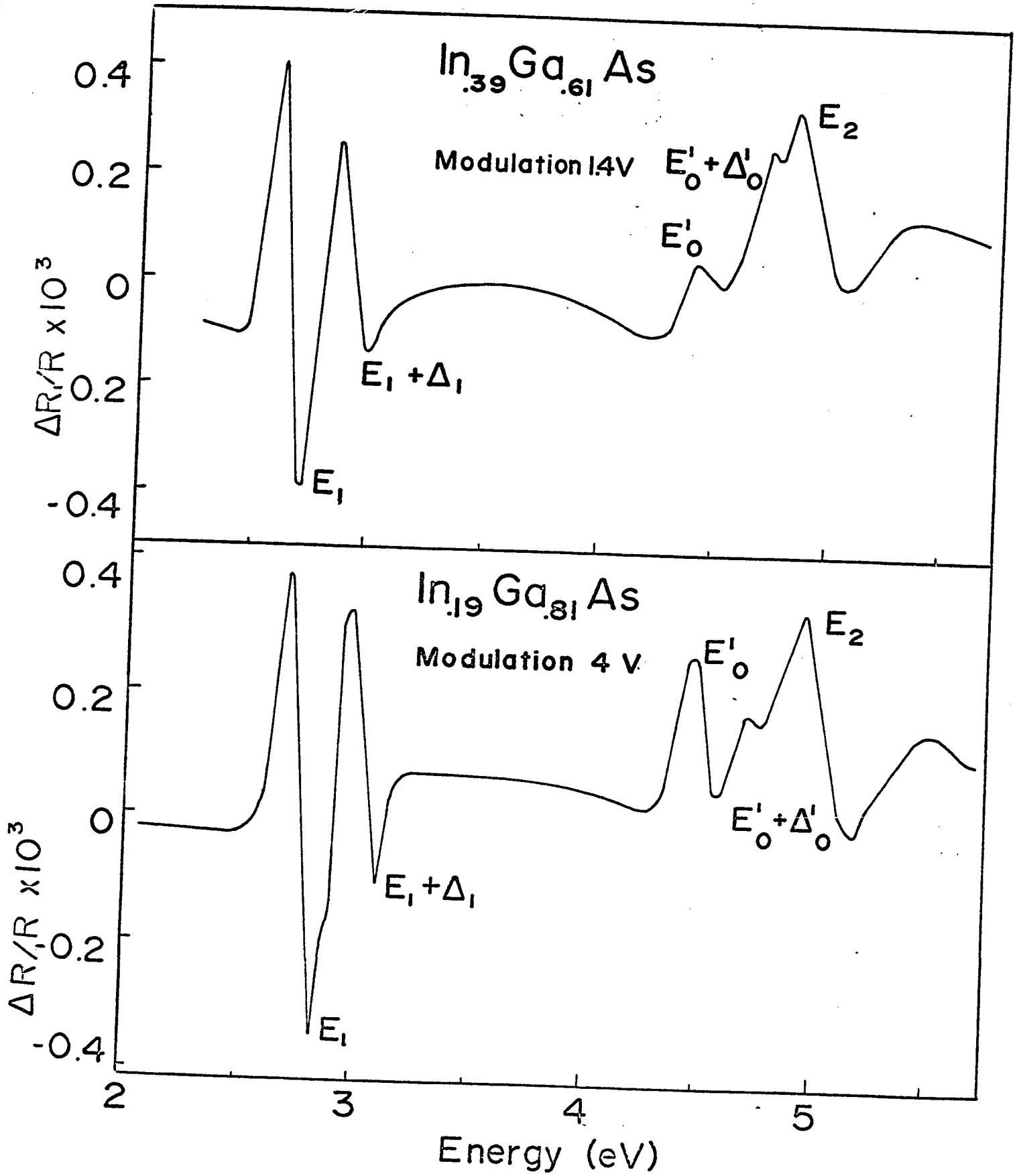

FIG 32 The Electroreflectance Spectra of $In_{1-x}Ga_xAs$ at room temperature for x = 0.61 and x = 0.81 .

$x = 0.7$, and tends to revert to the GaAs type of case where it is small. At the same time $E_1(2) + \Delta_1$ reappears. At all times the sign of $E_1(1)$ corresponded with the carrier sign of the specimen, reversing when a few p-type specimens from the directionally frozen ingot ($0.82 < x < 0.53$) were used. Due to the reasons mentioned above, the ultra-violet signals were very weak and noisy in the range $0.1 < x < 0.6$, and they seemed to be very sensitive to the d.c. bias and amplifier phase setting. The few peaks which were observed seemed to be in the opposite direction to $E_1(1)$ for $\sim 0.3 < x < 0.82$, except for two of the p-type specimens ($x = 0.71$) and $x = 0.79$) which had peaks in the same direction as $E_1(1)$. The sensitivity to bias and phase setting might mean that the E_o' and E_2 peaks were changed by one of these factors, whereas the E_1 peaks were not changed, being less sensitive. The discolouration problem prevented a satisfactory investigation of this effect.

The variation of the E_1 peak energies with composition is shown in Fig. 33. It can be seen that $E_1(1)$ and $E_1(d)$ are both linear within experimental error, and accurately project to the corresponding values in GaAs (C 49, T 12), $E_1(2)$ lies approximately 0.05eV above a line drawn between the same peaks in the compounds, with this value decreasing somewhat for small values of x. $E_1(1) + \Delta_1$ is approximately linear, but lies above the expected values by ~0.03eV. As

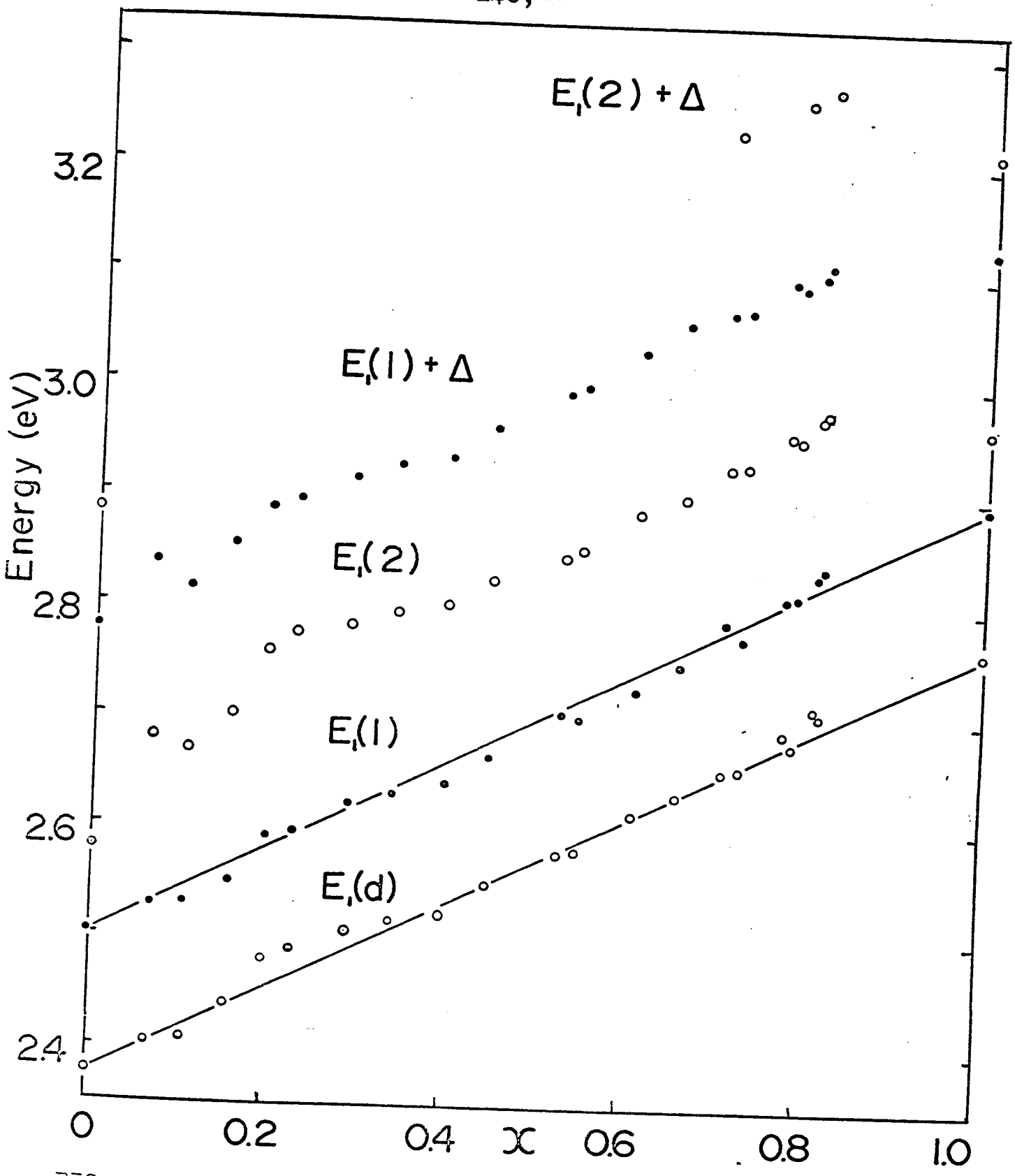

FIG 33 The Variation of the E_1 Transition Energies with Composition for $In_{1-x}Ga_xAs$.

explained earlier, $E_1(2) + \Delta_1$ was observed only in the compounds and alloys with $x > 0.7$; the alloy values lie almost 0.1eV above a linear relation between the corresponding values in the compounds. The values of

$$\Delta_1(1) = [E_1(1) + \Delta_1] - [E_1(1)]$$

are shown in Fig 34, and the large error bars (sum of inaccuracies of estimating the two peak energies from the recorder chart) are partly due to the noisy spectra obtained over most of the alloy range. $E_1(1)$ was usually accurate to ± 0.005eV and $E_1(1) + \Delta_1$ to ± 0.010eV, so most values of $\Delta_1(1)$ are accurate to ~± 0.015eV, or ± 5%. The value of $\Delta_1(1)$ can be seen to be constant at ~0.29eV. for a large range of x, falling off to ~0.28eV in InAs (probably an insignificant amount), and decreasing for $x > 0.8$ to the GaAs value of 0.23eV. The values of $\Delta_1(0) = E_1(2) - E_1(d)$ generally follow a similar form, the InAs value being ~ 0.20eV, the alloy values falling ~ .03eV below those of $\Delta_1(1)$, and GaAs having a value of 0.20eV.

The variation of the ultra-violet peaks with composition shown in Fig. 34 is somewhat less detailed than the similar graph from which values could be taken. Even so, all the transitions seemed to vary linearly with alloy composition. Typical errors in estimating these transition energies from the charts are E_o', ± 0.01eV;

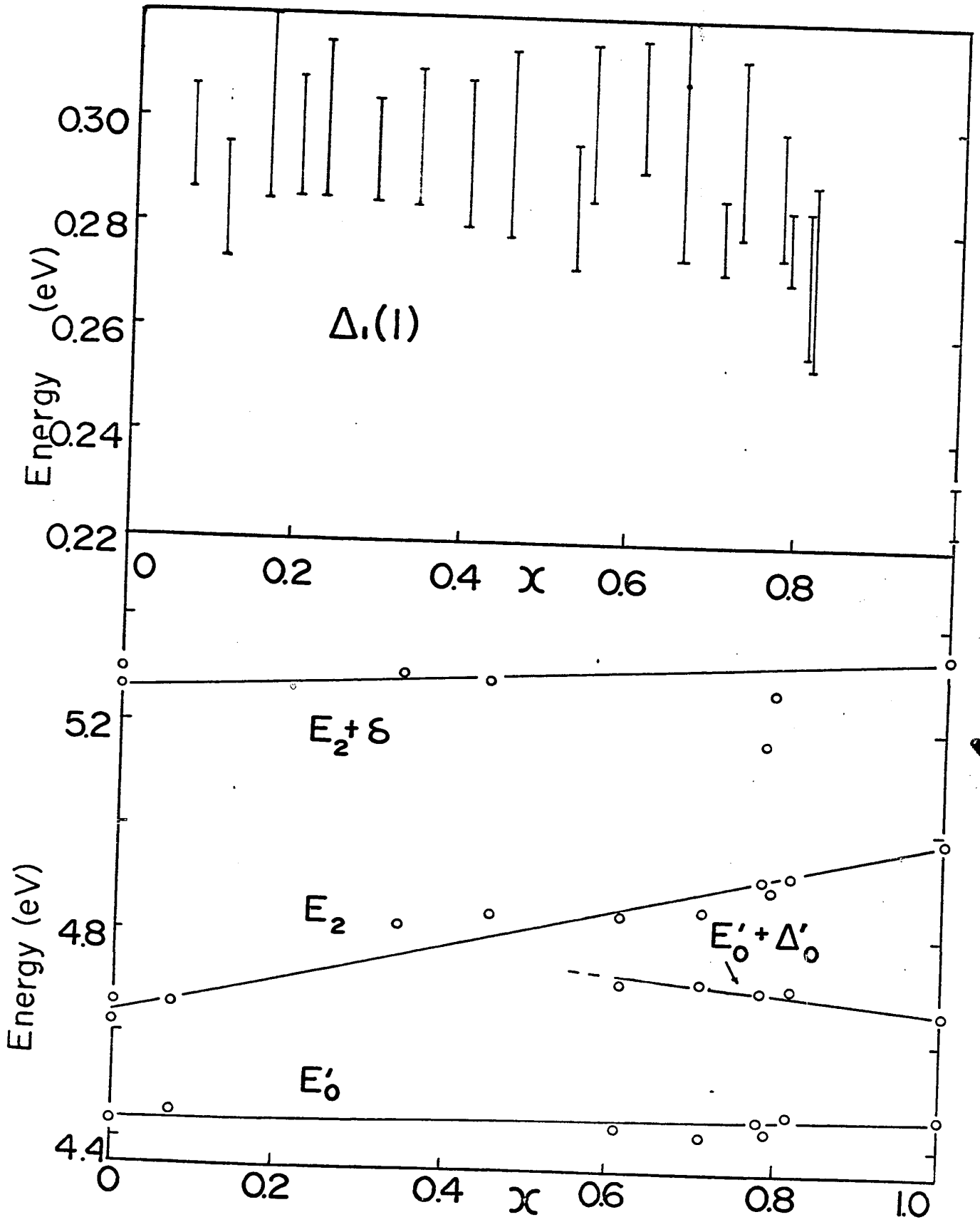

FIG 34 The Variation of $\Delta_1(1)$ and the E_o' and E_2 Transition Energies with Composition for $In_{1-x}Ga_xAs$.

$E_o' + \Delta_o'$ and E_2, ± 0.03eV; $E_2 + \delta$, ± 0.06eV. The projection of $E_o' + \Delta_o'$ leads to a value for Δ_o' (InAs) of ~0.4eV, but because of the relatively large combined error in estimating Δ_o', and the limited range of x for which the higher transition was observed, this value could vary between 0.3 and 0.6eV The E_2 splitting, δ, varies approximately linearly from 0.35eV in GaAs to 0.50eV in InAs.

All of the observed transition energies for the compounds agree well with those reported in the literature (C 49, S 46).

5.5 DISCUSSION.

The transition assignments shown in Figs 31 to 34 are all supported by the same arguments that were extended for GaAs in section 4.6.

The variation of $E_1(1)$ is linear within experimental error, as expected from the virtual crystal model. Such a variation was also observed by Woolley and Blazey (W 30), but not by Jones (J 6), in reflectance work. The variation of Δ_1 seems to be similar to that noticed in the GaAs - GaP results, being constant over part of the alloy range. It can be explained by a similar argument, except that in this case E_1 is linear. Also the anion is common instead of the cation, so Δ_o varies little (0.35eV in GaAs to 0.43eV in InAs), but $\Delta_1^?$ varies from 0.26eV (T 16) to 0.6eV (E 2). The shape of the upper valence band in the [III] direction is expected to change little between the III - V compounds, (C 37), but the lower band must change to accomodate the large $\Delta_1^?$ variation. Hence it is possible that the decreasing valence band separation as x is increased is compensated by a movement of the $E_1 + \Delta_1$ transition "Centre-of-gravity" toward the L edge It is of course possible that the E_1 transitions also move; as x is increased from 0 to 1, E_1 increases from 2 5 to 2 9eV, whilst E_o increases from 0.35 to 1.4eV. Any such movement would have to take place in a manner which keeps the variation of the E_1

transition linear with composition. As in the GaAs - GaP case, further conclusions cannot be drawn until better band structures of the compounds and alloys are available. A connection between the behaviour of Δ_1 between x = 0.8 and 1.0 and the sudden increase in E_o in the same region noted by Woolley et al. (W 15) is also a possibility.

The linear variation of E_o' with alloy composition is expected by the virtual crystal model, and had previously been demonstrated by reflectance work (W 30). The projected value of $E_o' + \Delta_o'$ in InAs gave a range of Δ_o' between 0.3 and 0.6eV; even the lowest value is still substantially higher than the 0.22eV calculated by the k.p method (C 49, P 53). The deviations between experiment and calculations usually show the calculated value to be too high, but this does not appear to be the case for InAs, although the proximity of the relatively large E_2 peak in the electroreflectance might have affected the peak positions. Both E_2 and $E_2 + \delta$ vary linearly with composition as expected by the virtual crystal model.

The accuracy of the above measurements would have been improved by the use of a low noise preamplifier ahead of the lock-in amplifier. Also measurements in the range $0.82 < x < 1.00$ would fill the missing gaps in the Δ_1 plot in particular, and possibly explain the apparent reversal

of the ultra-violet structure between GaAs and the x = 0.82 alloy specimen, especially as larger modulations may be used in this region. This would also give a better value of $E_o' + \Delta_o'$ in InAs, due to the increased range of measurements.

The use of the electroylte method of electroreflectance is limited in the infra-red by the cut-off of the water (~1eV), but measurements could be made of E_o for this system between x = 1.00 and 0.80 and of $E_o + \Delta_o$ down to x ~ 0.4. Such measurements would show if the sudden increase in E_o for x > 0.8 shown by Woolley et al. (W 15) is real, and would also give an accurate and direct value of Δ_o for InAs by a projection. (The value given in W 28 was obtained by an analysis of the infra-red absorption peaks in p-type material, and in section IV it was shown that the value of Δ_o for GaP obtained by a similar method was 20% too high).

SECTION VI

THE VARIATION OF EFFECTIVE MASSES AND ENERGY GAPS IN THE III - V ALLOYS

6.1 INTRODUCTION - EFFECTIVE MASS.

If the effect of an electric field on an electron in a crystalline solid is considered, an expression is obtained which is equivalent to Newton's second law, i.e.

$$\frac{dv}{dt} = \frac{1}{\hbar^2} (\nabla_k \nabla_k E).\underline{F}$$

The quantity $\frac{\nabla_k^2 E}{\hbar^2}$ has the dimensions of reciprocal mass, and is called the inverse effective mass tensor. Hence

$$\frac{dv_x}{dt} = \frac{1}{\hbar^2}\left(\frac{\partial^2 E}{\partial k_x^2} F_x + \frac{\partial^2 E}{\partial k_x \partial k_y} F_y + \frac{\partial^2 E}{\partial k_x \partial k_z} F_z\right) \quad \text{etc}$$

By a suitable choice of axes, the off-diagonal terms may usually be made zero, and for ellipsoidal constant energy surfaces, the tensor reduces to (for Ge in the ⟨111⟩ direction, for example)

$$\frac{1}{m^*_{ij}} = \begin{pmatrix} \frac{1}{m^*_{11}} & 0 & 0 \\ 0 & \frac{1}{m^*_{22}} & 0 \\ 0 & 0 & \frac{1}{m^*_{22}} \end{pmatrix} = \begin{pmatrix} \frac{1}{m_L} & 0 & 0 \\ 0 & \frac{1}{m_T} & 0 \\ 0 & 0 & \frac{1}{m_T} \end{pmatrix}$$

where m_L and m_T are the longitudinal and transverse effective masses respectively. The masses defined above are called band curvature effective masses, since they are directly related to the curvature of the energy band in $\underline{k}$ - space. Other definitions include the cyclotron effective mass and the density-of-states effective mass. These three definitions may be written, in order (for spherical energy surfaces, as a Γ_{1c}).

Band Curvature: $$m_1^* = \frac{\hbar^2}{(\nabla_k^2 E)}$$

Cyclotron: $$m_2^* = \frac{\hbar^2 k_F}{(\nabla_k E)_F}$$

Density-of-states: $$m_3^* = \frac{\hbar^3}{2E_F}\left(\frac{3n}{8\pi}\right)^{2/3}$$

where E_F = height of the Fermi level above the conduction band minimum,

k_F = Fermi radius, n = number of carriers/unit volume. The full derivation of and connection between these equations can be found in the standard texts (e.g. K 25, M 22; S 51) and will not be dealt with here. However, a few comments on their practical meanings will be necessary, in order to link theory and experiment later in this section.

Firstly, only for an isotropic parabolic conduction

band are the three effective masses identical. The band curvature effective mass, m_1^*, is that generally found from theoretical considerations. Optical experiments such as infra-red reflectivity, Faraday rotation and cyclotron resonance, will give the cyclotron effective mass, m_2^*, at the Fermi level. The density-of-states effective mass, m_3^*, is usually obtained from electrical measurements which give n and sometimes E_F, although it is possible to find the latter quantity from optical measurements also. This effective mass is also contained in the well known density-of-states equation:-

$$N(E)\,dE = \frac{4\pi}{h^3}\,(2m_3^*)^{3/2}\,E^{1/2}\,dE$$

The experimental results to be quoted later in this section are all obtained by optical methods, and are therefore cyclotron effective masses. By taking suitable precautions, these effective masses can be made equivalent to band curvature effective masses, so that direct comparion between theory and experiment is facilitated. These precautions usually take the form of measurements on several specimens of differing carrier concentrations, and extrapolating the results to the non-degenerate bottom of the band case. Alternatively,

if the movement of the Fermi level with doping is known, a correction factor can be applied. Such methods are usually satisfactory enough to ensure agreements within the experimental error, but a careful approach has to be made in the cases of InSb and InAs, which both have a non-parabolic conduction band and a small density of states (see Section I).

In the following sub-sections, the term effective mass will refer to the band-curvature effective mass at the bottom of the conduction band (Γ_{1c}) when quoted in a theoretical sense, and to the cyclotron effective mass corrected to the same point when quoted experimentally.

6.2 SEMI-EMPIRICAL METHODS.

The k.p method of calculating band structure, due to Kane (K 26, K 27), which was briefly described in section 1.4, is also capable of yielding the effective masses of the electrons at the bottom of the conduction band and of the holes at the valence band maxima. For these calculations one requires a knowledge of the energy gaps involved, and the momentum matrix element which couples the p - functions corresponding to the light-mass and split-off valence bands with the s - functions corresponding to the conduction band. The theory referred to above gave

$$\frac{m}{m_c^*} = 1 + \frac{2}{3}\left[\frac{P^2}{\hbar^2}\left(\frac{2}{E_o} + \frac{1}{E_o + \Delta_o}\right)\right] \qquad \text{(xix)}$$

where $P^2 = \langle \Gamma_{2'} | \underline{p} | \Gamma_{25'} \rangle^2$ for diamond-type materials.

This approach was extended by Braunstein and Kane (B 4) who found expressions for the holes in a similar form and then applied the results to the III - V compounds in general. They pointed out that P^2 is approximately constant for all the III - V's, and then used the value of m_c^* for GaAs to calculate it, since the energy gaps and effective mass were well known in this compound. The various effective masses were then calculated for the rest of the III - V compounds, and

reasonable agreement with experiment found.

Cardona extended this work by taking into account interactions by the Γ_2' and Γ_{25}' states with other levels (C 13), and in the process made the work applicable to the III - V and II - VI compounds, whereas Kane's approach was essentially applicable only to the group IV elements. In this manner expressions were derived for the effective masses at Γ (conduction and valence bands), with estimates of the same quantities at L and X. He found, for the polar materials,

$$\frac{m}{m^*(\Gamma_{1c})} = 1 + \frac{P^2}{2E_o}\left[\left(\frac{E_o' + E_{IV}}{3}\right)\left(\frac{2}{E_o} + \frac{1}{E_o + \Delta_o}\right) - \left(\frac{E_o' - E_{IV}}{E_o' - E_o}\right)\right] \quad (xx)$$

where E_o, Δ_o and E_o' refer to the energy gaps in the compound.

E_{IV} is the E_o' gap for the corresponding group IV material, and P^2 has a value of $\approx$ 23eV for the III - V compounds. Cardona was able to apply such corrections because of the great wealth of information on the higher transitions available through reflectance measurements.

The success of this formula on the III - V's prompted thoughts of applying it to the III - V alloys, since measurement of the necessary energy gaps had been made on several of the alloy systems. The lowest direct

energy gap had been found for InSb - InAs, InSb - GaSb and InAs - GaAs. By the virtual crystal model, a linear variation of energy with composition is expected for transitions not involving a sensitive level such as Γ_{1c}; this has been borne out in reflectance measurements on InSb - GaSb and InAs - GaAs (Ref 30). Equation (xx) was used to calculate the effective mass at the bottom of the conduction band, $m^*(\Gamma_{1c})$, for the three alloy systems mentioned above and for GaAs - GaP; the latter was included because reflectance measurements were being made upon it at the time.

6 3 CALCULATIONS.

The initial results (T 33) were calculated using the best values available at the time, but data acquired since then warranted a complete recalculation for this thesis. In particular, the reflectance and electroreflectance results described in sections III, IV and V and the results given in C 49 were used. Certain results were not available, and suggestions are made later in the section about this. Each of the quantities involved in equation (xx) will be discussed in turn, and the results obtained will be outlined and compared with experiment in section 6.4

E_o:- The lowest direct energy gaps for InSb - InAs (T 34, T 59), InSb - GaSb (T 5, T 12, T 16) and InAs - GaAs (T 15), were taken from the literature and had all been found by careful optical absorption measurements on good homogeneous specimens. Results by other workers for InAs - GaAs (A 2, H 45) were not used for reasons given in section 6 5. The energy gap for the GaAs - GaP alloys was taken from the electroreflectance results described in section IV and T 12. Good results have not been obtained for any other III - V alloy systems as far as the author is aware, and this fact is also commented on in section 6 5

Values of the energy gaps were taken every 0.2 mole fraction for use in the calculations.

Δ_o:- This quantity had been found only for GaAs - GaP (section IV, T 12), and was shown to be linear with alloy composition. As the virtual crystal model predicts such a variation for energy gaps involving non-sensitive levels, a linear interpolation between the values for the compounds was used in the calculations for all the systems except GaAs - GaP, where the experimental values were used.

E_o':- This energy gap had also been shown to be linear with alloy composition in InAs - GaAs (T 30, section V) and GaAs - GaP (T 12, T 16, T 42), and so linear interpolations between the best values for the compounds (C 49, T 12) were used for all the systems. As pointed out in section 4.6, the transition measured by electroreflectance accurately represents the $\Gamma_{15v} - \Gamma_{15c}$ gap.

E_{IV}:- The corresponding values of E_o' in the group IV elements (Si, Ge, α-Sn) were taken from electroreflectance (C 49, S 38), photoemission (C 28) and reflectance (C 23) measurements, a best value being chosen for each case. The values for each of the III - V compounds were found from the usual hypothetical group IV "compound" e.g. GaSb corresponds to Ge - Sn

All of the above energy gaps are room temperature values, since the only available experimental evidence of alloy effective masses were taken at this temperature. The effects of temperature on the calculation are discussed later in this sub-section. The best values of the energy gaps for the III - V compounds involved in the alloy systems of interest are listed in Table 8. Using these energy gaps, values of the momentum matrix P^2 were calculated for each compound, by substituting the best available values of the effective mass in equation (xx). Taking a mean value of P^2 for all the III - V's is pointless in alloy work, because it renders comparison with experiment difficult; only one part of the graph can agree with experiment.

The values of P^2 cover a range of 18.2 to 28.2eV, by no means constant. However, the above theories strictly apply only at 0^oK. Ehrenreich has shown (see e.g. [22]) that for $T > 0^oK$, the quantity E_o in equation (xix) (and hence (xx) also) is not identical with the experimentally determined $E_o(T)$. Instead, it is coupled with the temperature dependence of the curvature of the conduction band at $\underline{k} = 0$ By assuming that $m^*(\Gamma_{1c})$ remains approximately constant as the temperature is lowered to $\approx 0^oK$, and that the usual temperature

TABLE 8 Data used in Alloy Effective Mass Calculations

Compound	E_c(eV)	Δ_o(eV)	E_o'(eV)	E_{IV}(eV)	$\frac{m^*}{m}(\Gamma_{1c})$ exp.	P^2, calc.
GaP	2.75	0.10 (T12)	4.78	3.3	0.135 (P53)	28.2
GaAs	1.43	0.33 (T12)	4.46	3.2	0.067 (C4)	26.2
GaSb	0.72	0.80 (C49)	3.27	2.7(5)	0.047 (H47, Z6)	19.7
InP	1.34	0.10 (C49)	4.72	2.8(5)	0.073 (E1)	24.2
InAs	0.353	0.42 (M28)	4.44	2.7(5)	0.027 (C4)	21.2
InSb	0.183	0.80 (C49)	3.16	2.3	0.015 (C13)	18.2

coefficients apply, new values of $P^2(0^oK)$ can be calculated (Λ_o is assumed not to vary with temperature, see S 46).

For InSb, $\frac{m^*(\Gamma_{1c})}{m}$ = 015, $P^2(0^oK)$ = 26 3 (cf with 18 2)

For GaAs, $\frac{m^*(\Gamma_{1c})}{m}$ = 069, $P^2(0^oK)$ = 28 0 (cf with 26 2)

Thus on lowering the temperature from 300°K to 0°K, the value of P^2 increases by 45% for InSb and 7% for GaAs The only quantity which drastically affects m* (or P^2) on changing the temperature is the fundamental gap E_c; in both of the above cases, the percentage increase in the energy gap is almost the same as the resulting change in P^2, if m* is held constant In practice the effective mass varies with temperature, but the literature often reports conflicting results For InSb, most authors show a decrease with increasing temperature (e g M 22, S 57), whilst for InAs and GaAs (C 4) and InP (C 19), a slight increase was obtained Some Russian work (U 1) showed large increases (8 to 15%) as T was raised from 100°K to 300°K for InSb, InAs and GaAs As pointed out by Cardona et al (C 52) an increase in m* with increasing temperature is usually expected because of the non-parabolicity of the conduction band However, the thermal expansion of the lattice affects the band structure, and

the net result is usually a small increase or decrease. Therefore the above approximation ($m^* \sim$ constant) is a reasonable one for most III - V compounds.

6 4 RESULTS.

The results are shown in Fig. 35. The first impression is that the curves have similar forms to their respective energy gap variations with alloying. This, of course, is to be expected, since equation (xxi) shows that $\frac{m^*}{m}$ is proportional to E_o to a first approximation. A plot of $\frac{m^*(\Gamma_{1c})}{m}$ against E_o for the III - V compounds yields a linear relation of the form (W 33).

$$\frac{m^*(\Gamma_{1c})}{m} = K.E_o, \quad \text{where } K \sim 0.05eV^{-1} \qquad \text{(xxi)}$$

The deviation from linearity is therefore expected, and proportionally is almost the same as that of the energy gap variation. The four systems will now be discussed.

InSb - InAs:- This system has the largest deviation, and the non-linear variation should therefore be the most easily detectable. The only experimental evidence available to date is that by Potter and Kretschmar (P 20) from thin film work. These films had high carrier concentrations ($2 < n < 10$, $\times 10^{\xi}$ cm^{-3}), and the calculations gave values of $\frac{m^*}{m\gamma_F}$, where

$$\gamma_F = \left(1 + \frac{E_F}{E_o + 2/3\,\Delta_o}\right) \Big/ \left(1 + \frac{E_F}{E_o + \Delta_c}\right) \text{ and } 1.0 < \gamma_F < 1.5$$

The values of E_o estimated by Potter and Kretschmar were very high because of the high carrier concentrations, and

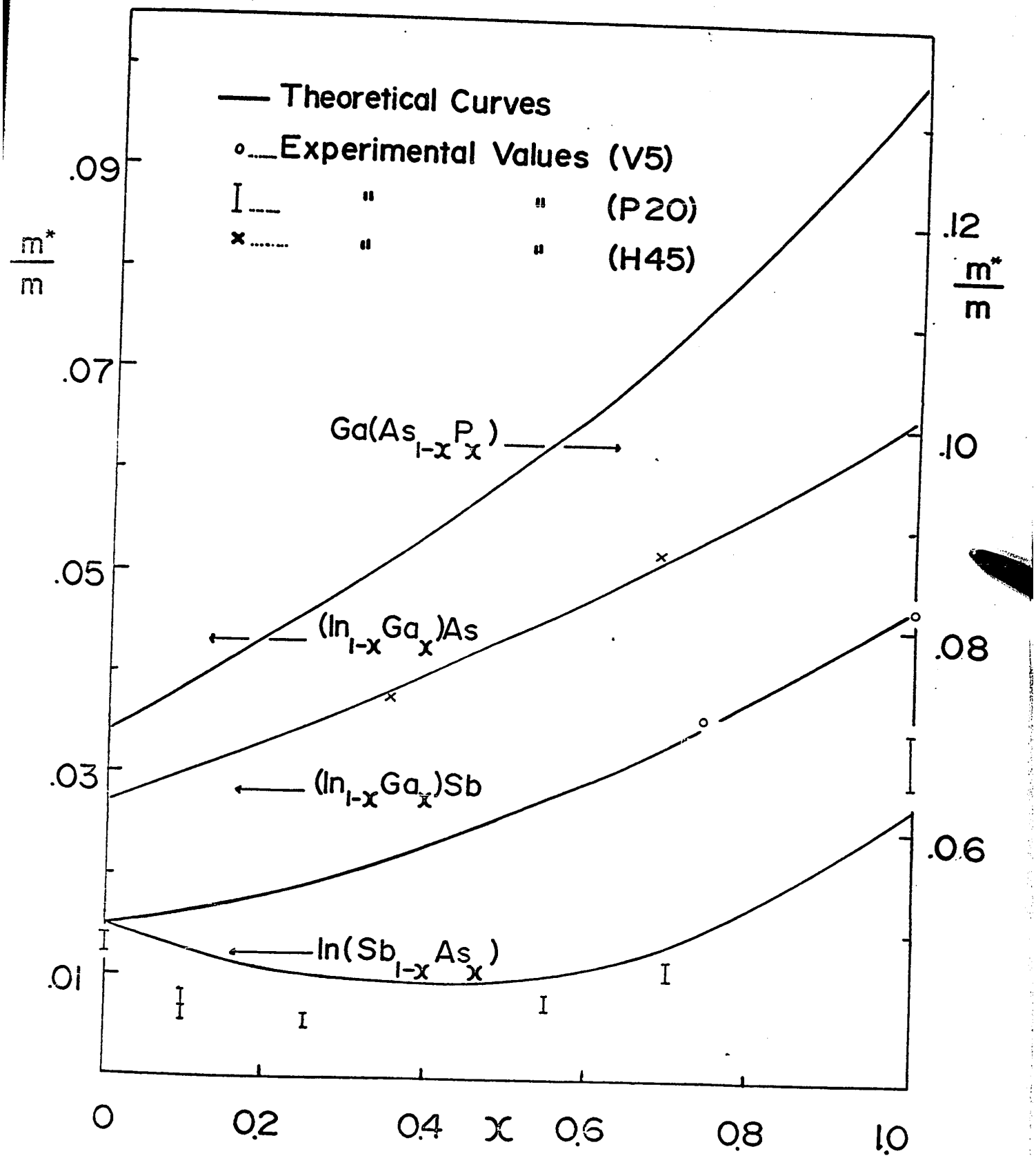

FIG 35 The Theoretically Predicted Variation of the Effective Masses of Four III-V Alloy Systems. Experimental data is also shown.

their values of $\frac{m^*}{m\gamma_F}$ were therefore of little use in determining the variation with alloy composition. As γ_F depends on E_F, its value depends on the carrier concentration, but Woolley et al (W 25, W 44) have shown that the Fermi position is high in highly degenerate InSb and InAs. Values of effective mass were therefore recalculated from P 20, using $\gamma_F = 1.25$ and $\gamma_F = 1.50$ and non-degenerate energy gap values (W 34). The resulting pairs of values are shown as the ends of error bars in Fig. 35. Although the agreement is not good, it is sufficient, bearing in mind the large experimental error, to show that the form of the calculated curve is reasonable. It is hoped that Faraday rotation measurements, on specimens having low carrier concentrations, being made in this department by Van Tongerloo, will yield more substantial proof.

InSb - GaSb:- The non-linearity in this system is also quite large, and the initial results of Van Tongerloo (V 5) using Faraday rotation show a good agreement with the theoretical curve. When combined with magnetoresistance measurements, Faraday rotation is capable of giving very accurate values of the effective mass, because the number of carriers in the (000) conduction band (N_o) can be found with much greater precision than by the Hall effect.

InAs - GaAs:- The only proof for this curve comes from

the two points given by Hockings et al (H 45). Their analysis, which used Cardona's method (C 4), on good homogeneous specimens, yields values which are probably good to ± 5% which are shown in Fig. 35. Therefore more measurements, made with high accuracy, are needed to really show the deviation expected by theory.

GaAs - GaP:- The amount of deviation for this system is the smallest of the four considered. The recent experimental results obtained by Hill (H 46) show an approximately linear variation of $\frac{m^*}{m}$, with a rate of increase with x about twice that expected, in the range $0 < x < 0.3$. Found from an analysis of free-carrier contributions to the electric susceptibility, these results are based to some extent on estimated values of the electrical properties of the alloys. Since the proximity of the higher bands will have a marked effect in this range, it was felt that a two-band analysis was necessary to give good results, and magnetoresistance measurements are currently being made by Kwan of this laboratory. When they are available, more satisfactory calculations of the effective mass may be made using Hill's data. It is also hoped that such a two-band analysis may be made with Faraday rotation and Vóigt effect measurements to find the effective mass over the entire alloy range.

6.5 ALLOY ENERGY GAP ANOMALY.

When the above effective mass calculations were being made, it was noticed that the form of the energy gap of the alloy systems considered always deviated from linearity in a concave manner. As pointed out by Mott and Jones (M 29), and extended by Parmenter (P 47), any deviations from the linearity predicted by the virtual crystal model should be due to the second order perturbation, and be proportional to the mean square deviation of the random perturbing potential from the average potential, V_{av}. Consider an alloy of x mole fraction of material A and (1 - x) mole fraction of B.

Then, $$V_{av} = xV_A + (1 - x)V_B$$

Deviations from V_{av} are

$$V - V_A = (1 - x)(V_B - V_A)$$

and $$V - V_B = x\,(V_A - V_B)$$

The probabilities of A or B materials being involved in a process (scattering, energy change etc.) are proportional to $(1 - x)^2$ and x^2 respectively. Hence the total probability is proportional to,

$$[x\,(1 - x)^2 + (1 - x)x^2] = x(1 - x).$$

i.e. Higher order effects predict a $K = x(1 - x)$ variation, where K = a constant, besides the linear variation predicted

by V_{av} alone.

This conclusion was first applied to the energy gaps of semiconducting alloys by Cardona (C 20), who measured the optical properties of the silver and cuprous halides and their alloys. He found reasonable agreement between a fitted curve of the form,

$$\Delta_2 E = C.x(1 - x) \qquad \text{(xxii)}$$

plotted as a deviation from linear behaviour, and the experimental results, for several of the excitonic peaks.

As far as the author was aware, no attempt had been made to investigate the form and magnitude of the deviation from linearity of the fundamental energy gaps of the various III - V alloy systems. In the light of the above predictions, parabolic expressions were fitted to the values of E_o for four alloy systems, (InSb - InAs, InSb - GaSb, InAs - GaAs and GaAs - GaP), of the form

$$E_o = A + Bx + Cx^2 \qquad \text{(xxiii)}$$

where x = mole fraction of compound #2.

$A = E_o$ for compound #1.

and $D = A + B + C = E_o$ for compound #2.

Then C is equivalent to the C obtained by Cardona (see equation (xxii)), and is equal to four times the deviation from linearity at x = 0.5.

InSb - InAs:- Two fits were made to the curve shown in Fig. 36, one for the optical absorption points and one for the same points plus some diffuse reflection data, the latter being shown as error bars. All data was taken from W 59, and corrected to a temperature of 290°K (see also W 34). Due to the large possible error in the diffuse reflection measurements, and the poor homogeneity of specimens in the range x = 0.5 to 0.6, it was felt that the first fit was more realistic; this is the solid line in Fig. 36. The small differences between the two fits can be seen in Table 9, which shows the values of A, C and D.

InSb - GaSb:- Two fits were made in this case also. The first involved optical absorption results taken at several different temperatures, a room temperature extrapolation being used (W 16). The second fit involved these points plus all those taken previously (at room temperature only), which are given in W 6 and W 12. Due to the large number of experimental points shown in the latter references, the equation fitted to the combined results is the one shown in Fig. 36. Again, both equations are represented in Table 9, and the difference is small. The correlation between the experimental points and the fitted curve can be seen to be very close.

InAs - GaAs:- The data used here is given in W 15, and

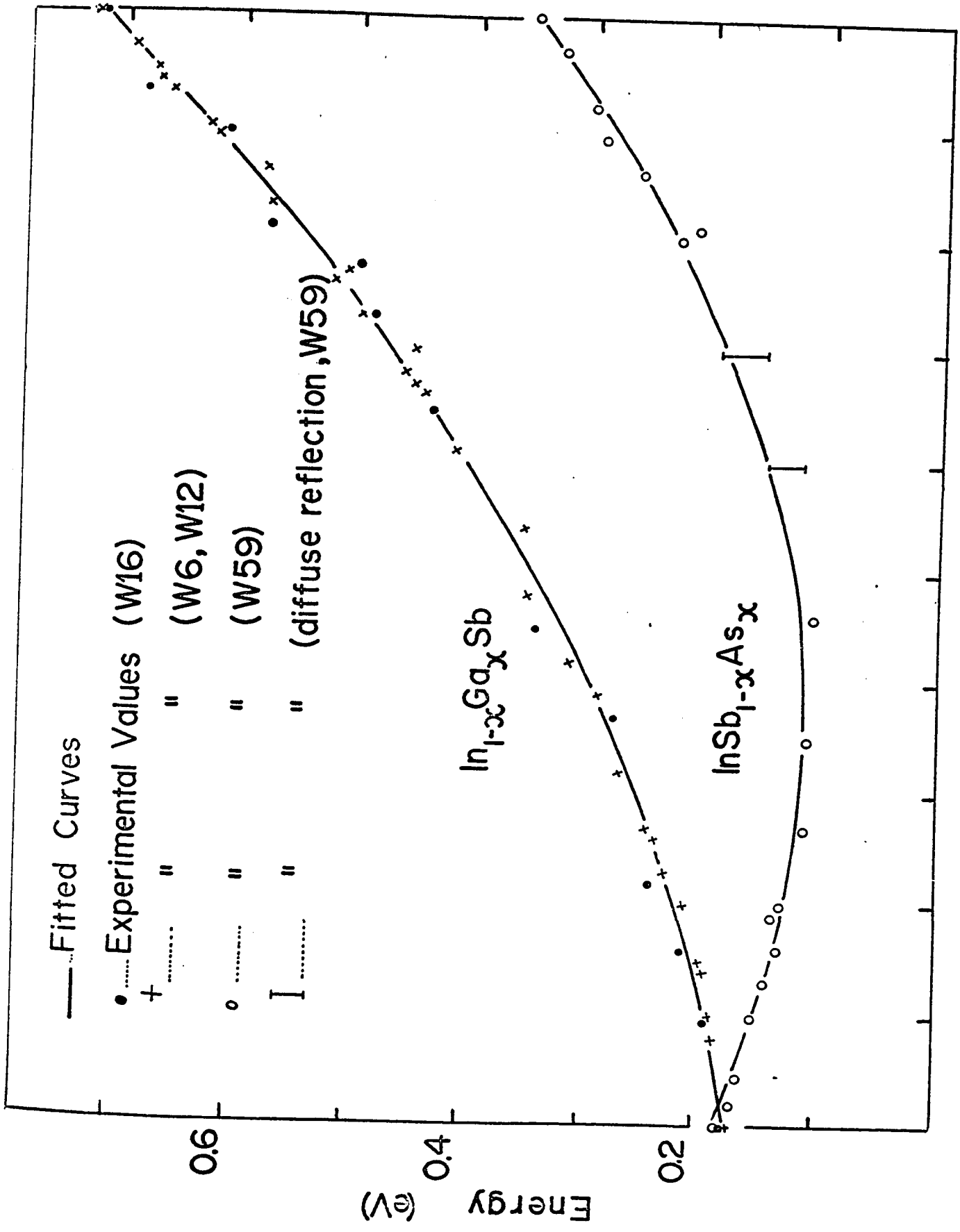

FIG 36 Variation of E_o for $InSb_{1-x}As_x$ and $In_{1-x}Ga_xSb$ with fitted curves.

is shown in Fig. 37. The parabolic fit is quite reasonable, in spite of the previous interpretation of a linear part (x = 0 to 0.8) and a sharp curve (at the GaAs end), expecially when it is borne in mind that the GaAs-rich specimens were annealed solid ingots which showed a large spread in composition. The graph obtained by Abrahams et al (A 2) was not used because their specimens were fairly inhomogeneous and the data showed a large scatter. Recent measurements by Hockings et al (H 45) show less scatter then the results of Abrahams et al, but the deviation from linearity is greater than that obtained by Woolley's group. This will be commented upon later, but both sets of values are shown in Table 9.

GaAs - GaP:- These results were obtained from electroreflectance measurements, and have been discussed previously (sections 4.5 and 4.6). The quality of the parabolic fit was good (see Fig. 25) for both the E_o and $E_o + \Delta_o$ transitions, so both are included in Table 9. Optical absorption measurements have not given the variation of the direct gap very accurately, because of the influence of the nearby indirect transition. Any small deviation of a concave nature is probably compensated as x increases by the increasing proximity of the indirect transition. This can be seen in the literature; as the

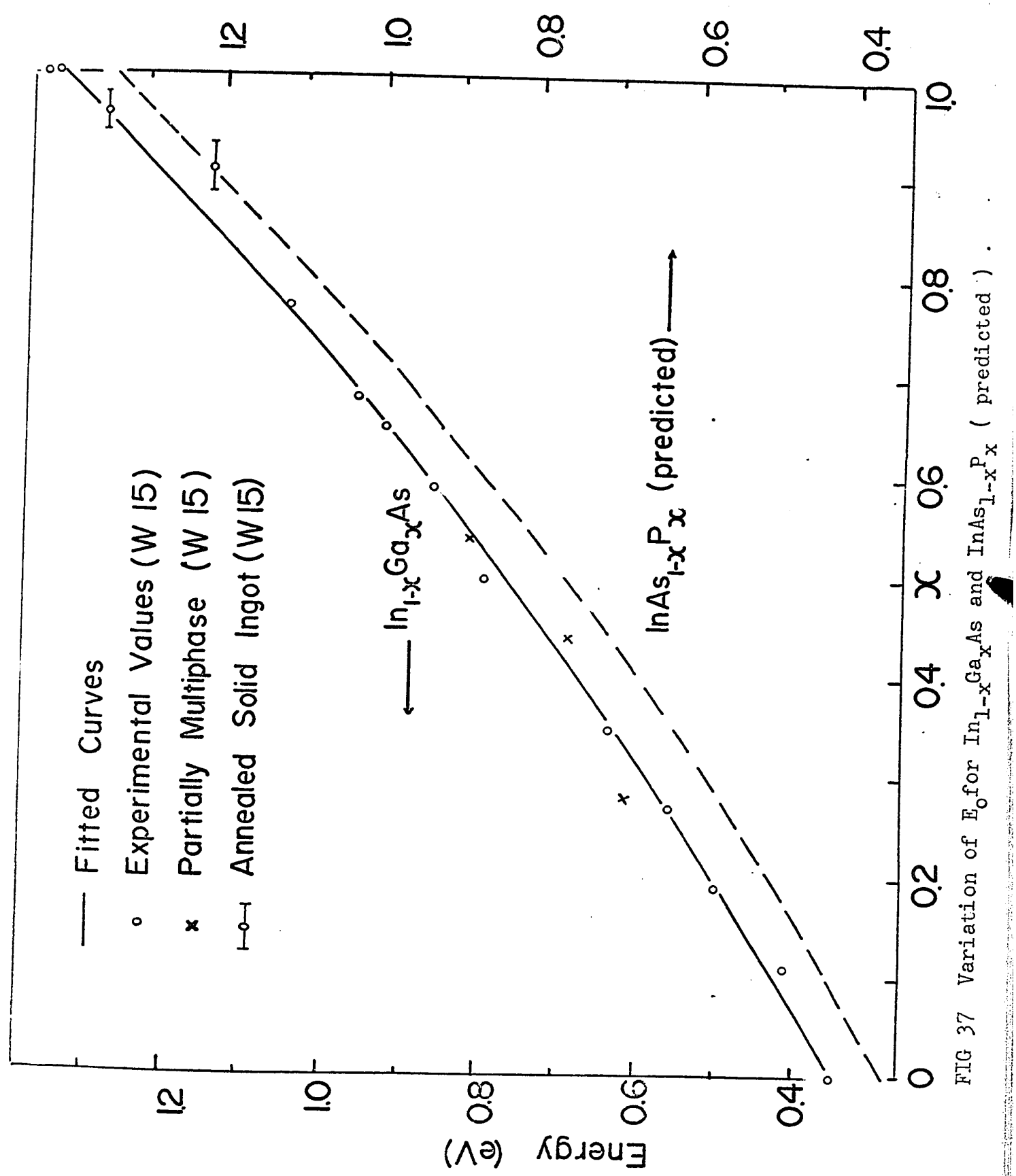

FIG 37 Variation of E_o for $In_{1-x}Ga_xAs$ and $InAs_{1-x}P_x$ (predicted) .

TABLE 9: Fitted energy gap Equations and References.

Alloy System	References	A (eV)	D (eV)	C (eV)	Measurements
InSb - InAs (1)	W 34, W 59	0.182	0.354	0.585	Opt. absorption
(2)	W 34, W 59	0.185	0.354	0.606	Opt. Absorption & Diff. Refl.
InSb - GaSb (3)	W 16	0.183	0.722	0.433	Opt. absorption
(4)	W 6, W 12, W 16	0.173	0.719	0.402	Opt. absorption
InAs - GaAs (5)	W 15	0.350	1.342	0.280	Opt. absorption
(6)	H 45	0.36	1.35	~0.6 (see text)	Opt. absorption
GaAs - GaP (7)	T 12	1.441	2.742	0.210	Electroreflectance
(8)	T 12	1.776	2.842	0.182	Electroreflectance
InAs - InP (9)	(C 49)	0.35	1.34	see text	-

Table 9. Coefficients of the parabolic equations fitted to some of the III - V compound alloy systems, (except (6) and (9)), with references for the source of the basic data and the method of measurement.

quality of the specimens and absorption edge analysis improved, the portion of the curve between x = 0 and 0.5 varied from convex to linear (F 1, A 1, P 52, R 8, in order of increasing quality). The optical absorption results of Subashiev and co-workers (A 7, S 30) showed all the minima, but as they took only a few points (mostly for $x > 0.7$) and assumed linear variations for the energy gaps, their results are not incompatible with the electroreflectance data. A recent paper by Neuse et al (N 7) showed the variation of the stimulated emission energy of alloy lasers with alloy composition; they obtained a curve of similar form to that mentioned above (Fig. 25). The photoresponse method of Spitzer and Mead (S 8) shows a linear variation of the direct gap with good accuracy. It is possible that their values for the compounds (GaP in particular) are too low, which would then lead to a concave deviation.

InAs - InP:- Early optical (F 1) and electrical (N 20) results indicated a linear variation of E_o with alloy composition, but few points were taken, and on specimens of doubtful homogeneity. A complete optical investigation by Oswald (O 4) showed that E_o varied linearly with temperature ($100^oK < T < 500^oK$), and with composition (for a given temperature). Only three alloy specimens were used,

and if modern values for the energy gap of InP (C 49) are substituted, the three alloy values fall below the linear variation between the compounds. Dubrovskii's results (D 1) were crudely analysed, and taken on inhomogeneous and structurally poor specimens. Results from experiments on spontaneous and stimulated emission in alloy diodes (A 3), using good values for the compounds (M 5, W 24), indicate that the energy gap falls below a linear variation by about 0.07eV for an alloy of equimolar composition. In the next sub-section it is proposed that this alloy system should also exhibit a concave deviation from linearity, but because the results are somewhat conflicting, no attempt was made to fit a parabola to any of them.

In none of the other III - V alloy systems has the direct gap been measured over a wide enough composition range and/or with great enough precision to be included in the above work. This is due to either a lack of high quality measurements, the difficulty of preparation, or the presence of an indirect lowest gap in one of the constituents (although the latter need not necessarily be a problem if electroreflectance measurements are feasible).

6.6 GENERAL FORMULA FOR III - V ALLOY ENERGY GAP ANOMALY.

It can be seen in Table 9 that the variation of the degree of departure from linearity, C, seems to depend on the energy gaps of the constituents of the alloy system i.e. as the combined energy gap (= A + D) increases, C decreases. An empirical investigation revealed the fact that C varied inversely as the square root of the mean energy gap i.e.

$$C = \frac{a}{\frac{1}{2}\sqrt{(A + D)}} = \frac{a}{\sqrt{E_o\ (\text{mean})}} \qquad \text{(xxiv)}$$

where a is a constant for the III - V compounds. A plot of the two quantities C and $\frac{1}{\sqrt{E_o\ (\text{mean})}}$ showed a linear relation passing through the origin, having a slope "a" of approximately $0.3 eV^{3/2}$ (Fig. 38). On this diagram the numbers associated with the different points correlate with those referred to in Table 9.

It is difficult to believe that the relation (xxiv) is completely fortuitous. However, further proof is needed before the equation can be quoted as a "law".

Most of the InAs - InP results mentioned in the previous sub-section are felt to be insufficiently accurate and/or insufficiently numerous to show the deviation from linearity accurately. It is interesting to note that

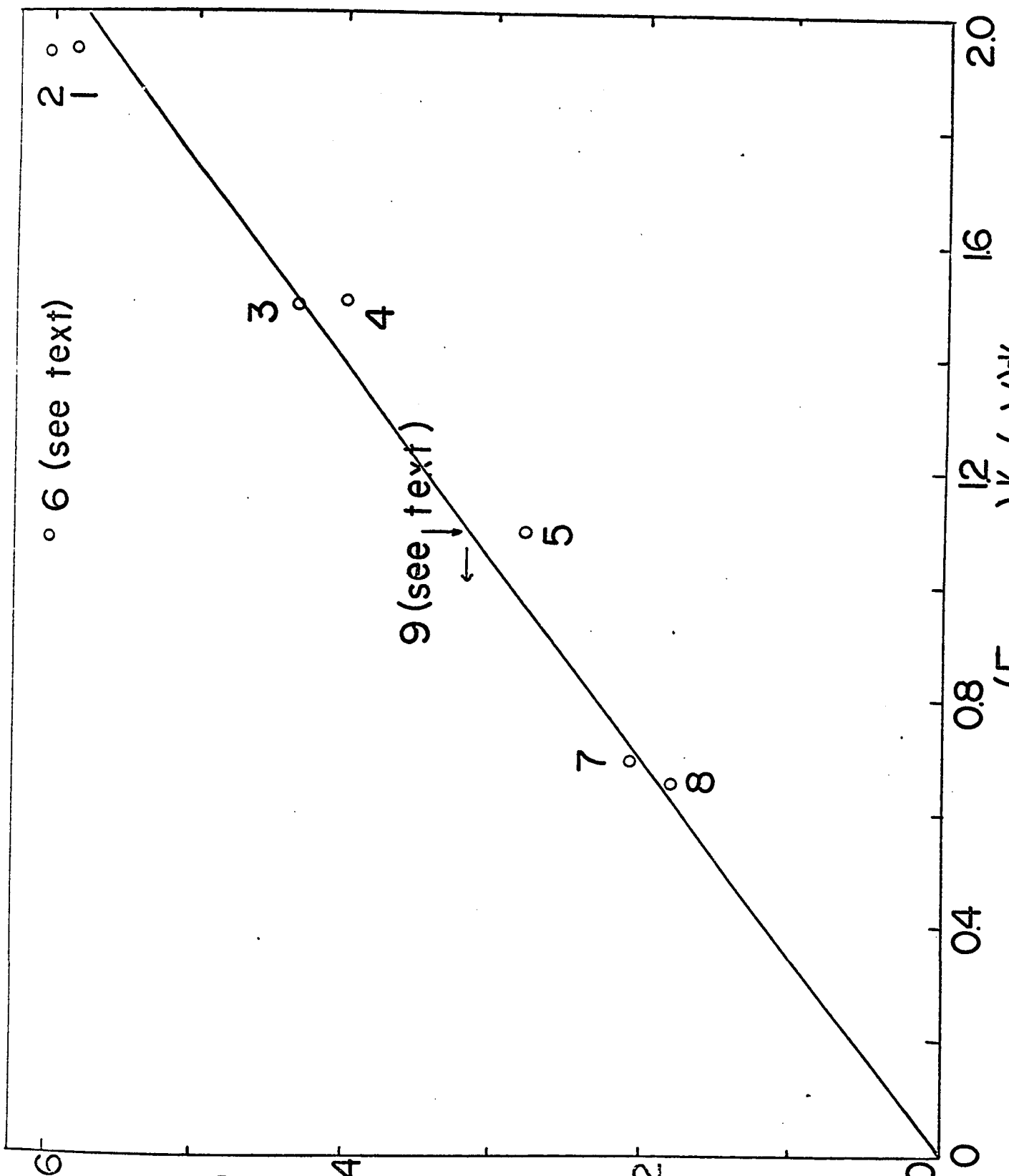

FIG 38 The Variation of C with E_o , (mean) for the III-V Alloys 9 see text).

if the above relation holds, the value of C can be predicted for any III - V alloy system, providing the energy gaps of the compounds are known. For InAs - InP, using the values shown in Table 9 (and Fig. 38), the value of C should be $\approx$ 0.32eV i.e. the maximum deviation from linearity should be $\approx$ 0.08eV at x = 0.5, an easily detectable quantity if good absorption or electroreflectance measurements are made. The curve predicted by such an analysis is shown in Fig. 37, and is seen to closely follow the InAs - GaAs results. Whilst the bulk of the available experimental results (see section 6.5) disagree with this curve, those of Alexander et al (A 3) appear to be very precise, and indicate the possibility of a deviation of this magnitude

The results of Hockings et al (H 45) mentioned in the previous sub-section also follow an approximately parabolic variation with C being of the order of 0.6eV (judged from a small graph). The results were all taken between x = 0.3 and x = 0.7, so it is possible that an unsufficiently accurate absorption edge analysis was performed The results of Minden (M 12) on luminescent diodes at 77°K indicate a value of C $\simeq$ 0.4eV, which is much closer to that obtained by Woolley et al (W 15).

In connection with these last few comments, it is interesting to note that experiments performed on less homogeneous alloys yielded larger deviations from linearity in the E_o plot than good specimens did (e.g. compare A 2 and H 45; I 5 and J 12). It is therefore possible that the experiments reporting larger deviations than expected utilised specimens which were insufficiently homogeneous.

6 7 DISCUSSION.

The applicability of Cardona's effective mass formula to the alloys has been demonstrated, although more results are needed, particularly on the InAs - GaAs and GaAs - GaP systems, before its general use can be advocated. Since such a relation seems reasonable, there seems little doubt that these results will bear out the theory. Accurate measurements now in progress on the InSb - InAs and InSb - GaSb systems should furnish the strongest proof, as the deviation is most marked in these alloys.

A more precise way of calculating these effective masses would be to apply a full k.p analysis, as used in P 53 for the III - V compounds, to the alloys. The variation of the various energy gaps with composition is either well known (E_o), or is linear between the corresponding values in the compounds (Δ_o, E_o', E_1 etc). Hence such an approach would be feasible As the first-principles type of band calculation has yet to prove accurate for the compounds, there is little point in attempting to apply it to the alloys.

The variation of the quantity C with energy, demonstrated in the preceding section and Fig. 38, is interesting, and the results sufficient to warrant a

theoretical investigation Further experimental work of a confirmatory nature might prompt such a study, and some of the III - V systems which yield reasonably large deviations are (with the predicted value of C in paraentheses).

InAs - InP (0.32eV)

GaAs - GaSb (0.28eV)

InP - GaAs (0.24eV)

Other systems which involve a component having an indirect gap are.

InSb - AlSb (0.27eV)

GaSb - AlSb (0.24eV)

InP - GaP (0.22eV)

Whilst some of these cannot be measured in full with the electrolyte electroreflectance technique, Seraphin's technique or optical absorption measurements (for the direct-gap systems) could be used. Some suggestions for future lines of approach to this problem are made in the next section.

SECTION VII

CONCLUSIONS

7.1 SUMMARY OF RESULTS.

Apparatus was constructed to measure the relative reflectance of small semiconductor specimens to a high degree of precision. Results on the GaAs - GaP alloy system at room and liquid nitrogen temperatures (J 42) led to a revised band structure for GaP that was later confirmed by photoemission experiments and band structure calculations. High energy (> 4eV) reflectance results on the same alloy system were also made (T 16)

Electroreflectance measurements on the GaAs - GaP system yielded more accurate results than those obtained by reflectance (T 12), and combined with the high energy reflectance results provided some interesting results on the magnitude of the valence band splitting in the L direction from the zone centre to the edge. General conclusions concerning the valence band splitting at Γ, Δ and L for the III - V compounds were then made, and the contributions of the cation and anion to these splittings examined.

Alloys of the InAs - GaAs system were prepared by a directional freeze technique and found to be satisfactory over only a limited range of composition. A new technique, named travelling freeze, was developed and tried,

and found to give specimens over most of the composition range with a greater homogeneity than had been obtained by directional freezing. Apparatus similar to that used for the electroreflectance measurements on the GaAs - GaP alloy system was set up. Measurements of the electroreflectance spectra of InAs - GaAs alloys then allowed further conclusions to be made on the band structure of the alloys compared with previous reflectance work (W 30).

The utility of alloy investigations in determining the properties of the constituent compounds, as well as of the alloys, has been demonstrated in the past (e.g. M 22, W 53), and is substantiated by the above work. The use of electroreflectance for the first time in alloy investigations yielded precise results (T 12), and was shown to be a powerful tool in optical work, having several advantages over normal reflectance techniques.

Some semi-empirical calculations were made of effective masses in some typical III - V alloy systems, and compared with the limited amount of experimental data available. An empirical formula for the variation of the fundamental energy gap in the III - V alloys was developed, and variations predicted for the systems for which experimental data is not avilable.

In the next sub-section suggestions are made for

future lines of research which would complement the above investigations and further the work of this group on semiconducting alloys involving the III - V compounds.

7.2 FUTURE WORK AND SUGGESTIONS.

Some suggestions have already been made at the end of sections III - VI. These will be summarised and additional suggestions made

GaAs - GaP:- Electrical work designed to make Hill's effective mass calculations (H 46) more accurate is presently being performed in this laboratory. It is hoped that two-band Faraday rotation measurements will also yield good values of the effective masses.

InAs - GaAs:- The preparation of the GaAs - rich ($0.8 < x < 1.0$) alloys is feasible by the travelling-freeze method, and will be tried. Such specimens would be capable of confirming through electroreflectance measurements the missing parts of Figs. 33 and 34, but more important, would give the variation of E_o and $E_o + \Delta_o$ in this region, which could be compared with the optical absorption results (J 15 in particular). In this connection, it will be noted that an electrolyte having a low energy cut-off of less than 1eV would be extremely useful for electroreflectance measurements of E_o and $E_o + \Delta_o$ on the III - V compounds and alloys.

Other Systems:- In the light of the InAs - GaAs results (E_1 complex in particular), electroreflectance measurements on the InSb - InAs, InSb - GaSb, InAs - InP etc.

alloy systems should give interesting results; the first of these is capable of giving an accurate value of E_o' in InAs.

High-energy reflectance data would be capable of substantiating some of the suggestions made in section 4.6. Any experimental results on the variation of effective masses and fundamental energy gaps in the III - V alloys would be useful in extending the calculations made in section VI.

Finally, the need for the further theoretical work on the virtual crystal model and the band structure of the semiconducting III - V alloy systems should be stressed. Experimental methods have become accurate and results are numerous; satisfactory quantitative explanations are lacking for many of these results, and so any theoretical work on the alloys which is capable of reducing such a backlog would be most welcome.

REFERENCES

In the list that follows, the following abreviations are used for the Proceedings of the International Conference on Semiconductor Physics.

Prague - 5th Conference, Prague (1960);
Academic Press, N.Y.

Exeter - 6th Conference, Exeter (1962);
The Institute of Physics & the Physical Society, London.

Paris - 7th Conference, Paris (1964);
Dunod, Paris and Academic Press, N.Y.

A 1. J.J. Allen, J.W. Hodby.
Proc. Phys. Soc., 82, 315 (1963)

2. H.S. Abraham, R. Braunstein, F.D. Rosi.
Jnl. Phys. Chem. Solids, 10, 204 (1959)

3. F.B. Alexander et al.
Appl. Phys. Letts, 4, 13 (1964)

5. N. Kinslie, M. Pilkuhn, H. Rupprecht.
Jnl. Appl. Phys. 35, 105 (1964).

A 7. S.A. Abagyan, A.V. Lishina, V.V. Subashiev.
Sov. Phys. Sol. State, 6, 2266 (1965)

9. S.A. Abagyan, V.V. Subashiev, S.P. Singkhal.
ibid. 7, 153 (1965)

11. J.W. Allen et al.
Appl. Phys. Letts. 7, 78 (1965)

13. E. Adler, E. Erlbach.
Phys. Rev. Letts, 16, 67 (1966)

17. Ya. Agaev, D.N. Naseldov.
Sov. Phys. Sol. State, 2, 758 (1960)

19. R.L. Aggarwal, L. Rubin, B. Lax.
Phys Rev Letts, 17, 8 (1966)

20. D.E. Aspnes.
Phys. Rev., 147, 554 (1966)

B 2. F. Bassani, D. Brust.
Phys. Rev., 131, 1524 (1963)

4. R. Braunstein, E.O. Kane.
Jnl. Phys. Chem. Solids, 23, 1423 (1962)

B 7. F Bassani, M Yoshimine.
Phys. Rev., 130, 20 (1963)

10. W.M. Becker, A.K. Ramdas, H.Y. Fan.
Jnl. Appl. Phys, 32, 2094 (1961)

12. D. Brust.
Phys. Rev., 134A, 1337 (1964)

17. R. Braunstein, A.R. Moore, F. Herman.
ibid., 109, 695 (1958)

21. T.K. Bergstresser, M.L. Cohen, E.W. Williams,
Phys Rev. Letts, 15, 662 (1965)

25. I.S. Baukin, V.I. Ivanov-Omskii, B.I. Kolomiets.
Sov. Phys. Sol.State, 7, 1019 (1965)

36. J.F. Black, S-M Ku.
Jnl. Electrochem. Soc., 113, 249 (1966)

39. F. Braun.
Ann. Phys. Chem., 153, 556 (1874)

40. J. Bardeen, W.H. Brattain.
Phys. Rev., 75, 1208 (1949)

41. F. Bloch.
Zeit. Phys, 52, 555 (1928)

B 42. L. Brillouin.

Jnl. Phys. Radium, 1, 377 (1930)

43. E. Burstein.

Phys. Rev., 93, 632 (1954)

44. L.C. Barcus et al.

ibid., 111, 167 (1958)

45. G. Busch, O. Vogt.

Helv. Phys. Acta, 33, 437 (1960)

46. I.I. Burdiyan, A.S. Borshchevskii.

Zhur. Tech. Phys., 28, 2684 (1958)

48. I.I. Burdiyan, B.T. Kolomiets.

Sov. Phys. Sol. State, 1, 1067 (1959)

49. K.W. Blazey.

Ph.D. Thesis, Nottingham (1963)

50. H.E. Bennett, J.F. Koehler.

Jnl. Opt. Soc. Am., 50, 1 (1960)

52. C.N. Berglund.

Jnl. Appl. Phys, 37, 3019 (1966)

55. B. Batz.

Solid State Comm., 4, 241 (1966)

C 2. M. Cardona, D.L. Greenaway.
Phys. Rev., 125, 1291 (1962)

3. M. Cardona, G. Harbeke.
Jnl. Appl. Phys, 34, 813 (1963)

4. M. Cardona.
Phys. Rev., 121, 752 (1961)

5. M. Cardona.
Jnl. Appl. Phys, 32, 958 (1961)

7. M. Cardona.
Zeit, Phys, 161, 99 (1961)

8. M. Cardona.
Jnl. Appl. Phys. 32, 2151 (1961)

10. M. Cardona, D.L. Greenaway.
Phys. Rev., 131, 98 (1963)

13. M. Cardona.
Jnl. Phys. Chem. Solids, 24, 1543 (1963)

16. M. Cardona, D.L. Greenaway.
Phys. Rev., 133, 1685 (1964)

19. M. Cardona.
Prague, p.388 (1960)

C 20. M. Cardona.

Phys. Rev., 129, 69 (1963)

22. D.A. Cusano, G.E. Fenner, R.O. Carlson.

Appl. Phys. Letts, 5, 144 (1964)

23. M. Cardona.

Paris, p.181 (1964)

27. M. Chester, L. Fritsche.

Phys. Rev., 139A 518 (1965)

28. M.L. Cohen, J.C. Phillips.

ibid., 139A 912 (1965)

29. M. Cardona.

Jnl. Appl. Phys, 36, 2181 (1965)

33. M. Cardona, F. Pollak.

Phys. Rev., 142, 530 (1966)

34. M. Chester, P.H. Wendland.

Phys. Rev. Letts, 13, 193 (1964)

35. M. Cardona, F. Pollak, J.G. Broerman.

Phys. Letts, 19, 236 (1966)

37. M.L. Cohen, T.K. Bergstresser.

Phys. Rev., 141, 789 (1966)

C 41. R.W. Conrad, C.E. Jones, E.J. Williams.
Jnl. Electrochem. Soc., 113, 287 (1966)

42. J. Callaway.
Solid State Phys, 7, 100 (1958).

43 J. Callaway.
"Energy Band Theory" N.Y. Academic Press, (1964)

44. N. Codere, E.H. Van Tongerloo, J.C. Woolley.
Physics in Canada, 22, 56 (1966)

45. M. Cardona, F. Pollak, K.L. Shaklee.
Phys. Rev. Letts, 16, 644 (1966)

46. J. Callaway.
Phys. Rev., 130, 549 (1963)

47. J. Callaway.
ibid, 134A 998 (1964)

48. M. Cardona.
Private communication.

49. M. Cardona, K.L. Shaklee, F. Pollak.
To be published.

50. M. Cardona et al.
Solid State Comm., 4, 319 (1966)

C 52. M. Cardona, W. Paul, H. Brooks.
Helv. Phys. Acta, 33, 329 (1960)

D 1. G.B. Dubrovskii.
Sov. Phys. Sol. State. 5, 699 (1963)

8. J.P. Dismukes et al.
Jnl. Appl. Phys, 35, 2899 (1964)

15. G. Dresslhaus, A.F. Kip, C. Kittel.
Phys. Rev., 98, 368 (1955)

16. G. Dresselhaus et al.
ibid., 100, 1218 (1955)

E 1. H. Ehrenreich.
Jnl. Appl. Phys, 32, 2155 (1961)

2. H. Ehrenreich, H.R. Philipp, J.C. Phillips.
Phys. Rev. Letts, 8, 59 (1962)

7. W.E. Engeler et al.
ibid., 14, 1069 (1965)

8. W.E. Engeler, M. Garfinkel, J.J. Tiemann.
ibid., 16, 239 (1966)

14. H. Ehrenreich.
Jnl. Phys. Chem. Solids, 12, 97 (1959)

F 1. O.G. Folberth.

Zeit Naturforsch, 10A 502 (1955)

2. H. Flicker, P.G. Herkart.

Bull. Am. Phys. Soc., 9, 61 (1964)

4. T.A. Fulton, D.B. Fitchen, G.E. Fenner.

Appl. Phys. Letts, 4, 9 (1964)

7. G.E. Fenner.

Phys. Rev., 134A 1113 (1964)

10. G.E. Fenner.

ibid., 137A, 1000 (1965)

11. A. Frova, P. Handler.

ibid., 137A 1857 (1965)

14. A. Frova, C.M. Penchina.

Phys. Status, Sol., 9, 767 (1965)

16. A. Frova, et al.

Phys Rev., 145, 575 (1966)

17. M. Faraday.

Exp. Res. in Elec., series 4, 433 (1833)

18. H.Y. Fan, M.L. Shepard, H. Spitzer.

Proc. Photocond. Conf., p.184, Wiley (1954)

F 19. T.E. Fischer.

Private communications, (1965)

Phys. Rev., 147, 603 (1966)

21. A. Frova, P. Handler.

Paris, p.157 (1964)

22. W. Franz.

Zeit. Naturforsch, 13A 484 (1958)

G 2. D.L. Greenaway.

Phys. Rev. Letts, 9, 97 (1962)

5. V. Gerhardt.

Phys. Letts, 9, 117 (1964)

10. G.J. Gobeli, E.O. Kane.

Phys. Rev. Letts, 15, 142 (1965)

16. S.V. Galginaitis.

Jnl. Appl. Phys, 36, 460 (1965)

19. M. Glicksman.

Jnl. Phys. Chem. Solids, 8, 511 (1959)

20. M. Glicksman.

Phys. Rev., 100, 1146 (1955)

G 21. N.A. Goryunova, N.N. Fedorova.
Jnl. Tech. Phys. Moscow, 24, 1339 (1955)

22. N.A. Goryunova, I.E. Gorshkov.
Jnl. Nheong Khum, 3, 668 (1958)

23. G. Giesecke, H. Pfister.
Acta Cryst., 11, 369 (1958)

H 2. J.W. Hodby.
Proc. Phys. Soc., 82, 324 (1963)

4. N. Holonyak et al.
Appl. Phys. Letts, 3, 47 (1963)

9 F. Herman.
Rev. Mod. Phys, 30, 102 (1958)

10. N. Holonyak.
Trans Met. Soc. AIME, 230, 276 (1964)

11. N. Holonyak, S.F. Bevacqua.
Solid State El., 7, 488 (1964)

19. N. Holonyak.
Proc. I.E.E.E., 52, 104 (1964)

27. F. Herman.
Paris, p.3 (1964)

H 30. C. Hilsum

ibid., p.1127 (1964)

38. F. Herman et al.

Quantum Theory of Atoms, Molecules, and the Solid State Academic Press (1966)

40. E.H. Hall.

Am. Jnl. Math., 2, 287 (1879)

41. F. Herman.

Phys. Rev., 95, 847 (1954)

42. F. Herman.

ibid., 89, 518 (1953)

43. F. Herman.

ibid., 93, 1214 (1954)

45. E.F. Hockings et al.

Jnl. Appl. Phys., 37, 2879 (1966)

46. D.E. Hill.

Bull. Am. Phys. Soc., 11, 205 (1966)

47 H.B. Harland, J.C. Woolley.

Can. Jnl. Phys, in press.

I 5. V.I. Ivanov-Omskii, B.T. Kolomiets.
Sov. Phys. Sol. State. 1, 512 (1959)

6. V.I. Ivanov-Omskii, B.T. Kolomiets.
ibid., 2, 363 (1960)

J 3. E.J. Johnson, H.Y. Fan.
Phys. Rev., 139A 1991 (1965)

4. H. Jones.
"The Theory of Brillouin Zones and Electronic States in Crystals". North-Holland (1960)

5. E.R. Johnson, S.M. Christian
Phys. Rev., 95, 560 (1954)

6. C.E. Jones.
Applied Spectroscopy 20, 161 (1966)

K 4. S-M Ku.
Jnl. Electrochem. Soc., 110, 991 (1963)

5. S-M Ku, J.F. Black.
Solid State El., 6, 505 (1963)

25. C. Kittel.
"Introduction to Solid State Physics"
Wiley (1956)

K 26. E.O..Kane.

Jnl. Phys. Chem. Solids, 1, 83 (1956)

27. E.O. Kane.

ibid., 1, 249 (1957)

30. E.O. Kane.

Phys. Rev., 146, 558 (1966)

31. L.V. Keldysh.

Jnl. Exp. Th. Phys., 7, 788 (1958)

32. L.V. Keldysh, V.S. Vavilov, K.I. Britsyn.

Prague, p.824 (1960)

L 1. D. Long.

Jnl. Appl. Phys. 33, 1682 (1962)

4. F. Lukes, E. Schmidt.

Phys. Letts, 2, 288 (1962)

7. F. Lukes, E. Schmidt.

Exeter, p.389 (1962)

M 1. T.S. Moss.

Jnl. Appl. Phys, 32, 2136 (1961)

2. C.A. Mead, W.G. Spitzer.

Phys. Rev. Letts, 11, 358 (1963)

M 5. I. Melngailis.

Proc. I.E.E.E., 51, 1154 (1963)

12. H.T. Minden.

Jnl. Electrochem. Soc., 112, 300 (1965)

22. O. Madelung.

"Physics of III - V Compounds" Wiley (1964)

23. T. Muto.

Sci. Papers Inst. Phys. Chem.

Res. Tokyo 34, 377 (1938)

24. J.F. Miller.

Jnl. Electrochem. Soc., 107, 527 (1960)

25. G.G. MacFarlane et al.

Phys. Rev., 108, 1377 (1957)

26. G.G. MacFarlane et al.

ibid., 111, 1245 (1958)

27. T.P. McLean.

Progr. Semiconductors 5, 53 (1960)

28. F. Matossi, F. Stern.

Phys. Rev., 111, 472 (1958)

29. N. Mott, H. Jones.

"The Theory of the Properties of Metals and Alloys", Oxford, (1936)

N 1. A Nussbaum.
Proc. I.R.E. 50, 1762 (1962)

6. L. Nordheim.
Ann Phys. Leipzig, 9, 607 (1931)

7. C.J. Neuse et al.
Sold State El., 9, 735 (1966)

O 3. E. Otsuka et al.
Jnl. Phys. Soc. Japan, 20, 727 (1965)

4. F. Oswald.
Zeit. Naturforsch, 14A, 374 (1959)

P 2. H.R. Philipp, H. Ehrenreich.
Phys. Rev., 129, 1550 ,(1963)

3. W. Paul.
Jnl. Appl. Phys. 32, 2082 (1961)

4. H.R. Philipp, E.A. Taft.
Phys. Rev., 113, 1002 (1959)

5. H.R. Philipp, E.A. Taft.
ibid., 120, 37 (1960)

6. J.C. Phillips.
Jnl. Phys. Chem. Solids, 12, 208 (1960)

P 13. L. Pincherle.
Exeter, p.541 (1962)

20. R.F. Potter, G.G. Kretschmar.
Infra-red Phys, 4, 57 (1964)

21. M.H. Pilkuhn, H. Rupprecht.
Trans. Met. Soc. A.I.M.E. 230, 282 (1964)

29. M.H. Pilkuhn, H. Rupprecht.
Jnl. Appl. Phys. 36, 684 (1965)

36. J.C. Phillips.
Solid State Phys. 18, (1966)

42. F.H. Pollak, M. Cardona.
Jnl. Phys. Chem. Solids, 27, 423 (1966)

43. F.H. Pollak, M. Cardona, K.L. Shaklee.
Phys. Rev. Letts, 16, 942 (1966)

47. R.H. Parmenter.
Phys. Rev., 97, 587 (1955)

48. R.H. Parmenter.
ibid., 99, 1759 (1955)

49. R.H. Parmenter.
Jnl. Phys. Chem. Solids, 6, 6 (1958)

P 50. W. Paul.

Jnl. Phys. Chem. Solids, 6, 6 (1958).

51. J.C. Phillips.

Phys. Rev. Letts, 10, 329 (1963).

52. F.A. Pizzarella.

Jnl. Electrochem. Soc., 109, 226 (1962)

53. F.H. Pollak, C.W. Higginbotham, M. Cardona.

To be published.

54. J.C. Phillips.

Proc. Int. School Phys. "Enrico Fermi"

Varenna Lectures, Suppl. Nuovo Cim., (1965)

55. W. Paul.

Private Communication.

R 8. M. Rubenstein.

Jnl. Electrochem. Soc., 112, 426 (1965)

10. J.H. Racette.

Semiconductor Dev. Concepts. Oct. 31, 62 (1963)

18. V. Rehn.

Bull. Am. Phys. Soc., 11, 205 (1966)

S 1. F. Stern.
Jnl. Appl. Phys. 32, 2166 (1961)

8. W.G. Spitzer, C.A. Mead.
Phys. Rev., 133, 872 (1964).

18. B.O. Seraphin, R.B. Hess.
Phys. Rev. Letts, 14, 138 (1965)

19. B.O. Seraphin, R.B. Hess.
Paris, p. 165 (1964)

21. V.V. Sobolev, N.N. Syrbu.
Sov. Phys. Sol. State, 6, 2018 (1965)

23. V.V. Sobolev.
ibid., 6, 2488 (1965)

26. R. Sirrine.
Jnl. Electrochem. Soc., 111, 750 (1964)

28. B.O. Seraphin, N. Bottka.
Phys. Rev., 139A, 560 (1965)

29. B.O. Seraphin, N. Bottka.
Phys. Rev. Letts, 15, 104 (1965)

30. V.K. Subashiev, S.A. Abagyan.
Paris, p. 225 (1964)

S 31. B.O. Seraphin, R.B. Hess, N. Bottka.
Jnl. Appl. Phys., 36, 2242 (1965)

34. K.L. Shaklee, F.H. Pollak, M. Cardona.
Phys. Rev. Letts, 15, 883 (1965)

36. V.K. Subashiev, G.A. Chalikyan.
Sov. Phys. Sol. State, 7, 992 (1965)

37. B.O. Seraphin, N. Bottka.
Appl. Phys. Letts, 6, 134 (1965)

38. B.O. Seraphin.
Phys. Rev., 140A, 1716 (1965)

39. K.L. Shaklee, M. Cardona, F.H. Pollak.
Phys. Rev. Letts, 16, 48 (1966)

46. B.O. Seraphin.
Jnl. Appl. Phys., 37, 721 (1966)

48. B.O. Seraphin, N. Bottka.
Phys. Rev., 145, 628 (1966)

50. W. Smith
Jnl. Soc Tel. Engr., 2, 31 (1873)

51. R.A. Smith.
"Semiconductors", Cambridge (1959)

S 52. A. Sommerfeld.
Zeit Phys., 47, 1 (1928)

53. H. Stöhr, W. Klemm.
Z. Anorg. Allgem. Chem., 241, 305 (1939)

54. M.C. Steele, F.D. Rosi.
Jnl. Appl. Phys., 29, 1517 (1958)

55. M.D. Sturge.
Phys. Rev., 127, 768 (1962)

57. S.D. Smith, C.R. Pidgeon, V. Prosser.
Exeter, p.301 (1962)

T 1. J. Tauc, E. Antonick.
Phys. Rev. Letts, 5, 253 (1960)

2 J. Tauc, A. Abraham.
Prague, p.375 (1960)

3. J. Tauc, A. Abraham.
Jnl. Phys Chem Solids. 20, 190 (1961)

8. J.J. Tietjen, L.R. Weisburg
Appl. Phys. Letts, 7, 261 (1965)

T 12. A.G. Thompson et al.
Phys. Rev , 146, 601 (1966)

13. J.J. Tietjen, J.A. Amick.
Jnl. Electrochem. Soc., 113, 724 (1966)

15. K. Tharmalingam.
Phys. Rev., 130, 2204 (1963)

16. A.G. Thompson, J.C. Woolley, M. Rubenstein.
Can. Jnl. Phys, in press.

U 1. Yu. L. Ukhanov, Yu. V. Mal'tsev.
Sov Phys. Sol. State, 5, 2144 (1964)

V 4. V.S. Vavilov, K.I. Britsyn.
Sov. Phys Sol. State, 3, 1816 (1962)

5. E.H. Van Tongerloo
Univ. of Ottawa, Phys. Dept Report (1966)

W 1. J.C. Woolley, B.A. Smith, D.G. Lees.
Proc Phys. Soc., 69, 1339 (1956)

2. J.C. Woolley, B.A. Smith.
ibid., 70, 153 (1957)

W 3. J.C. Woolley, B.A. Smith.
ibid., 72, 867 (1958)

5. J.C. Woolley, D.G. Lees, B.A. Smith.
Jnl. Less-common Met., 1, 199 (1959)

6. J.C. Woolley, J.A. Evans, C.M. Gillet.
Proc. Phys. Soc , 74, 224 (1959)

11. J.C. Woolley, C.M. Gillet.
Jnl. Phys. Chem. Solids, 17, 34 (1960)

12 J.C. Woolley.
Prague, p.966 (1960)

15. J.C. Woolley, C.M. Gillet, J.A. Evans.
ibid., 77, 700 (1961)

16. J.C. Woolley, J.A. Evans.
ibid., 78, 354 (1961)

20. H. Weiss.
Zeit Naturforsch, 11A, 430 (1956)

24 K Weiser, R.S. Levitt.
Appl. Phys. Letts, 2, 178 (1963)

25. J.C. Woolley, E.W. Williams.
Jnl. Electrochem. Soc., 111, 210 (1964)

W 30. J.C. Woolley, K.W. Blazey.
Jnl. Phys Chem. Solids, 25, 713 (1964)

33. J.C. Woolley, A.G. Thompson.
Can Jnl. Phys, 42, 2030 (1964)

34. J.C. Woolley, J. Warner.
ibid., 42, 1879 (1964).

42. J.C. Woolley, A.G. Thompson, M. Rubenstein.
Phys Rev Letts, 15, 670 (1965)

43. E.W. Williams, C.E. Jones
Solid State Comm , 3, 195 (1965)

44 J.C. Woolley, E.W. Williams, R. Gagnon.
Jnl. Electrochem. Soc , 112, 1112 (1965)

45. P.H. Wendland, M. Chester.
Phys. Rev , 140A, 1384 (1965)

48. C.M. Wolfe et al.
Jnl. Appl. Phys, 37, 434 (1966)

53. J.C. Woolley.
Progr. Sol. State Chem, 1, 275 (1963)

54. H. Welker
Zeit. Naturforsch, 7A, 744 (1952)

30. J.C. Woolley, K.W. Blazey.
Jnl. Phys Chem. Solids, 25, 713 (1964)

33. J.C. Woolley, A.G. Thompson.
Can. Jnl. Phys, 42, 2030 (1964)

34. J.C. Woolley, J. Warner.
ibid., 42, 1879 (1964).

42. J.C. Woolley, A.G. Thompson, M. Rubenstein.
Phys Rev. Letts, 15, 670 (1965)

43. E.W. Williams, C.E. Jones
Solid State Comm., 3, 195 (1965)

44. J.C. Woolley, E.W. Williams, R. Gagnon.
Jnl. Electrochem. Soc, 112, 1112 (1965)

45. P.H. Wendland, H. Chester.
Phys. Rev, 140A, 1384 (1965)

48. C.M. Wolfe et al.
Jnl. Appl. Phys, 37, 434 (1966)

53. J.C. Woolley.
Progr. Sol. State Chem, 1, 275 (1963)

54. H. Welker.
Zeit. Naturforsch, 7A, 744 (1952)

W 55. A.H. Wilson.
Proc. Roy. Soc., A133, 458 (1931)

56. A.H. Wilson.
ibid , A134, 277 (1931)

57. J.C. Woolley
"Preparation of III - V Compounds"
pp. 3 - 20, Reinhold (1962)

58. J.C. Woolley, B.A. Smith
Proc Phys. Soc., 72, 214 (1958)

59. J. Warner.
Ph.D. Thesis, Nottingham. (1963)

61. R. Williams.
Phys. Rev , 117, 1487 (1960)

62. R. Williams.
ibid., 126, 442 (1962)

63. E.W. Williams.
Private Communication (1965)

Y 1. Y. Yacoby.
Phys Rev., 142, 445 (1966)

Y 2. Chang. Yu-Won, Yu Qi-Hua.
Acta. Phys. Sinica, 21, 1162 (1965)

3. Y. Yacoby.
Phys. Rev., 140A, 263 (1965)

Z 2. R. Zallen, W. Paul.
Phys Rev., 134A, 1628 (1964)

5. S. Zwerdling et al.
ibid., 114, 80 (1959)

6. S. Zwerdling et al.
Jnl. Phys. Chem. Solids, 9, 320 (1959)

CURRICULUM VITAE

NAME:	Alan G. Thompson
BORN:	Dartford, England, 1942
EDUCATED:	
Primary	West-Hill Primary School 1947-53
Secondary	Dartford Grammar School 1953-60
University	Nottingham University 1960-63
	University of Ottawa 1963-66
Course	Physics
Degree	B.Sc. (Honours) 1963.